Mutual Information Accumulation over Wireless Networks: Fundamentals and Applications

By

Hao Chen

Submitted to the Department of Electrical Engineering and Computer Science and the
Graduate Faculty of the University of Kansas
in partial fulfillment of the requirements for the
Doctor of Philosophy

Committee members

Lingjia Liu, Chairperson

Shannon Blunt

Victor Frost

Yang Yi

Zsolt Talata

Date defended: June 14, 2017

The Committee for Hao Chen certifies
that this is the approved version of the following dissertation :

Mutual Information Accumulation over Wireless Networks: Fundamentals and Applications

Lingjia Liu, Chairperson

Date approved: June 14, 2017

Abstract

Future wireless networks will face a compound challenge of supporting large traffic volumes, providing ultra-reliable and low latency connections to ultra-dense mobile devices. To meet this challenge, various new technologies have been introduced among which mutual-information accumulation (MIA), an advanced physical (PHY) layer coding technique, has been shown to significantly improve the network performance. Since the PHY layer is the fundamental layer, MIA could potentially impact various network layers of a wireless network. Accordingly, the understanding of improving network design based on MIA is far from being fully developed. The purpose of this dissertation is to study the fundamental performance improvement of mutual information accumulation over wireless networks and to apply these fundamental results to guide the design of practical systems, such as cognitive radio networks and massive machine type communication networks.

This dissertation includes three parts. The first part of this dissertation presents the fundamental analysis of the performance of mutual information accumulation over wireless networks. To begin with, we first analyze the asymptotic performance of mutual information accumulation in an infinite 2-dimensional(2-D) grid network. Then, we investigate the optimal routing in cognitive radio networks with mutual information accumulation and derive the closed-form cooperative gain obtained by applying mutual information accumulation in cognitive radio networks. Finally, we characterize the performance of mutual information accumulation in random networks using tools from stochastic geometry.

The second part of this dissertation focuses on the application of mutual information

accumulation in cognitive radio networks. An optimization problem is formulated to identify the cooperative routing and optimal resources allocation to minimize the transmission delay in underlay cognitive radio networks with mutual information accumulation. Efficient centralized as well as distributed algorithms are developed to solve this cross-layer optimization problem using the fundamental properties obtained in the first part of this dissertation. Simulation results show that mutual information accumulation can reduce more than 77% delay compared to conventional two-hop transmission in underlay cognitive radio network.

The third part of this dissertation focuses on the application of mutual information accumulation in massive machine type communication (massive MTC) network. A new cooperative retransmission strategy is developed for massive MTC networks. Theoretical analysis of the new developed retransmission strategy is conducted using the same methodology developed in the fundamental part of this dissertation. Monte Carlo simulation results and numerical results are presented to verify our analysis as well as to show the performance improvement of our developed strategy.

Acknowledgements

First and foremost, I would like to thank my advisor Dr. Lingjia Liu for his great guidance and countless support. I have learned a lot from Dr. Liu, especially on how to grasp the essence of problems and how to think in an intuitive way. I still remember our first discussion on how to improve the performance of the wireless networks in his office. His elegant interpretation methodology deeply attracted and affected me. In the past few years, he has taught me hand-by-hand on how to formulate ideas, solve problems and write rigorous technical reports. He has always been there to listen, discuss and give constructive guidance on my research. It is my fortunate to have the chance to work with him and it has been a truly stimulating and rewarding experience.

I would like to express my gratitude to Dr. Victor Frost, Dr. Shannon Blunt, Dr. Zsolt Talata and Dr. Yang Yi for serving on my dissertation committee and providing support during my whole Ph.D program. I would like to give my special thanks to Dr. Victor Frost for the discussion of network performance analysis during his class. I would like to thank Dr. Shannon Blunt and Dr. Erik Perrins for allowing me to audit their classes on signal processing and digital communication. I also would like to thank Dr. Jin Feng, Dr. Terry Soo and Dr. Harpreet S. Dhillon on the discussion of random process and stochastic geometry which have laid a solid foundation for me to write this dissertation. I would also like to thank Dr. John D. Matyjas and Dr. Michael J. Medley from Air Force Research Lab for their financial support on this work.

I would like to thank my colleagues and friends for their friendship and support during my Ph.D study at University of Kansas. Especially, I would like to thank Yan Li, Cenk Sahin, Zach Rohde, Rachad Atat, Rubayet Shafin, Susanna Mosleh, Ghaith Shabsigh,

Farhad Mahmood, and Hayder Almosa for their intensive discussions and collaborations. I would like to sincerely thank my friends, Yi Zhu, Bin Wang, Chaozheng Li, Panqiu Xia, Chao Lan, Luyao Shang, Robert Lutes, Brian Whitaker, Chuck Wa, Charlotte Wa and Xiaomeng Su for their friendship. I would like to thank Dr. Pinyi Ren, Dr. Li Sun, Dr. Hongxiang Li and Dr. Qinghe Du for their support during my Ph.D program application process. Without their help and support, I would not have had the chance to start my Ph.D program at KU. I am grateful to my friends and colleagues, Boon Ng, Young-Han Nam and Charlie Zhang at Samsung Research America. Their support and encouragement have accelerated the writing of this dissertation.

Finally and most importantly, I would like to express my profound gratitude to my family. I sincerely thank my father Mingwu Chen, my mother Qunying Ding, my grandfather Sijie Chen, my grandmother Suping Liu and all my relatives. This dissertation is dedicated to them for their infinite support, love and encouragement.

Contents

List of Figures

Chapter 1

Introduction

1.1 Motivation

According to the International Telecommunication Union (ITU) [2], the number of mobile cellular subscriptions globally is estimated to surpass 7.09 billions at the end of 2015, a number representing more than 96% of the world population. In the Americas, the impact of mobile cellular communications is even more significant with the current penetration rate of 108% [2]. Following this trend, in May 2015, it was predicted that there would be over 11.5 billion mobile-connected devices by year 2019, nearly 1.5 mobile devices per capita [3]. An important drive behind this is the worldwide rapid adoption of smart phones and mobile tablets. These devices are much more data-hungry: the data consumption of a single smart phone is equivalent to that generated by 37 featured phones; a mobile tablet can produce 2.5 times more traffic than the average smart phone [4]. As a result, Cisco Systems predicted a staggering 57% compound annual growth rate (CAGR) for global mobile cellular data traffic from 2014 to 2019: a 10-**fold increase**.

To meet the increasing communication demand, the future 5G systems must dramatically outperform previous generation systems and should support [5]:

- User experienced data rate: 0.1 $\sim$ 1 Gbps
- Connection density: 1million connections per square kilometer

- End-to-end latency: millisecond level
- Traffic volume density: tens of Gbps per square kilometer
- Mobility: higher than 500Km per hour
- Peak data rate: tens of Gbps

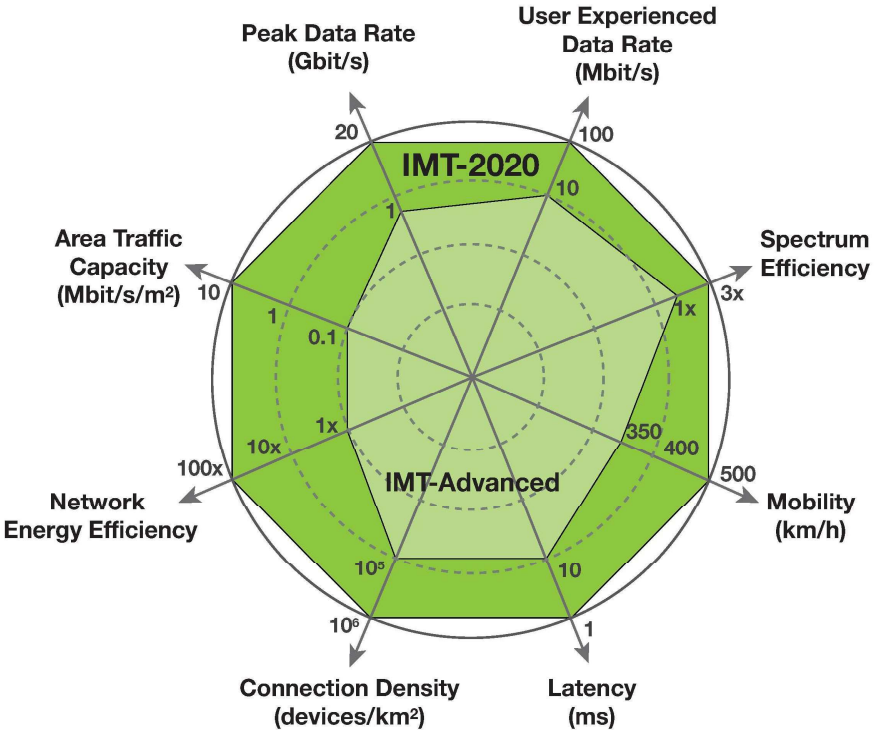

Figure 1.1: Key capabilities from IMT-Advanced (4G) to IMT-2020(5G)[1]

Figure 1.1 shows enhancement of key capabilities from 4G to 5G. As indicated in this figure, future 5G has to be able to *support large traffic volumes* and *provide reliable connections to ultra-dense mobile devices*. This is a challenging task, especially considering the unreliable nature of wireless channels. Conventionally, the design of wireless networks has borrowed the design of wired networks. Functionalities such as modulation, channel coding, resource allocation, routing are partitioned into separate network layers with minimum interaction between adjacent layers. Each lower layer serves as a black box abstraction for higher layers. For example, from a network layer point of view, the overall performance of the underlying physical and data link layer are modeled

as "bit pipes" that deliver data at a fixed rate with occasional random errors [6]. Recently various techniques, such as Massive Multi-Input and Multi-Output (Massive MIMO), polar codes, mutual information accumulation etc., have been developed to improve the physical layer performance of wireless networks. However, new network layer algorithms and protocols that can take full advantage of these physical layer techniques remain unexplored.

The rapid development in physical layer design is partially due to the Shannon information theory which describes fundamental relationships between the performance of point-to-point communication and system parameters. Unfortunately, there is no such simple yet fundamental theory for the capacity of a wireless network. Although the scaling laws [7] reveals significant insight on the performance of ad hoc networks, a tool that could provide a finer view is needed to guide the design of wireless networks. Stochastic geometry recently has been proven a powerful tool in characterizing the performance of cellular networks [8]. By modeling the location of nodes in a network as a spatial random process, stochastic geometry can be used to analyze the average performance of networks over many spatial topology realizations. However, how to use stochastic geometry to analyze the performance of multi-hop networks still remains an open problem. Especially, how to use stochastic geometry to analyze wireless networks with mutual information accumulation remains unexplored.

1.2 Mutual Information Accumulation

In this section, we introduce the details and potentials of mutual information accumulation. Mutual information accumulation is a natural extension of energy accumulation. In energy accumulation, a receiver can decode a packet as soon as the total received energy from multiple transmissions of that packet exceeds a certain threshold [9]. Energy accumulation can be achieved through repetition codes or chase combining in hybrid automatic repeat request (hyrid ARQ) [10], etc. Instead of accumulating energy, mutual information accumulation enables a node accumulate mutual information for a packet from multiple transmissions until it can decode the packet successfully [11].

In practice, mutual information accumulation can be realized through the use of rateless codes, of which Fountain [12] and Raptor codes [13], are examples. Rateless codes encode information bits into potentially infinite length codewords and additional parity bits are sent by the transmitter until the receiver is able to decode. Different from fixed coding-rate schemes, rateless codes can adaptively combat the dynamic wireless channels by just knowing the channel statistics [14], [11]. This advantage of mutual information accumulation (using rateless codes) is of vital importance in cognitive radio networks where the cost of gathering instantaneous channel state information is more difficult.

The difference between energy accumulation and mutual information accumulation can be seen clearly by considering communication over an additive white Gaussian noise (AWGN) channel over two time slots. For energy accumulation, the transmitter will send the same codeword across two time slots. Using maximal ratio combination, the receiver can obtain a throughput of $TW\log_2(1+2P/N_0)$ bits, where P is the transmit power spectral density, N_0 is the noise power spectral density, T is the slot duration, and W is the bandwidth. For mutual information accumulation, instead of transmitting the same codeword, independent codewords will be sent to the receiver over the two time slots, and the receiver will decode the data jointly. Accordingly, a throughput of $2TW\log_2(1+P/N_0)$ bits can be achieved. Since $(1+P/N)^2$ is greater or equal to $1+2P/N$, mutual information accumulation can obtain higher throughput than energy accumulation. It is interesting to observe that in the low signal-to-noise ratio (SNR) regime the approximation of $\log(1+SNR)\approx SNR$ holds. This suggests that the performance of energy accumulation is close to that of mutual information accumulation in this regime. However, as SNR increases, mutual information accumulation will have better performance.

Ever since the idea of mutual information accumulation was introduced to cooperative relay networks in [15, 14], many works have been conducted to solve the associated cooperative routing and resource allocation problems for a general wireless network. In [16], mutual information accumulation was introduced to an arbitrary wireless ad hoc network and the optimal/near-optimal routing and resource allocation strategies are identified. It has been shown that the performance

of the underlying wireless network with mutual information accumulation can be significantly enhanced. Scheduling problems in wireless networks using mutual information accumulation is investigated in [17]. The results suggest that by employing mutual information accumulation, the stability region of wireless networks can be expanded. Mutual information accumulation has been extended to the scenario of multi-packet transmission in a wireless network in [18]. In [11], the authors studied the optimal routing of a wireless network equipped with mutual information accumulation and showed that under the sum-bandwidth constraint, allocating all the system resources to a single user in each transmission slot can achieve the minimum delay in any one-dimensional networks. Recently, in [19] and [20], energy minimization problems are studied in wireless networks employing mutual information accumulation and efficient algorithms are introduced to solve the routing and power allocation problems.

1.3 Cognitive Radio Networks

Cognitive radio (CR), also known as dynamic spectrum access (DSA), has been regarded as one of the key techniques to improve the spectral efficiency of a wireless system. The basic idea of CR is to allow secondary users (SUs) to utilize primary users' (PUs') radio spectrum under the condition that the interference from the SUs to the PUs is constrained. In existing literature, several approaches have been introduced on how SUs should access PUs' radio spectrum: overlay cognitive radio [21], cooperation between PUs and SUs [22], underlay cognitive radio [23, 24] and, sensing based spectrum sharing [25].

In overlay cognitive radio networks, SUs will transmit after sensing PUs' spectrum idle. If PUs are sensed as busy or transmitting, SUs will stop transmitting. In the underlay cognitive radio approach, SUs and PUs are transmitting simultaneously on the same radio spectrum. In order to make sure that the interference from SUs to PUs are tolerable, SUs are usually required to transmit at a low power level resulting in a rather limited communication coverage. By introducing cooperation between PUs and SUs, a win-win situation can be achieved for both PUs and SUs. In

cooperative CRNs, SUs can act as relays for PUs. Therefore, the performance of PUs can be improved while SUs can earn more transmit opportunities. Sensing based spectrum sharing is a combination of overlay and underlay. To be specific, in sensing based cognitive radio networks, SUs will access the spectrum with a low probability/power when sensing PUs busy; SU will access the spectrum with a high probability/power when sensing PUs idle. This dissertation will focus on multi-hop cognitive underlay networks. Therefore, the following will give a detailed introduction on routing in multi-hop cognitive underlay networks.

In multi-hop cognitive radio networks, routing, which is to find a path from the source to the destination, is a fundamental and challenging issue [26]. To guarantee PUs' priority on spectrum access while optimizing SUs' performance by route selection, several approaches have been come up in current literature. To maximize SUs' end-to-end throughput, mixed integer linear/non-linear programming are employed to model the routing problem in [27] and [28]. Layered graph framework was introduced in [26] to exploit dynamic spectrums resource in routing from the perspective of graph theory. To reduce the control overhead, distributed routing algorithms for multi-hop cognitive radio networks were designed in [29] and [30], where routing performance depended on the design of routing metrics. The above mentioned routing algorithms in multi-hop cognitive radio networks were formulated based on either one of the following one-hop reception models [31]: the protocol model and the physical model. According to these models, if user A transmits a packet to user B that is one-hop away, the neighboring transmitters of this link have to keep silent and the neighboring receivers have to drop the received packets no matter whether it can decode it or not. In reality, neighboring users can partially overhear packets within a certain range of the transmitting user as pointed out in [32]. To take advantage of the broadcast nature of the wireless media, cooperative routing has been introduced to reduce the end-to-end energy consumption in routing packets between two users [33].

Using maximal ratio combining at the receiver, multiple partially overheard copies of the same data would enable the receiver to decode the data with higher reliability. This technique is usually called energy accumulation (EA) or accumulative relay (AR) [34]. Distributed space-time

codes [35] or amplify-and-forward relay [9] can be regarded as special cases of two-hop energy accumulation strategies. Energy accumulation routing in multi-hop wireless networks enables a node to store a copy of the received signal that is too weak for decoding and combine it with other copies of the same packet that arrives later [32]. It is shown in [34, 36, 37] that by energy accumulation, even the suboptimal routing and resources allocation algorithm can achieve $30\% \sim 50\%$ percent of energy reduction in multi-hop wireless networks. However, traditional routing methods like the layered graph framework [26] and mixed integer nonlinear programming [38] can not be directly applied in networks with energy accumulation or mutual information accumulation.

1.4 Massive Machine Type Communication

In February 2016, Cisco predicted the number of machine type devices (MTD) would grow from 604 million in 2015 to 3.1 billion by 2020 [39]. With the expected increase of machine type communication (MTC), a single macro-cell may need to support 10,000 or more devices in the future [40]. The challenges of designing a MTC network are different from those of a conventional broadband network because of the characteristics of MTC applications: small payloads, large numbers of devices, extended range and enhanced device energy efficiency [41]. Due to these characteristics, the current deployed 4G cellular technologies, which have extremely efficient physical and media access control layers performance, are still lagging behind supporting massive MTC. Therefore, to support massive MTDs is one of the main driving force of 5G networks. In most of the current MTC systems, MTDs communicates directly with the eNodeB in one cell. This single-hop paradigm may not be able to support massive MTD where hundreds or thousands of MTDs attempt to set up wireless communication links. Furthermore, MTDs located at the boundary of a cell suffer from a high outage probability due to the interference from other MTDs. A costly solution is to deploy more eNodeBs and split the cell into multiple small cells.

Instead of investing a huge amount of money on deploying extra eNodeBs or relays, cooperative communication has been demonstrated as an efficient and effective way to extend the coverage

region and improve the throughput of cellular networks [42] [43] [44] [45]. In [43], the authors introduced ad hoc GSM (A-GSM) system which integrates multi-hop communication into cellular networks. In [44] and [45], power allocation schemes were studied in two-hop relaying cellular networks and the performance gains were demonstrated by simulation results. Cooperative communication has been studied to extend the coverage range in heterogeneous M2M networks [46]. A two-hop transmission protocol to minimize total energy consumption in both flat and frequency-selective fading channels was studied in [47]. Guided routing protocols which aim at efficiently selecting relay nodes to enhance the delivery probability with partial network information were studied in [48] and [49]. It was shown in [50] that multi-hop cooperative communication could effectively reduce the end-to-end delay in a massive MTC network. However, there are still several key technique open questions remaining unsolved. The first question is relay selection with limited channel state information (CSI). Different from conventional relay selection with full CSI [42], it may be impossible for a MTD to estimate its wireless channels to potential relays due to the potentially huge amounts of overhead. The second question is the lack of systematic network performance analysis. Theoretical analysis on the performance of cooperative communication in a massive MTC network is challenging because the network performance depends on interference and network topologies. Due to the complexity of network performance analysis, most of the current literature only demonstrated the network-level benefits of cooperation using simulation results.

1.5 Stochastic Geometry and Wireless Networks

Information theory has played a central role in the design of the physical layer of a wireless communication system. However, information theory, which lays a foundation for improving the performance of point-to-point communication, has failed to characterize the performance of wireless networks. New tools need to be developed to analyze the performance and guide the design of wireless networks. Actually, one of the main challenge to analyze the performance of a wireless

network is the randomness in network topology and wireless channels. Recently, stochastic geometry has been regarded as a promising mathematical tool which can characterize the throughput, outage probability and transmission capacity of wireless networks.

Stochastic geometry deals with random spatial patterns [8]. By modeling the location of nodes as a stochastic process points in the two- or three-dimensional space, stochastic geometry can provide an average performance for wireless networks over different topologies just like the queueing theory provides averaged response times or congestion over all potential arrival patterns within a given parametric class. Hence wireless network modeling and analysis is a very natural application of stochastic geometry, and, indeed, the last decade has witnessed a significant growth in this area [8]. Using stochastic geometry as a tool to characterize interference in wireless networks can data back to 1978 [51], and was further advanced by Sousa and Silvester in the early 1990s [52]. Recently, stochastic geometry has been widely used to analyze the performance of cellular networks and D2D networks after the pioneering work of Andrews [53], Martin [8] and Baccelli [54].

For a cellular network, the downlink coverage probability and throughput for the typical user is given in [53]. Furthermore, the authors compare the theoretical result to the grid model and an actual base station deployment. They found that modeling the location of nodes as a Poisson point process (PPP) can provide a lower bound on coverage probability for the real systems performance. Fractional power allocation is studied using stochastic geometry to compare how power allocation strategies affect the performance of cellular systems [55]. Fractional frequency reuse is studied in [56] for cellular networks. Stochastic geometry is widely used to analyze the performance of wireless networks because it is tractable and can reveal fundamental relationship between system performance of system parameters. Recently researchers around the world are using stochastic geometry to analyze the performance of D2D networks [57], networks with carrier sensing [58], cognitive radio [59], heterogeneous networks [60] and networks with clustered devices [61].

Although stochastic geometry is quite success on characterizing the performance of 0ne-hop networks, e.g., cellular networks and D2D networks, it is quite challenging to characterize the performance of multi-hop networks. The main issue in multi-hop wireless network is that interfer-

ence in different locations and time-slots are correlated [62]. Furthermore, as indicated in [62], the effect of interference correlation depends on the path loss exponent. When temporal interference correlation is considered, it is proved in [63] that there is no diversity gain in simple retransmission schemes, even with independent Rayleigh fading over all links. This indicates that if in this time-slot a node is in outage, with high probability it will be in outage in the next time-slot. In [64], the authors characterize the transmission capacity of an ad hoc network with multi-hop transmissions and automatic repeat request on each hop under an assumption that interference is independent in different time. In [65], the author studied the throughput-delay-reliability tradeoff with ARQ in wireless ad hoc network without considering the spatiotemporal correlation of interference. Recently, correlation of interference is considered in [66] [67] for one-hop networks. Both results show that no-correlation assumption is significantly optimistic compared to the true performance.

Chapter 2

Fundamentals: Analysis of Wireless Networks with Mutual Information Accumulation

In this chapter, we study the fundamental performance of mutual information accumulation in various wireless networks. To begin with, we first analyze the performance of mutual information accumulation in an infinite 2-dimensional(2-D) grid network. Then, we study the optimal routing in cognitive radio networks with mutual information accumulation and characterize the cooperative gain we can obtain by applying mutual information accumulation in cognitive radio networks. Thirdly, we extend our work to random networks and characterize the performance of mutual information accumulation in a Poisson field of interferers using tools from stochastic geometry.

2.1 Asymptotic Analysis on MIA in 2-D Grid Network

The performance improvement of combing mutual information accumulation with cooperative routing for a simple 1-D wireless network was illustrated in [16]. It was shown that the cooperative gain converges to $\pi^2/6 \approx 1.64$ in the low signal-to-noise ratio (SNR) regime. In this section, we

characterize the cooperative gain for a two-dimensional (2-D) wireless network in the low SNR regime.

2.1.1 Problem Statement

Let us consider the routing problem for a simple 2-D grid network with $(N+1)^2$ nodes equally spaced in a $D \times D$ square area. Let $(0,0)$ be the coordinate of the source node and (N,N) be the coordinate of the destination node, as shown in Fig. 2.1. The source wants to transmit a message of B bits to the destination under the help of all other nodes in Fig. 2.1. The total system bandwidth is denoted as W_T and the transmit power spectrum density of each node is denoted as P. The channel power gain between two nodes, (i,j) and (m,n), is proportional to $(d_{(i,j),(m,n)})^{-\alpha} =$

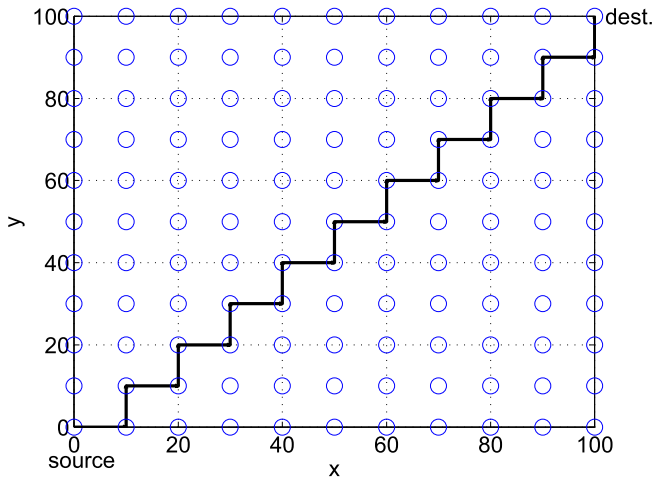

Figure 2.1: The topology of the 2-D grid network

$(N/D)^{\alpha}(\sqrt{(m-i)^2+(n-j)^2})^{-\alpha}$, where α is the path loss exponent. Small scaling fading is omitted here to simplify the analysis. The routing and resource allocation strategy is designed to minimize the end-to-end delay from the source to the destination. In the following, we provide an asymptotic analysis of the cooperative gain of this network in low SNR regime when the number of nodes goes infinite.

2.1.2 Performance Analysis

In the low SNR regime, the optimal route for the 2-D cooperative network using mutual information accumulation in this topology is tagged by the black line in Fig. 2.1. That is, the cooperative strategy that minimizes the transmission duration is: for the source, node $(0,0)$, keeps transmitting until node $(1,0)$ decodes the message. Then, node $(1,0)$ takes over the transmission. This is because node $(1,0)$ has better connections to the rest of the nodes in the route compared to node $(0,0)$. Therefore, it is better to allocate the full system bandwidth to node $(1,0)$ rather than reserving some for node $(0,0)$. Subsequent transmissions continue until the next node in the route (black line) decodes. The duration of each transmission is shorter than its previous one due to the fact that the receiving node has already accumulated some mutual information from the transmission of the previous nodes. On the other hand, the optimal route for non-cooperative multi-hop network can be obtained through Dijkstra's shortest path algorithm [68]. It is important to note that unlike the cooperative route where all nodes in the black line participate, in the non-cooperative network the optimal route depends on the transmission power of P. When P is sufficiently low, the optimal route is the same as the cooperative one. However, as P increases, some relay nodes are skipped. When P is sufficiently large, the minimum delay strategy is to let the source transmit to the destination directly.

Let the minimum delay of cooperative routing with mutual information accumulation be τ_{MIA} and the minimum delay of traditional multi-hop routing be τ_{NC}. In the following, we will refer the node by its location. The optimal route from the source to the destination is shown (black line) in Fig. 2.1 and the optimal decoding order is $(0,0)->(1,0)->(1,1)->(2,1)->\cdots->(N,N-1)->(N,N)$. The link capacity between node (i, j) and (m, n) is

$$C_{(i,j)(m,n)} = \log_2\left[1+\frac{PN^2/\Gamma}{D^2N_0\left((i-m)^2+(j-n)^2\right)}\right],$$

where we assume the path loss exponent is 2. When N is large and P is small, such that N^2P is

small, the spectral efficiency can be approximated as

$$C_{(i,j)(m,n)} \approx \log_2 e \frac{PN^2/\Gamma}{D^2 N_0 \left((i-m)^2+(j-n)^2\right)}. \tag{2.1}$$

The incremental delay for traditional multi-hop delay-optimal case $\Delta\tau_{nc}$ can be expressed as

$$\Delta\tau_{nc} = \frac{B}{C_{(i,j)(i,j+1)} W_T} \approx \frac{BN_0 D^2 \Gamma}{W_T P N^2 \log_2 e}. \tag{2.2}$$

For nodes which accumulate mutual-information, the incremental delay is reduced and in a large network the $A_{(i,j)(i+1,j)}$ and $A_{(i,j)(i,j+1)}$ will be the same and approach a steady state value $\Delta\tau_c$. For a specific node $(i,\ j)$, since the node is allocated the full bandwidth W_T, if its transmission lasts $\Delta\tau_c$, the corresponding time-bandwidth product is $A_{(i,j)(i+1,j)} = \Delta\tau_c W_T$ or $A_{(i,j)(i,j+1)} = \Delta\tau_c W_T$. As N becomes large, the steady state time-slots dominate the overall delay. The information accumulated at node $(k,\ k)$ can be divided into two parts: the first part is the information accumulated from nodes $(i,\ i)$, $1 \le i \le k-1$; the second part is the information accumulated from nodes $(i+1,\ i)$, $1 \le i \le k-1$. Therefore, the decoding condition for node $(k,\ k)$ can be expressed as,

$$\begin{aligned}
B &= \sum_{l=1}^{k} C_{(k-l,k-l)(k,k)} A_{(k-l,k-l)(k-l+1,k-l)} + \sum_{l=1}^{k} C_{(k-l+1,k-l)(k,k)} A_{(k-l+1,k-l)(k-l+1,k-l+1)} \\
&\approx \Delta\tau_c W_T \sum_{l=1}^{k} \log_2 e \frac{PN^2/\Gamma}{2D^2 N_0 l^2} + \Delta\tau_c W_T \sum_{l=1}^{k} \log_2 e \frac{PN^2/\Gamma}{D^2 N_0 (l^2+(l-1)^2)} \\
&= \Delta\tau_c W_T \log_2 e \frac{PN^2/\Gamma}{D^2 N_0} \sum_{l=1}^{k} \left(\frac{1}{2l^2} + \frac{1}{(l^2+(l-1)^2)} \right) \\
&\xrightarrow{N\to\infty,k\to\infty} \Delta\tau_c W_T \log_2 e \frac{PN^2/\Gamma}{D^2 N_0} \left(\frac{\pi^2}{12} + \frac{\pi}{2} \tanh(\frac{\pi}{2}) \right).
\end{aligned} \tag{2.3}$$

Therefore, the incremental delay is

$$\Delta\tau_c = \frac{BD^2 N_0 \Gamma}{W_T \log_2 e P N^2 \left(\frac{\pi^2}{12} + \frac{\pi}{2} \tanh(\frac{\pi}{2}) \right)}. \tag{2.4}$$

Therefore, the cooperative gain in two-dimension case is

$$\frac{\Delta\tau_{nc}}{\Delta\tau_c} = \frac{2N\Delta\tau_{nc}}{2N\Delta\tau_c} = \left(\frac{\pi^2}{12} + \frac{\pi}{2}\tanh(\frac{\pi}{2})\right) \approx 2.2631. \tag{2.5}$$

The cooperative gain of this 2-D grid network is simulated and plotted out in Fig.2.2 ($N = 100$, $D = 100$ m, $B = 20$ bits, $N_0 = 1$ W/Hz, and $\alpha = 2$) as a function of PW_T. Here W_T is the total

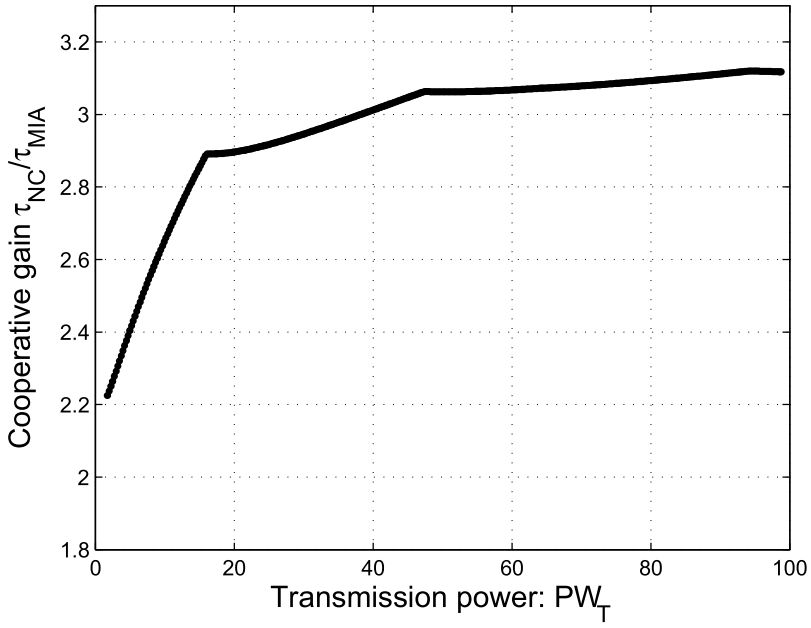

Figure 2.2: The cooperative gain of 2-D grid network

spectrum bandwidth of the system. It can be clearly seen in Fig.2.2 that the cooperative gain increases as transmit power increases. Furthermore, the cooperative gain curve is piece-wise. The non-differentiable break points correspond to the powers at which the optimal non-cooperative (shortest-path) route changes. As N becomes large and P approaches zero such that the product of N^2P stays small, we show that the cooperative gain converges to $\pi^2/12+\pi/2\tanh(\pi/2) \approx 2.2631$. Note that the cooperative gain for 1-D networks is characterized in [16] as $\pi^2/6 \approx 1.64$. Therefore, the cooperative gain in 2-D networks is larger than its courter part in 1-D networks. It is also important to note that the cooperative gain obtained here is very similar to that obtained in [33]. This is because the transmission strategy used in [33] is energy accumulation which performs

close to mutual information accumulation in the low SNR regime. Interestingly, the cooperative gain is not monotone increasing as a function of PW_T in each sub-domain as its corresponding one-dimensional case is. Instead, the cooperative gain first decreases and then increases as PW_T increases in each sub-domain. This can be explained by the fact that after selecting a new delay-optimal route, nodes will first works in the low SNR region and then works in the high SNR region as PW_T continues increasing. In the low SNR region, the end-to-end delay in non-cooperative networks can be expressed as C/SNR, where C is a constant decided by the length of packet, bandwidth and number of hops etc. While in the high SNR region, the delay can be expressed as $C/\log(1+SNR)$. Since $1/x$ decreases much faster than $1/\log(1+x)$ w.r.t. x, the delay as a function of power for non-cooperative networks decreases much faster when nodes are in low SNR region than in the high SNR region. Since there is no route change when transmit power increases in cooperative networks using mutual information accumulation, the increasing or decreasing trend will be dominated by τ_{NC}. This explains why the cooperative gain is not monotone increasing as shown in Fig. 2.2. This section shows that mutual information accumulation can achieve high cooperative gain in non-cognitive networks.

2.2 Analysis on MIA in Regular Cognitive Radio Networks

In this section, we analyze the fundamental performance of multi-hop underlay cognitive radio networks with mutual information accumulation.

2.2.1 Problem Statement

Consider an underlay cognitive network where PUs use orthogonal transmissions, such as orthogonal frequency-division multiplexing (OFDM) and different PU pairs occupy different subbands. N SUs try to access one subband of the cellular spectrum while keeping the total interference to the PU pair under a threshold. Accordingly, the underlay cognitive radio network considered in this paper can be modeled as a cognitive network with 1 PU transmitter, 1 PU receiver, 1 SU source,

1 SU destination and $N-2$ SU relays, as shown in Fig. 2.3. The spectrum bandwidth of a PU

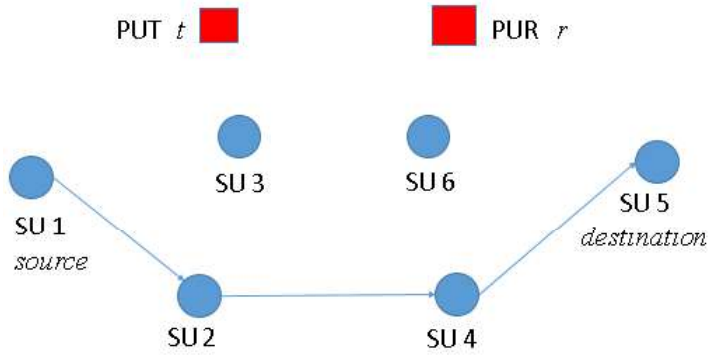

Figure 2.3: System model for MIA in cognitive radio networks

pair's subband is denoted as W_T and PU's interference threshold is denoted as I_T. The objective of SUs' network is to transmit a data packet with entropy B bits from the SU source to the SU destination with the help of the SU relay nodes. All SU relay nodes can actively help forwarding the data packet or keep silent on PU' spectrum, depending on the cooperative routing and resources allocation strategies.

Both PUs and SUs operate in half-duplex mode. All SUs use orthogonal frequency-division multiplexing (OFDM) and all transmitting SUs are allocated orthogonal time-bandwidth resources by transmitting in different time slots and on different OFDM sub-carriers. Therefore, all the transmitting SUs can transmit without interference with each other while all the receiving SUs can overhear the respective transmission. Let P_s denote the transmit power spectral density of SUs . The wireless channel between each pair of nodes is assumed to be a quasi-static flat-fading channel. The channel power gain between user i and user j is assumed to be h_{ij}. Let C_{ij} denote the achievable transmission rate per degree of freedom between node i and node j which can be expressed as [69]

$$C_{ij} = \log_2\left(1+\frac{h_{ij}P_s}{(N_0+h_{pj}P_p)\Gamma}\right)\frac{\text{bits}}{\text{sec}\cdot\text{Hz}},$$

where P_p is the transmit power spectral density of PU, Γ denotes the signal-to-noise (SNR) gap that defines the gap between the channel capacity and a practical modulation and coding scheme (MCS). The SNR gap depends on the MCS used and the targeted error probability. For a coded

quadrature amplitude modulation system, the gap is given by $\Gamma = 9.8 + \eta_m - \eta_c(\text{dB})$. η_m is the system design margin and η_c is the coding gain.

Equipped with mutual information accumulation, if SU i is allocated the time-bandwidth product A_i sec-Hz for transmission, the potential information flow from SU i to SU k can be expressed as $A_i C_{ik}$ bits. Assume that SUs are designed to use perfect rateless codes at all desired rates and that a receiver can combine information flows from two or more transmitters. If, for example, a pair of transmitting nodes, SU i and SU j, are allocated time-bandwidth products of A_i and A_j, respectively, our assumption means that SU k can decode the message as long as its mutual information accumulated exceeds the entropy, i.e.,

$$A_i C_{ik} + A_j C_{jk} \geq B.$$

Note that it is impossible to generate rateless codes that are perfect simultaneously at all possible rates. However, in practice, the overhead of rateless codes like fountain codes is bounded and not too large compared to perfect codes. Including an overhead factor $1+\varepsilon, \varepsilon > 0$, our computations can be achieved trivially by replacing B with $(1+\varepsilon)B$ [14] [70].

2.2.2 General Characteristics of the optimal route

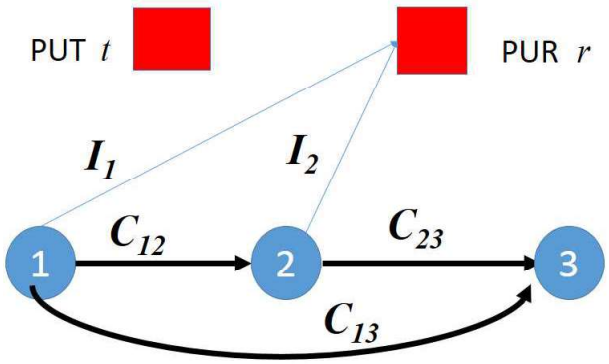

Figure 2.4: A simple three-node SU network

Let's first consider a basic three-node SU network shown in Fig. 2.4. Assume that node 1

and node 2 have already successfully decoded the codeword and both of these two nodes have a certain amount of energy that can support the following data transmission for a while. Node 3 still need to receive B_0 bits of mutual information before successfully decoding the codeword. The interference power spectral density of node 1 and node 2 to the PU receiver are denoted as $I_1 \triangleq h_{1r}P_1$ and $I_2 \triangleq h_{2r}P_2$, respectively. The link capacity among node 1, node 2, and node 3 are denoted as C_{12}, C_{13} and C_{23}. The interference power threshold set by the PU receiver is I_T and the total bandwidth is normalized to $W_T = 1$. Let θ_1 and θ_2 be the spectrum bandwidth allocated to node 1 and node 2, respectively. To decrease the transmission delay of node 3 is equivalent to maximize the sum of link capacity from both node 1 and node 2 to node 3, i.e.,

$$\begin{aligned} \arg\max_{\theta_1,\theta_2} \quad & \theta_1 C_{13} + \theta_2 C_{23} \\ s.t. \quad & \theta_1 + \theta_2 \leq 1, \\ & \theta_1 I_1 + \theta_2 I_2 \leq I_T, \\ & 0 \leq \theta_1, \theta_2 \leq 1. \end{aligned}$$

Note that here the sum-energy constraint is neglected since the route minimizes the end-to-end delay also minimizes the sum-energy [16]. The solution to the above linear programming problem is summarized in the following,

$$(\theta_1^*, \theta_2^*) = \begin{cases} (1,0), & \text{if } I_1 \leq I_T, C_{23} \leq C_{13}; \\ (0,1), & \text{if } I_2 \leq I_T, C_{23} \geq C_{13}; \\ \left(0, \frac{I_T}{I_2}\right), & \text{if } I_2 \geq I_T, C_{23} \geq \frac{I_2 C_{13}}{I_1}, I_1 \neq I_2; \\ \left(\frac{I_T}{I_1}, 0\right), & \text{if } I_1 \geq I_T, C_{23} \leq \frac{I_2 C_{13}}{I_1}, I_1 \neq I_2; \\ \left(\frac{I_T - I_2}{I_1 - I_2}, \frac{I_1 - I_T}{I_1 - I_2}\right), & \text{if } I_1 > I_T, I_2 < I_T, \text{and } C_{13} > C_{23} > \frac{I_2 C_{13}}{I_1}; \\ \left(\frac{I_2 - I_T}{I_2 - I_1}, \frac{I_T - I_1}{I_2 - I_1}\right), & \text{if } I_1 < I_T, I_2 > I_T, \text{and } C_{13} < C_{23} < \frac{I_2 C_{13}}{I_1}. \end{cases} \tag{2.6}$$

It is proven in [11] that the delay-optimal cooperative route for a wireless network is to let just one node to transmit within any time slot. However, this is not true in underlay cognitive radio net-

works. The delay-optimal cooperative route for underlay cognitive radio networks depends on both the interference conditions and the link capacity conditions. That is, under some interference and link capacity conditions, both node 1 and node 2 have the opportunity to participate in the transmission simultaneously. To be specific, the fifth and sixth items in (2.6) indicate that it is possible for node 1 and node 2 to conduct concurrent transmission and share the spectrum orthogonally in a time slot. Furthermore, we observe that if two nodes transmit concurrently in a time slot, one of the node's interference power spectral density has to be bigger than I_T while the other node's interference power spectral density has to be smaller than I_T. This observation is summarized into the following Lemma.

Lemma 1 *If two nodes, say node* 1 *and node* 2*, transmit concurrently in a time slot, then either* $I_1 > I_T, I_2 < I_T$ *or* $I_1 < I_T, I_2 > I_T$ *holds; and the total interference power spectral density to the PU receiver is* I_T.

Proof 1 *Node* 1 *and node* 2 *transmitting concurrently means that the bandwidth allocated to them (*θ_1 *and* θ_2*) are not zero. That is, the solution to maximize the sum of link capacity is either the fifth or the sixth item of* (2.6)*. This indicates either* $I_1 > I_T, I_2 < I_T$ *or* $I_1 < I_T, I_2 > I_T$*. Under this condition, the total interference power to the PU receiver is*

$$\frac{I_T - I_2}{I_1 - I_2} \times I_1 + \frac{I_1 - I_T}{I_1 - I_2} \times I_2 = I_T \quad or \quad \frac{I_2 - I_T}{I_2 - I_1} \times I_1 + \frac{I_T - I_1}{I_2 - I_1} \times I_2 = I_T.$$

Note that the delay-optimal route for a conventional wireless network can be found by letting $I_T \to \infty$. Under this situation, the solution becomes the first two terms of (2.6) which coincides with the intuition obtained in [11].

The analysis on the three-node SU network tells us the following intuition: after node 2 decodes the packet, it will take over the transmission and inform node 1 to stop transmitting if $\theta_1 = 0$; else if $\theta_1 > 0, \theta_2 > 0$, node 2 and node 1 will conduct concurrent transmission with bandwidth of θ_2 and θ_1, respectively; otherwise, node 2 will keep silent and node 1 will continue transmitting. However, equation (2.6) is just the optimal result for a three-node network. How should this result

be generalized and extended to a multi-node network and how can a new node make a decision on whether it should participate in the transmission after it decodes the data packet? We solve this problem by introducing the concept of *virtual node*. If there are two nodes, say node 1 and node 2, doing concurrent transmission at the same slot, these two nodes combined can be regarded as a virtual node $\hat{2}$. To be specific, by Lemma 1, the equivalent interference of this virtual node to the PU receiver is I_T and by equation (2.6) the equivalent link capacity between this virtual node and the destination can be expressed as $C_{\hat{2}N}$,

$$C_{\hat{2}N} = \theta C_{1N} + (1-\theta)C_{2N},$$

where, θ is the bandwidth allocation factor within the virtual node and can be expressed as

$$\theta = \begin{cases} \frac{I_T - I_2}{I_1 - I_2}, & \text{if } I_1 > I_T, I_2 < I_T; \\ \frac{I_2 - I_T}{I_2 - I_1}, & \text{if } I_1 < I_T, I_2 > I_T. \end{cases}$$

After introducing the concept of virtual node, if a new node which has decoded the message finds out that there are two nodes transmitting concurrently in the slot, this new node will make routing and resources allocation decision again by (2.6) where it should substitute its local information and the information of the virtual node. We have the following lemma for the routing and resource allocation for the new node.

Lemma 2 *If a node decodes the packet and finds out that a virtual node is transmitting in the network, this node will not transmit concurrently with the virtual node.*

Proof 2 *Lemma 1 tells us that the equivalent interference power spectral density of the virtual node to the PU receiver is I_T. Therefore, the routing and resources allocation result for the virtual node and the new decoding node belongs to the first four items in equation* (2.6)*, i.e., this virtual node will not transmit concurrently with the new decoding node.*

Lemma 2 indicates that, during a transmission slot Δ_i, there are at most two nodes transmitting concurrently in a slot. This result is summarized and proved in the following theorem.

Theorem 1 *For the underlay cognitive radio network of our interests, within a transmission slot, there are at most two SUs sharing PU's spectrum and transmitting concurrently.*

Proof 3 *We prove this theorem using the fundamental theorem of linear programming [71]. Assume there have been N nodes already decoded the message. Our goal is to find the best combination of transmitting nodes in the next slot to maximize the total throughput from these nodes, denoted as $i = 1, ..., N-1$, to the destination N. This problem can be summarized to the following linear programming problem:*

$$\max_{\theta_i} \sum_{i=1}^{N} \theta_i C_{i,N} \quad s.t. \begin{cases} \sum_{i=1}^{N} \theta_i \leq 1, \\ \sum_{i=1}^{N} \theta_i I_i \leq I_T, \\ 0 \leq \theta_i \leq 1, i = 1, 2, ..., N. \end{cases} \tag{2.7}$$

If the optimal feasible solution to the above optimization problem is $\theta_i = 1, i \in \{1, 2, ..., N\}$, this theorem holds since there is only one node transmitting. Otherwise, if $\theta_i < 1$, for all nodes, then there are only two active constraints in the standard format of linear programming problem. Therefore, there are at most two non-zero items, i.e., at most two non-zero θ_i, in the optimal basic feasible solution since the rank of the basis of the linear programming is at most 2.

The above theorem shows that there will be at most two nodes that share one transmission slot and therefore the cooperative routing and resources allocation over-head is limited. In the more general case where there are multiple primary receivers in the network, we can obtain the following corollary:

Corollary 1 *For the underlay cognitive radio network with M primary pairs, within a transmission slot, there are at most $M+1$ SUs sharing PU's spectrum and transmitting concurrently.*

The following theorem shows that under certain conditions, the distributed resource allocation algorithm can obtain optimal performance on end-to-end delay.

Theorem 2 *Assume a transmission order* $[1,2,\ldots,L]$ *has the property that the spectral efficiency from each node to the destination increases w.r.t. i, i.e.,* $C_{iN} \leq C_{(i+1)N}, 1 \leq i \leq N-1$. *If the path meets either the following two conditions:*

1) $I_i \geq I_{i+1}, 1 \leq i \leq N-1$*;*

2) $I_i < I_{i+1}, 1 \leq i \leq N-1$*, while* $C_{iN}/I_i \leq C_{(i+1)N}/I_{i+1}, 1 \leq i \leq N-1$*,*

then the optimal routing and resources allocation strategy for this path is in the following: assume current transmitting node is node $i, 1 \leq i \leq N-2$*, if node* $j, i < j \leq N-1$ *decodes the packet, then node* j *will take over the transmission and node i will stop transmitting. The spectrum bandwidth for node* j *is* $1_{(I_j \leq I_T)} + I_T/I_j \cdot 1_{(I_j > I_T)}$*, where* $1_{(I_j > I_T)}$ *is the indicator function. Here the optimality means to minimize the transmission delay or equivalently to maximize the equivalent link capacity to the destination.*

Proof 4 *We first prove condition 1). Assume node* $i, 1 \leq i \leq N-2$ *is transmitting and node* $j, i < j \leq N-1$ *first decodes the packet. If* $I_j \leq I_T$*, since* $C_{jN} \geq C_{iN}$*, all the spectrum bandwidth, i.e.* $W_T = 1$*, should be assigned to node* j *by the second item in equation* (2.6)*. The spectrum resource for node i is* 0*, therefore, node i will stop transmitting. If* $I_j > I_T$*, since* $I_j < I_i$*, we can get* $C_{iN}/I_i \leq C_{jN}/I_j$*. Then* I_T/I_j *part of spectrum should be assigned to node* j *in order to maximize SU's throughput by the third item in equation* (2.6)*. The spectrum resource for node i is* 0*, therefore, node i will also stop transmitting. Therefore, we can conclude that as long as node* j *decodes the packet successfully, it will take over the transmission with bandwidth* $1_{(I_j \leq I_T)} + I_T/I_j \cdot 1_{(I_j > I_T)}$*. This ends the proof of condition 1). The proof of condition 2) is very similar to that of condition 1), therefore it can be omitted.*

2.2.3 One-dimensional underlay cognitive radio network

In this section, we analytically characterize the cooperative gain for a one-dimension underlay cognitive radio network using mutual information accumulation. The network topology is shown in the following Fig. 2.5. $N+1$ SU nodes are deployed equally in a line from $(0,0)$ to $(D,0)$. The PU transmitter (PUT) is located at $(0,d_1)$ and the PU receiver (PUR) is located at $(1,d_1)$. The path

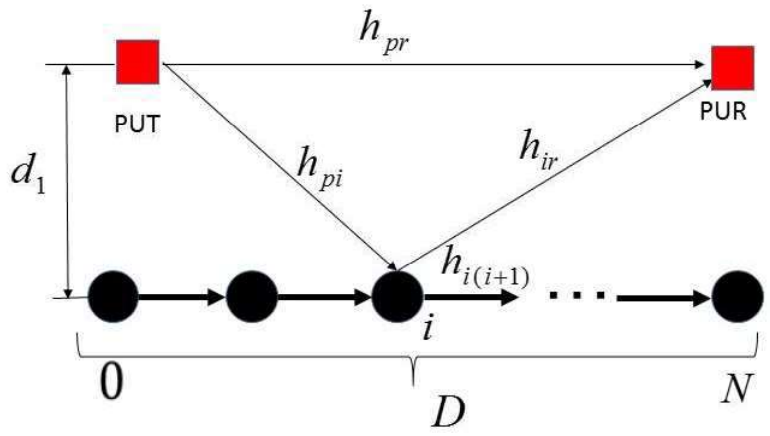

Figure 2.5: one-dimensional special case in underlay cognitive radio networks

loss exponential is $\alpha = 2$. We assume the noise at the SU receivers (SUR) can be ignored compared to the interference from PUT and all SUs transmit at the same fixed power P_s. The channel power gain between each pair of two nodes are proportional to the distance $d^{-\alpha}$. Denote the SU source node as node 0 and the destination as node N. In the low signal-to-interference ratio (SIR) regime, i.e., P_s is very small, the spectral efficiency of the channel between node i and the destination node N can be expressed as,

$$C_{iN} = \log_2\left(1 + \frac{P_s\left(D - iD/N\right)^{-2}}{P_p\left(d_1^2 + D^2\right)^{-1}\Gamma}\right) \approx \frac{P_s\left(d_1^2 + D^2\right)}{P_p(D - iD/N)^2\Gamma}.$$

Obviously, as the node index increases, the corresponding spectral efficiency to the destination increases. Node i's interference power spectral density to PUR can be expressed as

$$I_i = P_s\left(d_1^2 + (D - iD/N)^2\right)^{-1},$$

which is also increasing as the node index increases. The ratio between spectral efficiency and interference spectral density can be expressed as

$$\frac{C_{iN}}{I_i} = \frac{d_1^2 + D^2}{P_p\Gamma}\left(1 + \frac{d_1^2}{(D - iD/N)^2}\right).$$

As i increases, C_{iN}/I_i also increases. By Theorem 2, this indicates that in this 1-D cognitive radio network, as long as node i decodes the information, it will take over the transmission from the previous transmitting node. Accordingly, the optimal routing and resources allocation strategies are similar to those for conventional wireless networks described in [16], i.e., the data packet is transmitted one-by-one and in each transmission order, the whole available spectral bandwidth will be allocated to the current transmitting node. The overall delay can be computed by solving $A_{01}C_{01} = B, A_{12}C_{12} + A_{01}C_{02} = B$ or in general

$$\sum_{i=0}^{k-1} A_{i(i+1)}C_{ik} = B,$$

for each $k, 1 \leq k \leq N$, which we can write as

$$\begin{pmatrix} C_{01} & 0 & \cdots & 0 \\ C_{02} & C_{12} & \ddots & 0 \\ \vdots & \vdots & \ddots & 0 \\ C_{0N} & C_{1N} & \cdots & C_{(N-1)N} \end{pmatrix} \begin{bmatrix} A_{01} \\ A_{12} \\ \vdots \\ A_{(N-1)N} \end{bmatrix} = B\mathbf{1}, \tag{2.8}$$

where $\mathbf{1} = [1, 1, \ldots, 1]^T$ and the available spectrum means the SU will be assigned the bandwidth to guarantee that the total interference at the PUR is less than I_T. Therefore, there are three different cases based on different interference conditions:

The first case is $I_0, I_1, I_2, \ldots, I_{N-1} \geq I_T$. In this case, for each node i, the available spectrum bandwidth is I_T/I_i. The delay of cooperative routing using mutual information accumulation can be expressed as

$$\tau_C = \sum_{i=1}^{N} \Delta_i = \sum_{i=1}^{N} A_{(i-1)i}I_{i-1}/I_T = \frac{B}{I_T}\mathscr{I}^T\mathscr{K}^{-1}\mathbf{1},$$

where $\mathscr{K}^{-1}$ is the inverse of the spectrum efficiency matrix shown in (2.8) and $\mathscr{I} = [I_0, I_1, \ldots, I_{N-1}]^T$. Since P_s is small, the multi-hop route crossing every node one-by-one is delay optimal both for the

cooperative routing with mutual information accumulation and traditional multi-hop delay-optimal routing. The optimal delay of traditional multi-hop routing can be expressed as

$$\tau_{NC} = \frac{B}{I_T} \sum_{i=0}^{N-1} \frac{I_i}{C_{i(i+1)}}. \tag{2.9}$$

The second case is $I_0, I_1, I_2, \ldots, I_{N-1} \leq I_T$. In this case, each node can fully use its spectrum and the cooperative delay is the same as that in [16],

$$\tau_C = B\mathbf{1}^T \mathscr{K}^{-1}\mathbf{1}. \tag{2.10}$$

The third case is that there exists a node M which meets that $I_i \leq I_T, i \leq M$ and $I_i > I_T, i > M$, i.e., $M = \{M : I_M \leq I_T, I_{M+1} > I_T\}$. In this case, the optimal end-to-end delay of traditional multi-hop routing can be divided into two parts: the first part is the delay from node 1 to node M. Since node 1 to node M's interference is less than or equal to I_T, this part of nodes can use the full spectrum; the second part is the delay from node $M+1$ to node N. Since these nodes' interference is larger than I_T, this part of nodes can only use $I_T/I_i, M < i \leq N-1$ part of the full spectrum, i.e.,

$$\tau_{NC} = \sum_{i=0}^{M} \frac{B}{C_{i(i+1)}} + \sum_{i=M+1}^{N-1} \frac{BI_i}{I_T C_{i(i+1)}}. \tag{2.11}$$

Accordingly, the delay obtained by cooperative routing using mutual information accumulation can be expressed as,

$$\tau_C = B\widehat{\mathscr{I}_{\mathscr{M}}}\mathscr{K}^{-1}\mathbf{1}, \tag{2.12}$$

where $\widehat{\mathscr{I}_{\mathscr{M}}} = [1,1,\ldots,1,I_{M+1}/I_T,\ldots,I_{N-1}/I_T]$. Therefore, the cooperative gain can be summarized as,

$$G_c = \frac{\tau_{NC}}{\tau_C} = \begin{cases} \frac{\Sigma_{i=0}^{N-1} \frac{I_i}{C_{i(i+1)}}}{\mathscr{I}^T \mathscr{K}^{-1}\mathbf{1}}, & I_0 \geq I_T; \\ \frac{\Sigma_{i=0}^{N-1} \frac{1}{C_{i(i+1)}}}{\mathbf{1}^T \mathscr{K}^{-1}\mathbf{1}}, & I_{N-1} \leq I_T; \\ \frac{\Sigma_{i=0}^{M} \frac{1}{C_{i(i+1)}} + \Sigma_{i=M+1}^{N-1} \frac{I_i}{I_T C_{i(i+1)}}}{\widehat{\mathscr{I}_{\mathscr{M}}}^T \mathscr{K}^{-1}\mathbf{1}}, & I_M \leq I_T, I_{M+1} > I_T. \end{cases} \tag{2.13}$$

Note that from (2.13) we can find the cooperative gain in underlay cognitive radio network is quite different from the result in traditional ad hoc network as discussed in [16]. Specifically, the cooperative gain of traditional ad hoc network can be regarded as a special case of underlay cognitive radio network when I_T is sufficiently large. Furthermore, in the special case of mutual information accumulation, i.e., each node can only accumulate information from its previous transmit node, the spectral efficiency matrix will be $\mathscr{K} = diag\{C_{01}, C_{12}, \cdots, C_{(N-1)N}\}$. Then the cooperative gain in underlay cognitive radio network will be 1. That is, the hop-by-hop transmission in traditional ad hoc network can also be regarded as a special case of networks with mutual information accumulation where each node can only accumulate information from its previous transmitting node.

2.2.4 Evaluation Results

Fig. 2.6 shows both the simulation and theoretical results on the cooperative gain as a function of PUR's interference power threshold I_T in the 1-D cognitive radio network which is shown in Fig. 2.5. The simulation parameters are in the followings. The PUT is placed at $[0, 0.8]$, and the PUR is located at $[1, 0.8]$. The SU source is fixed at $[0, 0.5]$ and the SU destination is fixed at $[1, 0.5]$. Other parameters include $W_T = 1$ Hz, $E_T = 20$ Joule, $N_0 = 0$ W/Hz, $P_p = 1$ W/Hz, $\alpha = 2$ and $B = 3$bits. There are 20 SU nodes equally deployed in the 1-D network. From Fig. 2.6, we can see that the theoretical results match very well with the simulation results. This verifies our simulation codes as well as our theoretical analysis. Furthermore, it is important to note that the cooperative gain is much higher when PU's interference constraint is tight. That is, as the

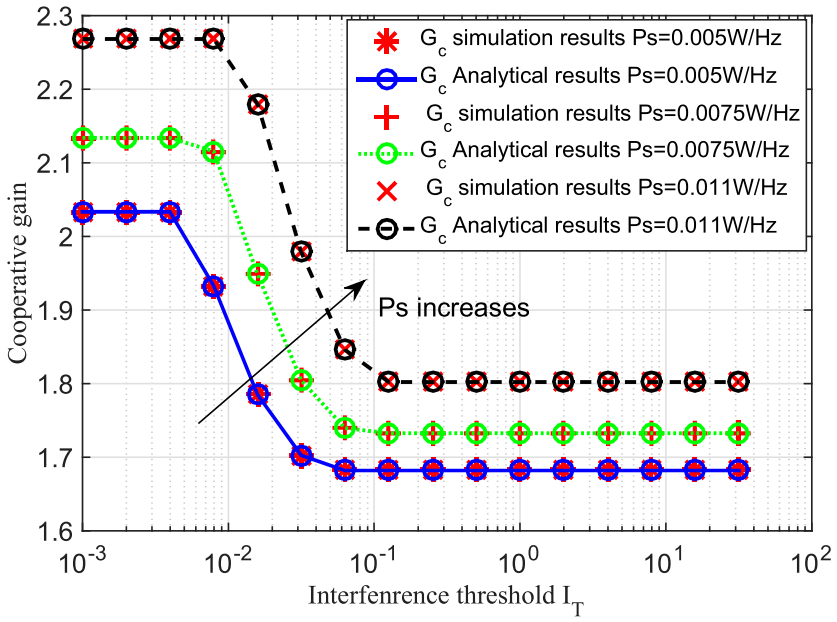

Figure 2.6: Simulation and theoretical results on cooperative gain as a function of I_T

interference power threshold decreases, the cooperative gain will increase. This result suggests that in underlay cognitive radio networks, using mutual information accumulation will bring significant benefits especially in the case where PUs have tight interference power constraint. Finally, it is shown in Fig. 2.6 that as P_s increases, the cooperative gain increases. It is clear that when P_s increases, the end-to-end delay of both shortest path and mutual information accumulation routing will decrease. However, the decrease speed of mutual information accumulation routing is much faster than that of shortest path routing. This is because for any transmission slot all nodes can benefit from the increase of P_s in mutual information accumulation routing as opposed to only one node can benefit from the increase of P_s in the traditional multi-hop routing.

2.3 Analysis on MIA in Random Networks

It has been shown in [72] that mutual information accumulation can significantly reduce end-to-end delay in a multi-hop wireless network. However, theoretical results on the performance of mutual information accumulation with interference from random networks still remain unknown.

In this section, we theoretically analyze the performance of mutual information accumulation in random networks using tools from stochastic geometry. To be specific, we first model the various network topologies as a Poisson point process. Then we analyze the coverage probability of the two-hop network under retransmission, energy accumulation and mutual information accumulation strategies at the receiver side. Finally, simulations results and numerical results are presented to verify the correctly of our analysis and provide system design guidance.

2.3.1 Problem Statement

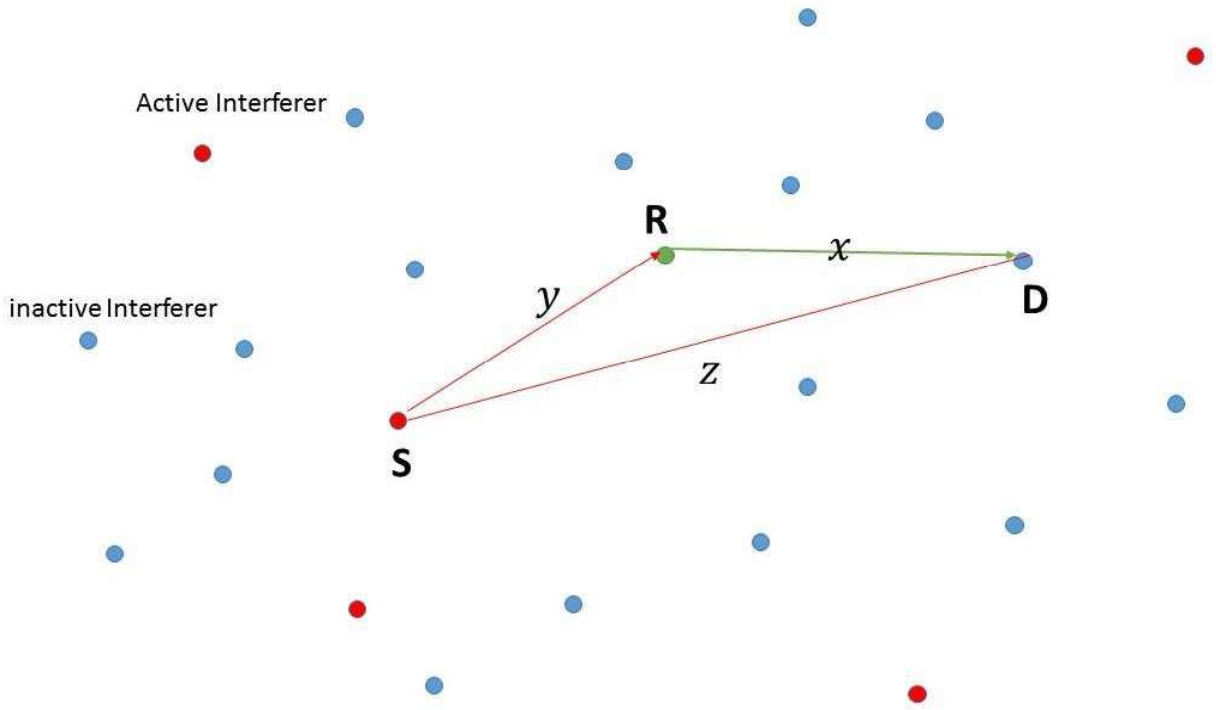

Figure 2.7: System model for MIA in random networks

Consider a two-hop network with source node S, relay node R and destination node D. The distance of the source-relay link, source-destination link and relay-destination link are denoted as y, z and x, respectively. Other nodes in the network are modeled as a Poisson Point process(PPP) Φ with a intensity of λ as shown in Fig 2.7. All other nodes will randomly access a common band of spectrum using slotted ALOHA protocol with access probability of p. Therefore, for any time-slot

i, the locations of interference nodes in this network can be modeled as a PPP $\Phi_{a,i}$ with intensity of $\lambda_a = p\lambda$. The destination or relay can successfully decode packets if its received signal-to-interference-ratio(SIR) is greater than a threshold T or accordingly its spectral efficiency is greater than $C_0 = \log(1+T)$. Here we assume the system works in interference limited regime and the noise power is omitted to simplify our analysis. Extension to including the analysis of noise power is straight forward and is omitted here. Channels of the link is modeled as a combination of the power-law path loss and Rayleigh block fading. Assume all nodes in the network transmit with the same power P, the received power at the receiver side can be expressed as $P_r = PG_{s,d,i}x^{-\alpha}$, where $G_{s,d,i} \sim \exp(1)$ is the small scale fading gain between the link from node s to node d in time slot i and $\alpha > 2$ is the path loss exponent. The small scaling fading between different link in the same time slot and between the same link in different time slots are assumed to be i.i.d. If the relay node can decode the packet in the first slot while the destination node fails to decode the packet, the relay node will retransmit the packet or the re-encoded packet to the destination. The destination can try to decode the retransmitted packet directly, named in the following as retransmission strategy. Or the destination node can try to combine the packet received in the first time slot and the packet received in the second time slot using maximum ratio combination (MRC), named in the following as MRC or energy accumulation (EA). Or the destination can combine the packet in the first time slot and the packet received in the second time slot as a long code-word and decode the packets using mutual information accumulation, named in the following as MIA strategy. In the following, we will theoretically analyze and compare the performance of retransmission, MRC and MIA using tools from stochastic geometry.

2.3.2 Performance Analysis on Retransmission, EA and MIA

We first analyze the coverage probability of the transmission in the first slot. Denote $I_{d,1}$ and $SIR_{s,d,1}$ as the interference and SIR received at the destination in the first time slot. The received

SIR can be expressed as

$$SIR_{s,d,1} = \frac{P_r}{I_{d,1}} = \frac{PG_{s,d,1}z^{-\alpha}}{\sum_{\mathbf{x}\in\Phi_{a,1}} PG_{\mathbf{x},d,1}\|\mathbf{x}-D\|^{-\alpha}}. \tag{2.14}$$

The coverage probability is defined as $P_1 = \mathbb{P}(SIR_{s,d,1} > T)$. Note that the probability here should consider the randomness from small scale fading, random access and network topologies. The randomness of network topologies is modeled as Poisson point process and the interference from nodes in different locations can be characterized by tools from stochastic geometry. To be specific, the coverage probability in the first time slot can be calculated in the following steps. Similar procedures can be found in the book [8]. We present details of the calculation here to show how we deal with different randomness using tools from stochastic geometry.

$$\begin{aligned}
P_1 &= \mathbb{P}(SIR_{s,d,1} > T) \\
&\overset{a}{=} \mathbb{E}_{\Phi,\{G_{\mathbf{x},d,1}\},Aloha}\left[\exp(-TI_{d,1}/Pz^{\alpha})\right] \\
&= \mathbb{E}_{\Phi,\{G_{\mathbf{x},d,1}\},Aloha}\left[\Pi_{\mathbf{x}\in\Phi}\exp(-TG_{\mathbf{x},d,1}\|\mathbf{x}-D\|^{-\alpha}z^{\alpha})\right] \\
&\overset{b}{=} \mathbb{E}_{\Phi}\left[\Pi_{\mathbf{x}\in\Phi}\left(1-p+\frac{p}{1+Tz^{\alpha}\|\mathbf{x}-D\|^{-\alpha}}\right)\right] \\
&\overset{c}{=} \exp\left(-\lambda p\int_{\mathbb{R}^2} 1-\frac{1}{1+Tz^{\alpha}\|\mathbf{x}-D\|^{-\alpha}}d\mathbf{x}\right) \\
&= \exp\left(-2\pi\lambda p/\alpha z^2 T^{2/\alpha}B(1-2/\alpha,2/\alpha)\right) \\
&= \exp(-c_1\lambda p z^2 T^{2/\alpha}),
\end{aligned} \tag{2.15}$$

where $\overset{a}{=}$ comes from averaging over the small scale fading $G_{s,d,1}$; $\overset{b}{=}$ comes from averaging over the access policy of slotted ALOHA and small scale fading of $G_{\mathbf{x},d,1}$; $\overset{c}{=}$ comes from the probability generating functional (PGFL) [8]; $B(x,y)$ is the Beta function; $c_1 = 2\pi/\alpha B(1-2/\alpha,2/\alpha)$ is a constant only related to the path loss exponent. Equation (2.15) characterizes the one-hop coverage probability of the random network by taking account of small scale fading, random access and random topologies. Network optimization can be conducted based on this equation to further optimize the network performance by adjusting the related parameters.

In the following, we analyze the coverage probability under retransmission. If the relay node can decode the packet in the first slot, then the relay node can forward the packet to the destination in the second slot. The successful decoding condition after two-slot transmission includes two events: 1) the destination can decode the packet in the first slot; 2) the destination fails to the decode the packet in the first slot while the relay decodes the packet in the first slot, the destination decodes the packet from the relay in the second time slot. Note that in the first time slot the interference is from Poisson field of $\Phi_{a,1}$ and in the second slot the interference is from Poisson field of $\Phi_{a,2}$. Mathematically, the coverage probability can be expressed as

$$P^{Re} = \mathbb{P}(SIR_{s,d,1} < T, SIR_{s,r,1} > T, SIR_{r,d,2} > T) + \mathbb{P}(SIR_{s,d,1} > T). \tag{2.16}$$

As each nodes in the network will access the spectrum with a probability of p independently, $\Phi_{a,1}$ and $\Phi_{a,2}$ are not independent. Therefore, we cannot split the analysis into two time slots. Instead the coverage probability in two time slots has to be considered jointly. Furthermore, the interference at the relay node and the interference at the destination node are also correlated. The closer the relay node to the destination node, the stronger the correlation between the interference at the relay node and the interference at the destination node. These phenomenon are called the spatio-temporally correlated interference which makes the analysis of two-hop networks challenging and complex. The coverage probability under retransmission strategy is summarized in the following Lemma.

Lemma 3 *Under retransmission strategy, the coverage probability of a two-hop network in a Poisson field of interference can be expressed as*

$$P^{Re} = P_1 + \exp\left(-\lambda \int_{\mathbb{R}^2} 1 - \left(1 - p + \frac{p}{1 + \|\boldsymbol{x} - \boldsymbol{R}\|^{-\alpha} T y^{\alpha}}\right)\left(1 - p + \frac{p}{1 + \|\boldsymbol{x} - \boldsymbol{D}\|^{-\alpha} T x^{\alpha}}\right) d\boldsymbol{x}\right)$$
$$- e^{-\lambda \int_{\mathbb{R}^2} 1 - \left(1 - p + \frac{p}{(1 + \|\boldsymbol{x} - \boldsymbol{R}\|^{-\alpha} T y^{\alpha})(1 + \|\boldsymbol{x} - \boldsymbol{D}\|^{-\alpha} T z^{\alpha})}\right)\left(1 - p + \frac{p}{1 + \|\boldsymbol{x} - \boldsymbol{D}\|^{-\alpha} T x^{\alpha}}\right) d\boldsymbol{x}}. \tag{2.17}$$

Proof 5 *See Appendix A.1 for details.*

Lemma 3 captures the coverage probability under retransmission strategy. Note that, the coverage probability is averaged over various network topologies. The expression of the coverage probability is complex as there is a two-dimensional integration inside the exponent function.

Similar to the retransmission strategy, energy accumulation (EA) strategy allows the relay to retransmit the same packet to the destination if the relay can decode the packet in the first time slot. If the receiver of the destination can do MRC, then the actual SIR at the destination after the second slot can be expressed as $SIR_{s,d,1} + SIR_{r,d,2}$. Therefore, compared to retransmission strategy, MRC or energy accumulation can achieve better coverage probability. Mathematically, the coverage probability of energy accumulation can be expressed as

$$P^{EA} = \mathbb{P}(SIR_{s,d,1} < T, SIR_{s,r,1} > T, SIR_{r,d,2} + SIR_{s,d,1} > T) + \mathbb{P}(SIR_{s,d,1} > T). \tag{2.18}$$

Compared to the analysis of retransmission, calculation of the coverage probability of energy accumulation strategy is more challenging as it is related to the sum of two random variables. The main idea to attack this challenge is to analyze the coverage probability under a given topology or a given realization ϕ of the Poisson point process Φ. Under a given topology, we can first analyze the coverage probability under a fixed $SIR_{r,d,2}$ and then average the coverage probability over the distribution of $SIR_{r,d,2}$. Note that here the distribution of $SIR_{r,d,2}$ is the distribution under a fixed topology, which is quite complex than the distribution of $SIR_{r,d,2}$ under Poisson point process. The theoretical result of coverage probability is summarized in the following Lemma and the detailed proof can be found the Appendix.

Lemma 4 *Under energy accumulation strategy, the coverage probability of a two-hop network in*

a Poisson field of interference can be expressed as

$$P^{EA} = P_1 + \int_0^{\infty} \int_{\mathbb{R}^2} \frac{p\lambda \|\boldsymbol{x}\text{-}\boldsymbol{D}\|^{-\alpha} x^{\alpha}}{(1+\|\boldsymbol{x}\text{-}\boldsymbol{D}\|^{-\alpha} x^{\alpha}\omega)^2} \left(1 - p + p\frac{1}{1+(T-\omega)^{+} z^{\alpha}\|\boldsymbol{x}\text{-}\boldsymbol{D}\|^{-\alpha}} \frac{1}{1+\|\boldsymbol{x}\text{-}\boldsymbol{R}\|^{-\alpha} T y^{\alpha}}\right) d\boldsymbol{x}$$
$$\cdot e^{-\lambda \int_{\mathbb{R}^2} 1-\left(1-p+\frac{p}{1+\|\boldsymbol{y}\text{-}\boldsymbol{D}\|^{-\alpha} x^{\alpha}\omega}\right)\left(1-p+p\frac{1}{1+(T-\omega)^{+} z^{\alpha}\|\boldsymbol{y}\text{-}\boldsymbol{D}\|^{-\alpha}} \frac{1}{1+\|\boldsymbol{y}\text{-}\boldsymbol{R}\|^{-\alpha} T y^{\alpha}}\right) dy} d\omega$$
$$- e^{-\lambda p \int_{\mathbb{R}^2} 1-\frac{1}{1+\|\boldsymbol{x}\text{-}\boldsymbol{D}\|^{-\alpha} T z^{\alpha}} \frac{1}{1+\|\boldsymbol{x}\text{-}\boldsymbol{R}\|^{-\alpha} T y^{\alpha}} d\boldsymbol{x}}. \tag{2.19}$$

Proof 6 *See Appendix A.2 for details.*

If the relay can decode the packet in the first time slot, the relay can re-encode the packet and forward the re-encoded packet to the destination. The destination can accumulate the mutual information of this packet by treating the two received information bits as a long code-word. The successful decoding condition under mutual information accumulation now becomes that as long as the mutual information accumulated at the destination is larger than a threshold, the destination can decode the packet. Compared to energy accumulation strategy, mutual information accumulation can further improve the performance. The coverage probability under the mutual information accumulation strategy can be expressed as

$$P^{MIA} = \mathbb{P}(SIR_{s,d,1} < T, SIR_{s,r,1} > T, \log(1+SIR_{r,d,2}) + \log(1+SIR_{s,d,1}) > \log(1+T)) + \mathbb{P}(SIR_{s,d,1} > T). \tag{2.20}$$

Using the same analysis technique, the coverage probability under the mutual information accumulation can be derived and is summarized in the following Lemma.

Lemma 5 *Under mutual information accumulation strategy, the coverage probability of a two-hop*

network in a Poisson field of interference can be expressed as

$$P^{MIA} = P_1 + \int_0^{\infty} \int_{\mathbb{R}^2} \frac{\lambda p \|\boldsymbol{x}\text{-}\boldsymbol{D}\|^{-\alpha} x^{\alpha}}{(1+\|\boldsymbol{x}\text{-}\boldsymbol{D}\|^{-\alpha} x^{\alpha}\omega)^2} \left(1 - p + p \frac{1}{1+\frac{(T-\omega)^+ z^{\alpha} \|\boldsymbol{x}\text{-}\boldsymbol{D}\|^{-\alpha}}{1+\omega}} \frac{1}{1+\|\boldsymbol{x}\text{-}\boldsymbol{R}\|^{-\alpha} T y^{\alpha}}\right) d\boldsymbol{x}$$
$$\cdot e^{-\lambda \int_{\mathbb{R}^2} 1-\left(1-p+\frac{p}{1+\|\boldsymbol{y}\text{-}\boldsymbol{D}\|^{-\alpha} x^{\alpha}\omega}\right)\left(1-p+p\frac{1}{1+\frac{(T-\omega)^+ z^{\alpha}\|\boldsymbol{y}\text{-}\boldsymbol{D}\|^{-\alpha}}{1+\omega}} \frac{1}{1+\|\boldsymbol{y}\text{-}\boldsymbol{R}\|^{-\alpha} T y^{\alpha}}\right) d\boldsymbol{y}} d\omega$$
$$- e^{-\lambda p \int_{\mathbb{R}^2} 1-\frac{1}{1+\|\boldsymbol{x}\text{-}\boldsymbol{D}\|^{-\alpha} T z^{\alpha}} \frac{1}{1+\|\boldsymbol{x}\text{-}\boldsymbol{R}\|^{-\alpha} T y^{\alpha}} d\boldsymbol{x}}. \tag{2.21}$$

Proof 7 *See Appendix A.3 for details.*

Even though we obtained the coverage probability for retransmission strategy, energy accumulation strategy and mutual information accumulation strategy, the expression of the coverage probability is very complex. Especially, the expression of the coverage probability of mutual information accumulation. In the following, we are focusing on simplifying and approximating these expressions so that the relationship between the network parameters and network performance can be more intuitive.

2.3.3 Approximation and Simplification

In this subsection, we develop some tricks to approximate the simplify the coverage probability. The complex expression of coverage probability makes it difficult to get design intuition and optimize network performance. The direction of approximation is to reduce the number of integrations. One trick we can use is that for any $\mathbf{x}$, $\|\mathbf{x}-D\| \approx \|\mathbf{x}-R\| \approx \|\mathbf{x}-R/2-D/2\|$, i.e., the distance from $\mathbf{x}$ to D and from $\mathbf{x}$ to R can be approximated by the distance from $\mathbf{x}$ to the middle point of the segment from D to R as shown in Fig. 2.8. Note that this approximation is accurate only when $\mathbf{x}$ is far away compared to the distance from D to R. However, numerical results show that this approximation is still accurate when we do integration on $\mathbb{R}^2$. Under this approximation, the coverage

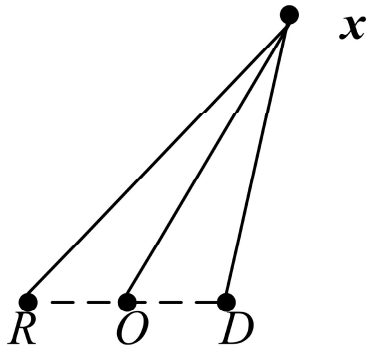

Figure 2.8: Illustration of the distance approximation

probability of retransmission can be simplified as

$$P^{Re} \approx P_1 + \exp\left(-\lambda \int_{\mathbb{R}^2} 1 - \left(1-p+\frac{p}{1+\|\mathbf{x}\|^{-\alpha}Ty^{\alpha}}\right)\left(1-p+\frac{p}{1+\|\mathbf{x}\|^{-\alpha}Tx^{\alpha}}\right) d\mathbf{x}\right) - e^{-\lambda \int_{\mathbb{R}^2} 1-\left(1-p+\frac{p}{(1+\|\mathbf{x}\|^{-\alpha}Ty^{\alpha})(1+\|\mathbf{x}\|^{-\alpha}Tz^{\alpha})}\right)\left(1-p+\frac{p}{1+\|\mathbf{x}\|^{-\alpha}Tx^{\alpha}}\right) d\mathbf{x}}. \tag{2.22}$$

By some mathematic simplifications, the following two-dimensional integrations can be expressed as followings:

$$\begin{aligned}
&\int_{\mathbb{R}^2} 1 - \left(1-p+\frac{p}{1+\|\mathbf{x}\|^{-\alpha}Ty^{\alpha}}\right)\left(1-p+\frac{p}{1+\|\mathbf{x}\|^{-\alpha}Tx^{\alpha}}\right) d\mathbf{x} \\
&= p(1-p)c_1T^{2/\alpha}(y^2+x^2) + p^2c_1T^{2/\alpha}\frac{x^{\alpha+2}-y^{\alpha+2}}{x^{\alpha}-y^{\alpha}}; \\
&\int_{\mathbb{R}^2} 1 - \left(1-p+\frac{p}{(1+\|\mathbf{x}\|^{-\alpha}Ty^{\alpha})(1+\|\mathbf{x}\|^{-\alpha}Tz^{\alpha})}\right)\left(1-p+\frac{p}{1+\|\mathbf{x}\|^{-\alpha}Tx^{\alpha}}\right) d\mathbf{x} \\
&= p(1-p)c_1T^{2/\alpha}x^2 + p(1-p)c_1T^{2/\alpha}\frac{y^{\alpha+2}-z^{\alpha+2}}{y^{\alpha}-z^{\alpha}} \\
&+ p^2c_1T^{2/\alpha}\frac{x^{2\alpha+2}(y^{\alpha}-z^{\alpha}) - y^{2\alpha+2}(x^{\alpha}-z^{\alpha}) + z^{2\alpha+2}(x^{\alpha}-y^{\alpha})}{(x^{\alpha}-y^{\alpha})(y^{\alpha}-z^{\alpha})(x^{\alpha}-z^{\alpha})},
\end{aligned} \tag{2.23}$$

where $c_1 = \frac{2\pi}{\alpha} B(1-\frac{2}{\alpha}, \frac{2}{\alpha})$. Therefore, the coverage probability under retransmission strategy can be simplified as

$$\begin{aligned} P^{Re} \approx\ & e^{-c_1\lambda p z^2 T^{2/\alpha}} + e^{-p(1-p)\lambda c_1 T^{2/\alpha}(y^2+x^2) - p^2\lambda c_1 T^{2/\alpha}\frac{x^{\alpha+2}-y^{\alpha+2}}{x^\alpha - y^\alpha}} \\ & - e^{-p(1-p)\lambda c_1 T^{2/\alpha} x^2 - p(1-p)\lambda c_1 T^{2/\alpha}\frac{y^{\alpha+2}-z^{\alpha+2}}{y^\alpha - z^\alpha} - p^2\lambda c_1 T^{2/\alpha}\frac{x^{2\alpha+2}(y^\alpha - z^\alpha) - y^{2\alpha+2}(x^\alpha - z^\alpha) + z^{2\alpha+2}(x^\alpha - y^\alpha)}{(x^\alpha - y^\alpha)(y^\alpha - z^\alpha)(x^\alpha - z^\alpha)}}. \end{aligned} \tag{2.24}$$

After approximation and simplification, the previous two-dimension integration is removed from the final expression. In the following, we are going to simplify the coverage probability of energy accumulation strategy. The result is summarized in the following Lemma and details can be found in the Appendix.

Lemma 6 *Under energy accumulation strategy, the coverage probability of a two-hop network in a Poisson field of interference can be approximated as*

$$\begin{aligned} P^{EA} \approx & \int_0^\infty \left(p\lambda c_3 x^2 \omega^{\frac{2}{\alpha}-1} - p^2\lambda x^\alpha c_2 h_0(a_0,b_0,c_0) \right) e^{-\lambda p(1-p)c_1 h_1(a_0,b_0,c_0) - \lambda p^2 c_1 h_2(a_0,b_0,c_0)} d\omega \\ & + e^{-c_1\lambda p z^2 T^{2/\alpha}} - e^{-\lambda p c_1 T^{2/\alpha}\frac{z^{\alpha+2}-y^{\alpha+2}}{z^\alpha - y^\alpha}}, \end{aligned} \tag{2.25}$$

where $a_0 \triangleq (T-\omega)^+ z^\alpha, b_0 \triangleq T y^\alpha, c_0 \triangleq x^\alpha \omega$, $h_0(a_0,b_0,c_0) \triangleq \frac{(a_0^2 {}_2F_1(1,2-\frac{2}{\alpha};3;1-a_0/c_0) - b_0^2 {}_2F_1(1,2-\frac{2}{\alpha};3;1-b_0/c_0))}{(a_0-b_0)c_0^{2-\frac{2}{\alpha}}}$; $c_1 = \frac{2\pi}{\alpha} B(1-\frac{2}{\alpha}, \frac{2}{\alpha})$; $c_2 \triangleq \frac{2\pi B(2-\frac{2}{\alpha}, 1+\frac{2}{\alpha})}{\alpha}$; $c_3 \triangleq \frac{2\pi B(1-\frac{2}{\alpha}, 1+\frac{2}{\alpha})}{\alpha}$; $h_1(a_0,b_0,c_0) \triangleq c_0^{2/\alpha} + \frac{b_0^{1+\frac{2}{\alpha}}}{b_0-a_0} + \frac{a_0^{1+\frac{2}{\alpha}}}{a_0-b_0}$, *and* $h_2(a_0,b_0,c_0) \triangleq \frac{(b_0)^{2+\frac{2}{\alpha}}}{(b_0-a_0)(b_0-c_0)} + \frac{(a_0)^{2+\frac{2}{\alpha}}}{(a_0-b_0)(a_0-c_0)} + \frac{(c_0)^{2+\frac{2}{\alpha}}}{(c_0-b_0)(c_0-a_0)}$.

Proof 8 *See Appendix A.4 for details.*

Note that both a_0 and c_0 are functions of ω. After simplification and approximation, there is only one integration left. Using the similar technique, the coverage probability under mutual information accumulation strategy can be approximated. Furthermore, we can find that the different between the energy accumulation equation (2.19) and the mutual information accumulation equation is small. If we define $a_1 = \frac{(T-\omega)^+ z^\alpha}{1+\omega}$ and replace a_0 in equation (2.25) with a_1, we can get the

approximation of the coverage probability under mutual information accumulation strategy, which is summarized in the following Lemma.

Lemma 7 *Under mutual information accumulation strategy, the coverage probability of a two-hop network in a Poisson field of interference can be approximated as*

$$P^{MIA} \approx \int_0^{\infty} \left(p\lambda c_3 x^2 \omega^{\frac{2}{\alpha}-1} - p^2 \lambda x^{\alpha} c_2 h_0(a_1,b_0,c_0) \right) e^{-\lambda p(1-p) c_1 h_1(a_1,b_0,c_0) - \lambda p^2 c_1 h_2(a_1,b_0,c_0)} d\omega$$
$$e^{-c_1 \lambda p z^2 T^{2/\alpha}} - e^{-\lambda p c_1 T^{2/\alpha} \frac{z^{\alpha+2} - y^{\alpha+2}}{z^{\alpha} - y^{\alpha}}}, \tag{2.26}$$

where $a_1 \triangleq \frac{(T-\omega)^+ z^{\alpha}}{1+\omega}, b_0 \triangleq T y^{\alpha}, c_0 \triangleq x^{\alpha}\omega$, $h_0(a_1,b_0,c_0) \triangleq \frac{(a_1^2 F_1(1,2-\frac{2}{\alpha};3;1-a_1/c_0) - b_0^2 {}_2F_1(1,2-\frac{2}{\alpha};3;1-b_0/c_0))}{(a_1-b_0)c_0^{2-\frac{2}{\alpha}}}$;
$c_1 = \frac{2\pi}{\alpha} B(1-\frac{2}{\alpha}, \frac{2}{\alpha})$; $c_2 \triangleq \frac{2\pi B(2-\frac{2}{\alpha}, 1+\frac{2}{\alpha})}{\alpha}$; $c_3 \triangleq \frac{2\pi B(1-\frac{2}{\alpha}, 1+\frac{2}{\alpha})}{\alpha}$; $h_1(a_1,b_0,c_0) \triangleq c_0^{2/\alpha} + \frac{b_0^{1+\frac{2}{\alpha}}}{b_0-a_1} + \frac{a_1^{1+\frac{2}{\alpha}}}{a_1-b_0}$,
and $h_2(a_1,b_0,c_0) \triangleq \frac{(b_0)^{2+\frac{2}{\alpha}}}{(b_0-a_1)(b_0-c_0)} + \frac{(a_1)^{2+\frac{2}{\alpha}}}{(a_1-b_0)(a_1-c_0)} + \frac{(c_0)^{2+\frac{2}{\alpha}}}{(c_0-b_0)(c_0-a_1)}$.

2.3.4 Evaluation Results

In this section, we provide both Monte Carlo simulation results and numerical results to verify our fundamental analysis and provide some system design guidance as well. Monte Carlo simulation steps are as follows: 1) select a sufficiently large region denoted as C and calculate the average number nodes in this area by $N = |C|\lambda$, where $|C|$ represent the area of the selected region; 2) put the source, relay and destination at three locations S, R and D; 3)for each round of simulation, generate the actual number of nodes according to Poisson distribution with an average of N and randomly distribute these number of nodes in the simulation region; 4) for each node, decide whether this node is active or not based on the slotted Aloha; 5) generate small scaling fading channel and calculate the received SIR. Details on the parameters of the simulation will be illustrated in the following.

Fig. 2.9 shows both Monte Carlo simulation results and numerical results on the coverage probability of one-hop transmission, two-hop decode and forward strategy, two-hop energy accu-

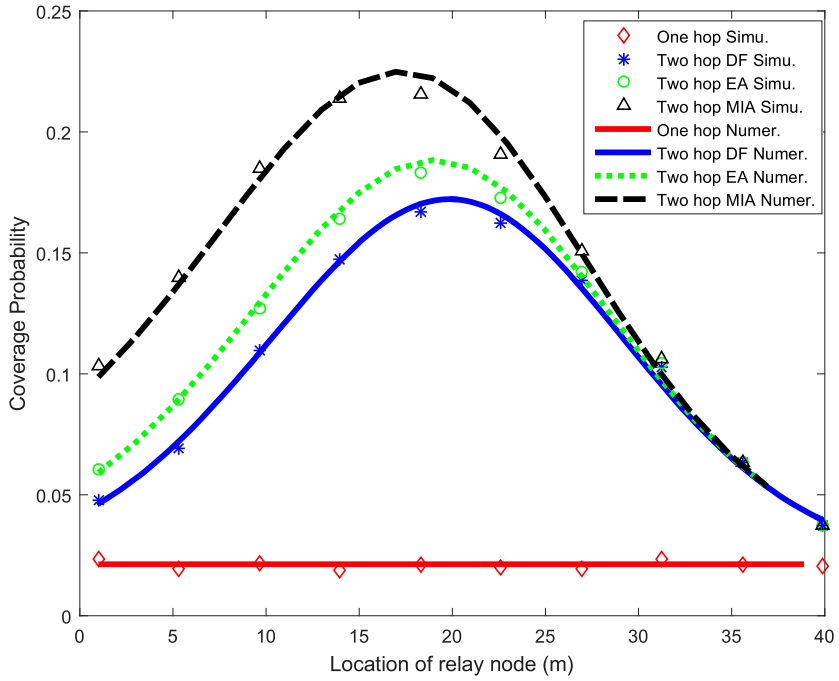

Figure 2.9: Coverage Probability of two-hop network

mulation and two-hop mutual information accumulation strategy. Numerical results on one-hop transmission strategy is obtained from equation (2.15); numerical results on two-hop decode and forward strategy is obtained from equation (2.16); numerical results on two-hop energy accumulation strategy is obtained from equation (2.19); numerical results on two-hop mutual information accumulation is obtained from equation (2.21). The simulation parameters are as follows: the intensity of the Poisson process of interference node $\lambda = 0.001m^{-2}$; the path loss exponent $\alpha = 4$; the SIR threshold for successfully decoding $T = 6$; the locations of the source node and the destination node are $S = (0,0), D = (40,0)$. The location of relay node changes from the source to the destination; the random access probability for the slotted Aloha $p = 0.2$. From this figure, we can observe that numerical results and Monte Carlo simulation results match very well, which verify our theoretical analysis. Furthermore, we can find that the optimal relay location will move closer to the source node when the cooperative strategy changes from decode and forward to energy accumulation and to mutual information accumulation. For example, the optimal location for the decode and forward strategy is at location of (19.46,0) with a coverage probability of 0.1721;

the optimal location for the energy accumulation strategy is at (18.95, 0) with a coverage probability of 0.1883; the optimal location for mutual information accumulation strategy is at (16.69,0) with a coverage probability of 0.2249. Therefore, under this simulation settings, we can find that mutual information accumulation can improve the coverage probability by 30.60% compared to decode-and-forward and can improve the coverage probability by 19.44% compared to energy accumulation.

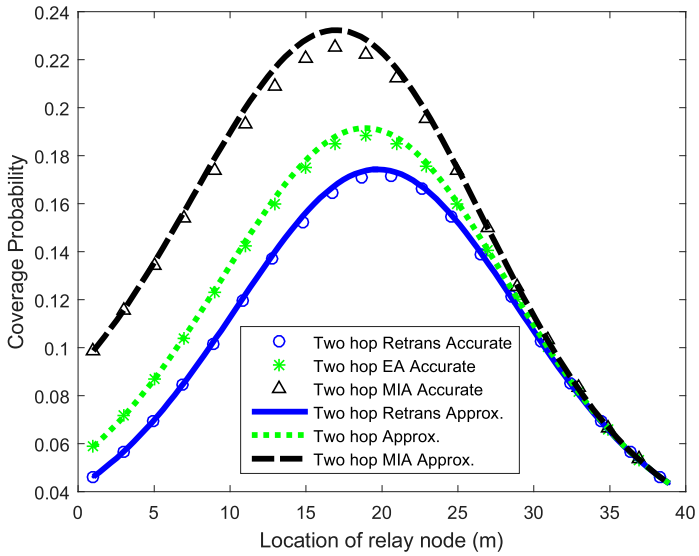

Figure 2.10: Approximation of coverage probability in two-hop network

Fig. 2.10 compares the accurate numerical results on coverage probability and the approximated results on coverage probability. Parameters are kept the same as the parameters in Fig. 2.9. From this figure, we can see that the approximation is close to the true value. Fig. 2.11 shows the coverage probability under different decoding threshold T. Other parameters are kept the same as the parameters in Fig. 2.9 except the decoding threshold which are marked in the figure. From this figure, we can observe that mutual information accumulation has better performance gain compared to energy accumulation when the decoding threshold is high. For example, when the decoding threshold $T = 6$dB, mutual information accumulation will achieve 13.49% gain on coverage probability compared to energy accumulation. However, the gain will be only 2% when the decoding threshold $T = 0$dB and 0.3% when the decoding threshold $T = -6$dB. This is because

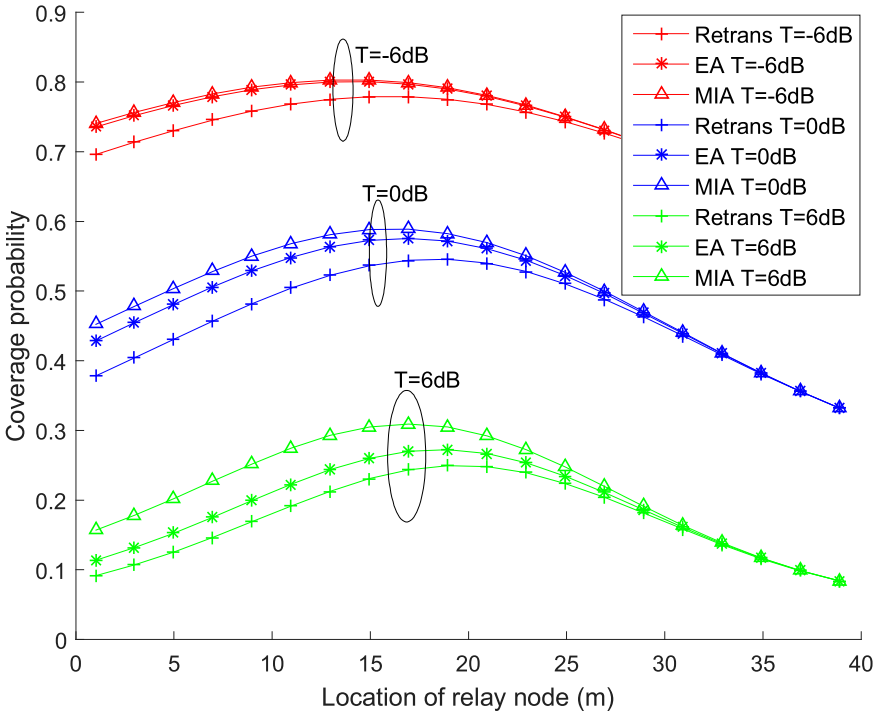

Figure 2.11: Coverage probability under different decoding threshold T

when the decoding threshold is low, the system works in low SNR regime where accumulating mutual information and accumulating energy will have similar performance as $\log(1+x) \approx x$ holds when x is small.

Fig. 2.12 shows the cooperative gain as a function of random access probability p. Here the cooperative gain is defined as the ratio between the coverage probability of mutual information accumulation and the coverage probability of retransmission strategy. In this figure, the distance of source-destination link $z = 90m$, the location of the relay node is set as at the optimal location which is obtained by one-dimensional search, $\lambda = 5 \times 10^{-5} m^{-2}$, $\alpha = 4$. It is clearly shown that the cooperative gain increases as the decoding threshold increases. Furthermore, this figure shows that the cooperative gain also increases as the random access probability p increases. When the random access probability increases, the interference in the network will increase. Therefore, we can conclude that mutual information accumulation can achieve much more cooperative gain in high interference scenarios. This conclusion is further confirmed in Fig. 2.13, where cooperative

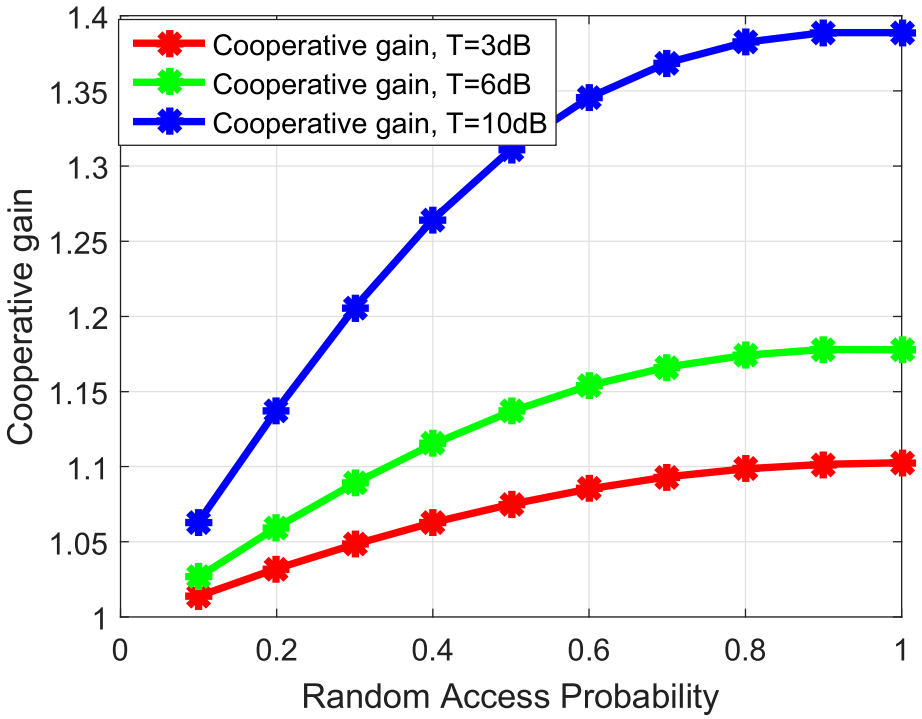

Figure 2.12: Cooperative gain as a function of random access probability p

gain as a function of network intensity is plot out. In this figure, $p = 0.5$, $z = 100m$ and $\alpha = 4$. As shown in this figure, cooperative gain increases as the network intensity increases.

2.4 Conclusions

In this chapter, we provide fundamentally theoretical analysis on the performance of mutual information accumulation over wireless networks. Asymptotic analysis shows that when the number of cooperating nodes goes to infinity, the cooperative gain in a two dimensional grid network will be greater than 2.6 which is much larger than the asymptotic cooperative gain in one-dimensional grid network. Furthermore, we study the characteristics of the optimal route in cognitive radio networks with mutual information accumulation and theoretically analysis the cooperative gain of mutual information accumulation in underlay cognitive radio networks. Analytical results show that mutual information accumulation can achieve higher cooperative gain especially in the scenario with tight interference tolerant threshold networks. Finally, we analyze the performance of

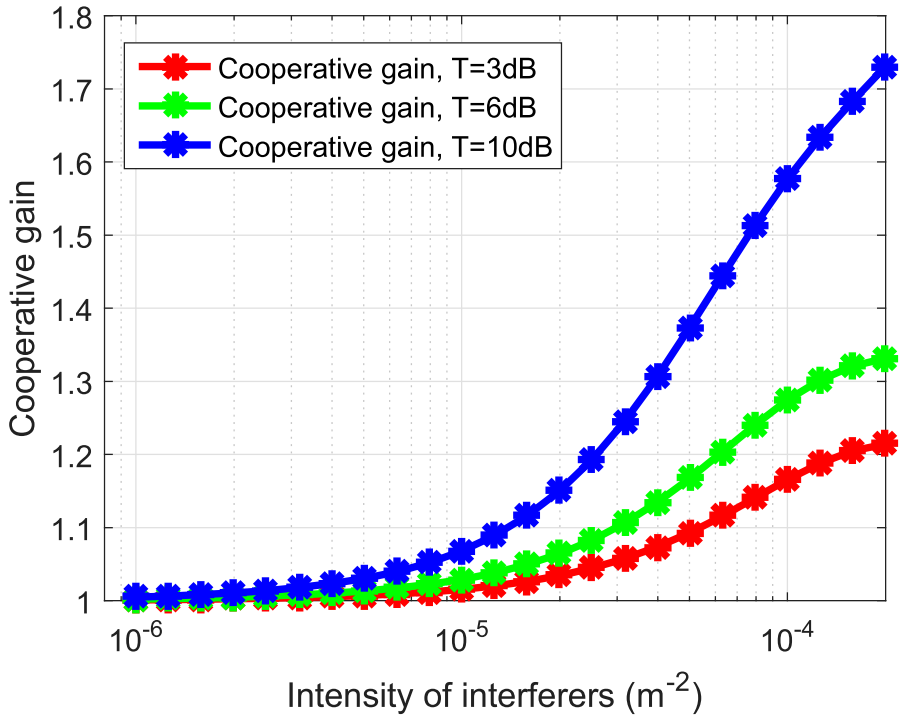

Figure 2.13: Cooperative gain as a function of network density λ

retransmission, energy accumulation and mutual information accumulation of a two-hop network with Poisson field of interference. An accurate approximation of the coverage probability is derived and verified by numerical results. This chapter lays a foundation for the following chapters on application.

Chapter 3

Applications: Mutual Information Accumulation in Cognitive Radio Networks

In this chapter, we are going to apply mutual information accumulation into underlay cognitive radio networks. In underlay cognitive radio networks, resource allocation and routing algorithms are studied to explore the advantage of mutual information accumulation. To be specific, both centralized and distributed resource allocation and routing algorithms are developed in underlay cognitive radio networks with mutual information accumulation. This chapter is organized as follows: Section 3.1 presents the system model of underlay cognitive radio network with mutual information accumulation; Section 3.2 presents the developed centralized routing and resource allocation algorithm for underlay cognitive radio networks with mutual information accumulation; Section 3.3 discussed the distributed routing and resource allocation algorithm for underlay cognitive radio networks with mutual information accumulation; Simulation results are presented in Section 3.4 and Section 3.5 concludes this chapter.

3.1 System Models

In this subsection, we will extend mutual information accumulation to underlay cognitive radio networks and investigate cooperative routing and resources allocation for such networks. Based on

various constrains, the following builds the mathematical model of resources allocation problem after a transmission order is given.

Let L be the total number of nodes in the transmission order. Denote T_i as the time at which user i decodes the message and $\Delta_i = T_i - T_{i-1}$ as the inter-user delay between user i and user j. Note that Δ_i can also be regarded as the length of the ith time-slot. For a given route/transmission order, the objective of the SU network will minimize end-to-end transmission delay:

$$T_L = \sum_{i=1}^{L} \Delta_i.$$

This linear objective function is optimized subject to the following constraints: (i) $\Delta_i \geq 0$ for all i, (ii) node i must decode by time $T_i = \sum_{\ell=1}^{i} \Delta_i$, (iii) the energy constraint(s), (iv) the constraint(s) on the use of time and bandwidth, and (v) the interference constraint for the primary users. We state constraints (ii)-(v) in turn.

First, there are L decoding constraints resulting from the nodes' positions in the transmission order. That is, the condition for successful decoding can be expressed as the accumulated mutual information exceeds the entropy:

$$\sum_{i=0}^{k-1} \sum_{j=i+1}^{k} A_{ij} C_{ij} \geq B, \quad k = 1, \ldots, L. \tag{3.1}$$

where A_{ij} denotes the time-bandwidth product assigned to the ith user in the jth time slot.

Second, we consider constraints on energy and bandwidth. There are per-node energy/power constraint [16], [73], [74] and sum-energy/power constraint [75], [76], [77] in the current literature. Per-node energy/power constraint is widely used to maximize the network life time as shown in [73], [74] while sum-energy/power constraint is widely used to maximize the network throughput as shown in [77]. Per-node energy constraint means that each node's consumed energy for transmitting the message should not exceed its own energy budget as follows,

$$\sum_{j=i+1}^{L} A_{ij} P_s \leq E_{T_i}, \quad 0 \leq i \leq L-1. \tag{3.2}$$

Sum-energy constraint means the total energy consumption for delivering the message throughout the SU network should not exceed the energy budget E_T:

$$\sum_{i=0}^{L-1} \sum_{j=i+1}^{L} A_{ij} P_s \leq E_T. \tag{3.3}$$

In this paper, we focus on the case of sum-energy constraint since we are trying to minimize the end-to-end delay in the networks instead of maximizing the network life time. Therefore, in the case where per-node energy constraint is considered, if a transmitting node runs out of energy, a new routing can be obtained by re-running the centralized algorithm over the available nodes as indicated in [74] or conducting routing repair procedure in the distributed algorithm. Sum-bandwidth constraint suggests that all the nodes in the SU network share a sum-bandwidth of W_T, i.e.,

$$\sum_{i=0}^{j-1} A_{ij} \leq \Delta_j W_T, \quad j = 1, \ldots, L. \tag{3.4}$$

Finally, to protect PU's quality of service, SUs should make sure that their total interference power to the PU receiver should not exceed I_T:

$$\sum_{i=0}^{j-1} A_{ij} h_{ir} P_s / \Delta_j \leq I_T, \quad \Delta_j \neq 0, j = 1, \ldots, L-1, \tag{3.5}$$

where h_{ir} is the channel gain from the ith SU to the PU receiver.

Therefore, the problem of minimizing SUs' end-to-end delay under sum-energy constraint, sum-bandwidth constraint and PU's interference power constraint can be written in the following optimization problem **OP1**:

$$\begin{aligned} &\min_{\Delta_i, A_{ij}} \sum_{i=1}^{L} \Delta_i \\ &s.t. (3.1), (3.3), (3.4), \text{and } (3.5). \end{aligned} \tag{3.6}$$

It is clear that given the transmission order, the resource allocation problem (3.6) is a linear programming problem and can be solved efficiently. However, how to find the optimal transmission

order is a NP-Hard problem. In the following, we presented a centralized heuristic solution.

3.2 Centralized Routing and Resource Allocation

Since the resource allocation problem for a fixed route/transmission order can be efficiently solved, the remaining question becomes how to find the optimal route/transmission order. Unfortunately, in [34] it is shown that finding the optimal route/transmission order for a wireless ad hoc network is NP-complete. It is clear that the additional constraint on interference power will only complicate the problem. In the following theorem, we show that the method to improve the transmission order introduced in [16] still holds in the underlay cognitive radio networks of our interests. Let $\mathbf{x}^* = \left[\Delta_1^*, \Delta_2^*, \ldots, \Delta_L^*, A_{01}^*, \ldots, A_{0L}^*, A_{12}^*, \ldots, A_{(L-1)L}^*\right]$ be the optimal solution obtained from **OP1** for a given route/transmission order. Denote the corresponding optimal end-to-end delay as $T_L^* = \sum_{i=1}^{L} \Delta_i^*$, we have the following theorem:

Theorem 3 *If $\Delta_i^* = 0$, use T_L^{**} to denote the optimal end-to-end delay (under the same sum-bandwidth, sum-energy, and interference power constraint) of the 'swapped' transmission order:*

$$[0, \ldots, i-2, i, i-1, i+1, \ldots, L] \quad if \quad i \leq L-1$$
$$[0, \ldots, L-2, L] \quad if \quad i = L.$$

We have $T_L^{**} \leq T_L^*$.

Proof 9 *We prove the theorem by constructing a feasible resource allocation solution for the 'swapped' transmission order which has a decoding delay equal to the optimal decoding delay of the original transmission order. Denote $\mathbf{x}^* = [\Delta_1^*, \Delta_2^*, ..., \Delta_L^*, A_{01}^*, A_{02}^*, ..., A_{0L}^*, A_{12}^*, ..., A_{(L-1)L}^*]$ as the optimal solution obtained from **OP1** for a given transmission order $[0, ..., i-2, i-1, i, i+1, ..., L]$.*

Define $\mathbf{x} = [\Delta_1, \Delta_2, ..., \Delta_L, A_{01}, A_{02}, ..., A_{0L}, A_{12}, ..., A_{(L-1)L}]$, *where*

$$\begin{aligned}
\Delta_i &= \Delta_i^*, 0 \le i \le L \\
A_{kl} &= A_{kl}^*, 0 \le k, l \le L, k \ne i-1, l \ne i \\
A_{i-1,i} &= 0, \\
A_{(i-1)j} &= A_{ij}^*, j \in \{i+1, \cdots, L\} \\
A_{ij} &= A_{(i-1)j}^*, j \in \{i+1, \cdots, L\}
\end{aligned} \tag{3.7}$$

We can find $\sum_{i=1}^{L} \Delta_i = \sum_{i=1}^{L} \Delta_i^*$ *and by Theorem 2 in [16], we know that* $\mathbf{x}$ *meets the decoding and sum-bandwidth constraint. To show that* $\mathbf{x}$ *is a feasible solution to the 'swapped' transmission order, we only need to show that* $\mathbf{x}$ *meets the interference constraint, i.e.,*

$$\sum_{l=0}^{j-1} A_{lj} P_s h_{lr} \le I_T \Delta_j, j = 1, 2, ..., L.$$

This is true because $\sum_{l=0}^{j-1} A_{lj} P_s h_{lr} = \sum_{l=0}^{j-1} A_{lj}^* P_s h_{lr} \le I_T \Delta_j^* = I_T \Delta_j, j = 1, 2, ..., L.$

This theorem indicates that if a user in the transmission order decodes the data packet before its previous user, a better delay performance can be achieved by moving forward this user in the transmission order. After executing the 'swapping' operation, the following 'deleting' operation can further improve the delay performance.

Theorem 4 *If user i's transmission time is* 0*, i.e.,* $t_i = \sum_{j=1}^{L} A_{ij} = 0$*, let* T_L^{**} *denote the optimal end-to-end delay (under the same sum-bandwidth, sum-energy, and interference power constraint) of the 'deleted' transmission order:*

$$[0, \ldots, i-1, i+1, \ldots, L] \quad if \quad i \le L-1.$$

Then, $T_L^{**} \le T_L^*$.

Proof 10 *Since the transmission time of user i is zero, it is clear that user i does not participate*

in the cooperative routing for the original transmission order. Therefore, deleting node i from the original transmission order will not cause extra delay. However, since we delete node i from the original transmission order, the feasible solution space of ***OP1*** *is enlarged as node i's successful decoding constraint is deleted. Therefore, the optimal delay of the new linear programming problem will be less or equal to that of the original linear programming problem.*

Considering both Theorem 3 and Theorem 4, we know that for any route/transmission order, the 'swapping' and 'deleting' operation can be used to obtain a better route/transmission order. The details of the iterative route optimization and resource allocation algorithms are summarized in Algorithm 1. It is important to note that the final route/transmission order is a swapped or deleted version of the initial one. Therefore, selecting the initial route/transmission order is of vital importance for the centralized resource allocation algorithm. Considering the protection of PU's quality of service, we can consider the initial route/transmission order as the one causing the minimal interference to the PU receiver. In Section 3.4, the transmission order obtained from distributed algorithm is used as the initial transmission order for the centralized resource allocation algorithm.

3.3 Distributed Routing and Resource Allocation

In this section, we introduce distributed cooperative routing and resources allocation algorithms for underlay cognitive radio networks. Distributed resources allocation algorithms for wireless networks using mutual information accumulation have been developed in [16] and [11]. However, they can not be directly applied to underlay cognitive radio networks. This is because these distributed routing and resources allocation algorithms did not take the interference to PUs into consideration. The distributed routing algorithms introduced in [29], [30], [78] addressed the issue of protecting PUs in cognitive radio networks. However, these distributed algorithms can not be directly applied to cognitive radio networks with mutual information accumulation since they failed to take full advantage of mutual information accumulation. Therefore, distributed coop-

Algorithm 1: Centralized cooperative routing and resources allocation algorithm

Input: System parameters:
$[P_1,\ldots,P_L], P_p, N_0, \alpha, I_T, E_T, \{h_{ij}|1 \le i,j \le N\}, \{h_{ir}|1 \le i \le N-1\}, \{h_{pi}|2 \le i \le N\}$;

Output: Route from the SU source to the destination and corresponding resources allocation A_{ij};

Initialization: Apply Dijkstra algorithm [68] to find the path from the source to the destination with the minimal interference to the PU receiver; take this minimal interference path as the initial transmission order ;

repeat

  solve the linear programming **OP1** to get the resources allocation solution for current transmission order;

  (Based on Theorem 3 swap the transmission order);

  if $\Delta_i = 0$ *and* $\Delta_{i-1} \neq 0, i = 1,\ldots,L$ **then**

    swap the positions of the two nodes in the order;

  if $\Delta_L = 0$ **then**

    drop node $L-1$ from the order;

  Based on Theorem 4 delete the silent node;

  if $t_i = 0$ **then**

    drop node i from the order;

until *An order with* $\Delta_i > 0$ *and* $t_i > 0$ *for all i is obtained*;

erative routing and resources allocation algorithms for underlay cognitive radio networks should take both link capacity, link interference to the PU receiver and the features of mutual information accumulation into account. It is important to note that the interference power constraint could completely change the structure of the optimal solution to the routing and resources allocation problem in the networks using mutual information accumulation. For example, it has been shown in [11] that the delay-optimal route under sum-bandwidth constraint allows only one user transmit in each transmission slot. However, due to the interference power constraint, there may be multiple users transmitting concurrently within a single transmission slot in underlay cognitive radio networks. Therefore, new distributed resources allocation algorithms need to be introduced. In the following, we will first develop the criteria under which there will be more than one node transmitting in a single transmission slot and then introduce a new distributed algorithm.

The details of the packet format in the distributed algorithm is shown in Fig. 3.1 and Fig. 3.2. The information contained in the control packet is θ_1 where θ_1 denotes the bandwidth allocated

for the current transmitting node. If the decoded node finds that it is a better forwarding node than the current transmitting one, it will set $\theta_1 = 0$ and send out the control packet. If the decoded node finds that it should transmit concurrently with the current transmitting node, it will add the calculated θ_1 in the control packet and send it out. The control packets are assumed to be sent out through a specific control channel and can be successfully and immediately received by the receivers. Since each time there is only one node decoding the message and the control packet is sent to inform the current transmitting node to stop or continue to transmit, it is a unicast instead of broadcast. Therefore, there will be no collision among control packets. After a node decides to take over the transmission, it will also add its own information to the header of the data packet. The information contained in the header of the data packet is V_flag, C_{iN} and I_i. V_flag is a one-bit information to indicate whether this node is part of the virtual node. C_{iN} is the current transmitting node's capacity to the destination and I_i is its interference to the PU receiver. If the current transmitting node is part of the virtual node, it will set V_falg TRUE, set C_{iN} field in the header of the data packet to the virtual node's equivalent capacity and set I_i in the header of the data packet to I_T; otherwise, it will set V_flag FALSE, add C_{iN} and I_i in the header of the data packet. These information is to help the next decoding node to do routing decision. Our new distributed cooperative routing and resources allocation algorithm is summarized in Algorithm 2.

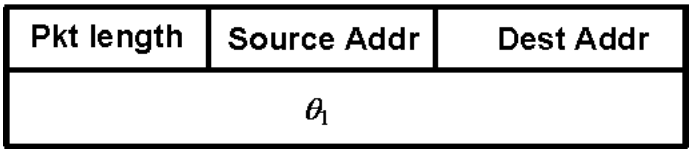

Figure 3.1: The format of control packet in the distributed algorithm

In the initialization stage of this distributed algorithm, I_i can be estimated by periodically sensing PU receiver's ACK packets or be estimated through the a priori knowledge on the location of PU receiver [79]; C_{iN} can be estimated through the sounding signals sent by the destination node as indicated in [16]. The complexity of the distributed algorithm lies in the calculation of equation (2.6) which consists of mathematical operations of comparison and division. Therefore, the computation complexity of this distributed algorithm for each node is $\mathcal{O}(1)$. The overhead of this

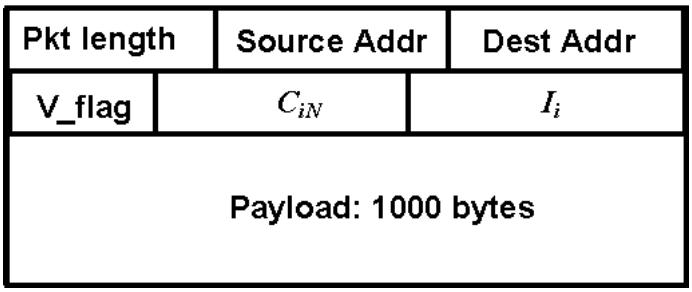

Figure 3.2: The format of data packet in the distributed algorithm

Algorithm 2: Distributed cooperative routing and resources allocation algorithm for underlay cognitive radio networks with mutual information accumulation

1 Initialization: (For node i) Estimate its interference power spectral density I_i to the PU receiver; estimate its channel to the destination and calculate C_{iN}; obtain the information of current transmitting node I_{i-1} and $C_{(i-1)N}$ from the header of the data packet it has decoded;
2 calculate θ_1, θ_2 by equation (2.6);
3 **if** $\theta_1 = 0, \theta_2 > 0$ **then**
4 Set $\theta_1 = 0$ in the control packet and send it out to inform current transmitting node to stop transmitting ; set V_flag FALSE; add C_{iN}, I_i in the header of the data packet and start to transmit;
5 **else if** $\theta_1 > 0, \theta_2 > 0$ **then**
6 Set θ_1 in the control packet with the calculated value θ_1 in step 2; send out the control packet; in the header of the data packet, set V_flag TRUE; set C_{iN} to the equivalent capacity of the virtual node; set I_i to I_T; transmit data packet with bandwidth θ_2;
7 **else**
8 node i keeps silent.

distributed algorithm lies in the information feedback about θ_1, link capacity of C_{iN} and I_i. To be specific, the newly decoded SU node needs to send out θ_1 to the current transmitting node. In the header of data packets, the capacity C_{iN} and interference I_i should be added. Refer to our current designed packet format, if C_{iN}, I_i and θ_1 is 2 bytes each, the total overhead of the distributed algorithm will not exceed 6 bytes for each data packet. Since the size of data packet can be on the order of 1000 bytes, the overhead of our distributed algorithm can be made quite small.

If all SU nodes are under per-node energy constraint and one node runs out of energy while transmitting, routing repair procedure will be conducted. The procedures are listed in the following: if there is only one node transmitting in current slot, this transmitting node will inform its

previous node in the transmission order to take over the transmission before running out of its energy. If one of the two nodes in the virtual node runs out of energy, the left node will continue to transmit. In case where SU source tries to send multiple packets to its destination, the source SU node can transmit the packets one-by-one. Specifically, the source can send out the first packet and wait for the ACK from the destination. If the source receives an ACK packet from the destination, it will send out another new packet until it finishes transmitting all its packets.

3.4 Simulation Results

In this section, we present simulation results to demonstrate the performance gains of mutual information accumulation and the effectiveness of our algorithms for underlay cognitive radio networks.

Fig. 3.3 gives an examples to compare the routing and resources allocation solutions between traditional multi-hop delay-optimal routing without mutual information accumulation and cooperative routing using mutual information accumulation in underlay cognitive radio networks. The system setup for Fig. 3.3 is in the following. All the nodes are distributed in the area of 1×1 (meter $\times$ meter). The PUT is placed at $[0.4, 0.8]$ and the PUR is located at $[0.6, 0.8]$. There are altogether 16 SU nodes in the system: the SU source (node 1) is placed at $[0.1, 0.4]$ and the SU destination (node 16) is located at $[0.9, 0.4]$. The other 14 SU relay nodes are uniformly distributed in the area. The total system bandwidth is set to be $W_T = 1$Hz and the total system energy is set to be $E_T = 20$Joule. Other parameters include $N_0 = 1$W/Hz, $P_s = 1$W/Hz, $P_p = 2$W/Hz, $I_T = 2$W, $\alpha = 2$, $\Gamma = 0$dB and $B = 1$bit. As shown in the figure, the traditional multi-hop delay-optimal routing (red dashed, obtained by Dijkstra algorithm) is $[1, 15, 4, 16]$. The corresponding bandwidth allocation results are labeled on the links. For example, when the source node transmits to node 15, it will use 82% of the total bandwidth due to the interference power constraint. The route for cooperative routing with mutual information accumulation is $[1, (8,1), (8,3), (8,6), 15, 4, (4,2), 16]$, where the second item $(8,1)$ means node 8 and node 1 will share PU's spectrum jointly in the

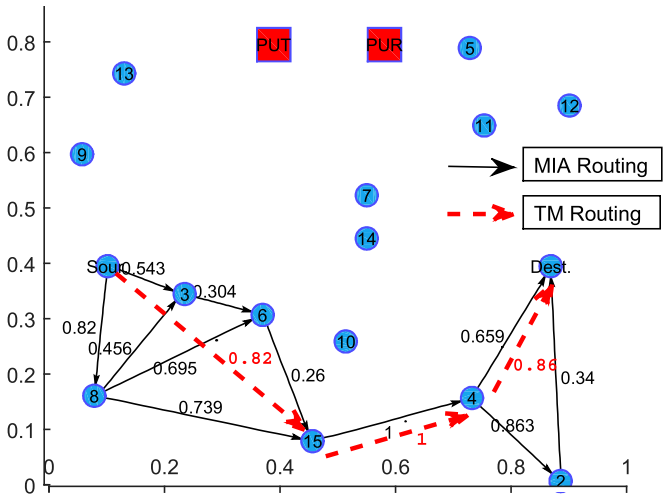

Figure 3.3: Compare of MIA routing with conventional multi-hop routing in the underlay CRN.

second slot and these two nodes can be regarded as a virtual node. Within the virtual node, node 1 will occupy 54.3% of the PU's spectrum and node 8 will occupy the rest 45.6% of the spectrum. From Fig. 3.3, we can see that the delay-optimal route of cooperative routing using mutual information accumulation for underlay cognitive radio network is very different from that using traditional multi-hop routing. It is important to note that the cooperative routing and resources allocation solution in [16] can be regarded as a special case of our algorithm where $I_T \to \infty$.

In Fig. 3.4, we show the cumulative delay distribution for the following four approaches: traditional multi-hop delay-optimal routing by using Dijkstra's algorithm (denoted as TM Routing delay-optimal in the figure), centralized algorithm for mutual information accumulation, distributed algorithm for mutual information accumulation, and optimal solution for mutual information accumulation obtained by exhaustive search. 6 SU nodes are randomly deployed in the network as SU relays. $I_T = 3$W, $\alpha = 3$. Other parameters are the same as those shown in Fig. 3.3. The cumulative delay distribution is based on 1000 runs. The average delay of the traditional multi-hop delay-optimal routing is 11.546sec, while the average delay of centralized and distributed cooperative routing using mutual information accumulation are 1.620sec and 1.622sec, respectively. The optimal delay obtained by exhaustive search is 1.608sec. On average, both the centralized and distributed cooperative routing algorithms can reduce up to 85.9% of the end-to-end delay compared to traditional multi-hop delay-optimal routing. Furthermore, compared to the optimal

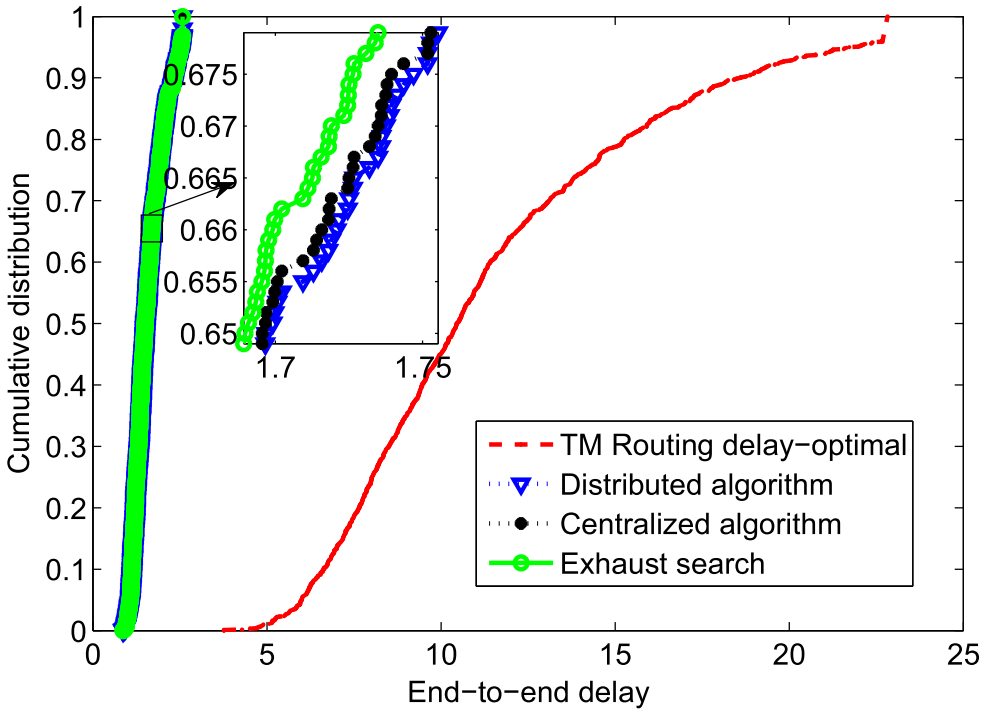

Figure 3.4: Compare of delay distributions of different algorithm

route and resource allocation strategies using exhaustive search, our proposed centralized and distributed algorithms only add 0.75% and 0.87%, respectively, additional delay. Under the same simulation parameters, if we change the number of SU nodes to 48, the centralized and distributed algorithms can, on average, reduce 77.7% and 77.5%, respectively, percent of the end-to-end delay compared to the traditional multi-hop delay-optimal routing. Finally, from Fig. 3.4, we can see that the introduced distributed algorithm can obtain almost the same performance on end-to-end delay compared to the centralized algorithm.

3.5 Conclusions

In this chapter, we introduce cooperative routing for underlay cognitive radio networks using mutual information accumulation and studied the associated problem of routing and resources allocation. An optimization problem has been formulated to identify the cooperative routing and optimal resources allocation for the minimum delay transmission. The problem is further decomposed into

two subproblems: routing problem and resources allocation problem. Efficient centralized as well as distributed algorithms were introduced to address these two problems. Since our solutions are linear programming based, they can be readily applied to large scale cooperative cognitive radio networks. Simulation results suggest that using the introduced resources allocation strategies, cooperative cognitive radio networks using mutual information accumulation can significantly reduce the end-to-end delay of SUs' transmission.

Chapter 4

Applications: Mutual Information Accumulation in Massive MTC Networks

In this Chapter, we explore the possibility and potential of applying mutual information accumulation into massive machine type communication (massive MTC) networks. In a massive MTC network, wireless connections between machine type devices (MTDs) and eNodeBs are unreliable due to the interference caused by uncoordinated random access of other MTDs. Conventionally, if an eNodeB fails to decode the packet, the MTD will retransmit the packet in the following available slot. However, it is with a high probability that the retransmission will fail again due to the correlated interference [80]. To address this problem, we first apply energy accumulation and mutual information accumulation in MTC networks to improve the network performance. Furthermore, we design and analyze a location-based cooperative strategy to further improve the performance of massive MTC networks. One of the main idea of the new design is to select an inactive MTD acting as a relay for outage MTDs. Unlike the work in [81] [82] where the authors assumed the packet was known at the relay (base station) in prior, the new designed protocol considers the case where the relay has no prior information about the packet. To be specific, an inactive MTD is selected as a relay if it has successfully decoded the packet and if it is located within a circular area around the eNodeB. Otherwise, if there is no inactive MTD that can decode the packet, the source

MTD will retransmit the packet. The chapter is organized as follows: Section 4.1 describes the system models. Section 4.2 presents the performance analysis. Simulation and numerical results are presented in Section 4.3 and Section 4.4 concludes the chapter.

4.1 System Model

We consider a static massive MTC network consisting of machine type devices (MTDs) and eNodeBs as shown in Fig. 4.1. The locations of MTDs are modeled as a homogeneous Poisson point process (HPPP) Φ with a density of λ. We assume MTDs transmit collected data to eNodeBs over a Random Access Channel (RACH) of LTE or LTE-A with a probability p by the one-stage protocol [83]. In the one-stage protocol, a MTD will transmit the data payload and device identity altogether in one packet without any other handshaking overhead. One-stage protocol is considered here because it may not be worthwhile to invest overhead on handshaking mechanism due to the small payload size of MTC. During a random access slot, we call the transmitting MTDs as active MTDs and the non-transmitting MTDs as inactive MTDs. Therefore, the locations of active MTDs in kth slot can be modeled as a HPPP Φ_a^k with a density of $p\lambda$; the locations of inactive MTDs in kth slot can be modeled as a HPPP Φ_{in}^k with a density of $(1-p)\lambda$. We assume that for each active MTD, its receiver (eNodeB) is located at a distance of z away. Extending this bipolar model to random link length is straight forward [84]. By Slivnyak's theorem, the performance of the MTC network can be represented by the performance of the typical MTD-eNodeB link [85].

Without loss of generality, the typical eNobeB is located at the origin of a two dimension topology. Assume the system operate in the interference-limited regime, i.e., the background thermal noise power is negligible compared to the total aggregate interference power. We call the typical eNodeB fails to decode a packet if the received signal-to-interference ratio (SIR) is less than a threshold T. The uplink channel of the considered massive MTC network is modeled as a combination of the power-law path loss and Rayleigh block fading. In this chapter, we focus on the uplink (link from MTD to eNodeB) performance analysis. We assume that all MTDs transmit

with the same power P_t. Therefore, the received power at the typical eNodeB from a MTD at a distance of z is $P_r = P_t G_{s,d,1} z^{-\alpha}$, where $G_{s,d,1} \sim \exp(1)$ is the small scale fading gain between the typical MTD s and the typical eNodeB d during the first transmission, and $\alpha > 2$ is the path loss exponent. The Rayleigh small scale fading is assumed to be i.i.d between different wireless links during different transmission slots.

Cooperative Strategy: The wireless connection between the typical MTD and the eNodeB is unreliable due to the interference caused by other uncoordinated and randomly accessing MTDs. If the destination or the eNodeB fails to decode the packet due to interference or fading, the MTD will retransmit the packet in the next available time slot. In the eNodeB side, the eNodeB can try to decode the retransmitted packet or the eNodeB can do energy accumulation by using MRC to combine the signal received from the first transmission and the signal received from retransmission. Another approach is that the MTD can transmit a redundancy version of the packet and the eNodeB will accumulate mutual information by combining the signal received from the first transmission and the signal received from the retransmitted redundancy version. Instead of letting the typical MTD retransmit the packet, we can also consider to select an inactive MTD act as a relay for the typical MTD according to the following conditions: 1) the inactive MTD decodes the packet in the first time-slot; 2) the inactive MTD is within a circular region $\mathscr{A}_r$ centered at the typical eNodeB with a radius of R_r. $\mathscr{A}_r$ is called the cooperative region. The inactive MTDs which meet the above two conditions are called potential relays. If potential relays decode the packet, they will send an acknowledge message (ACK) to the typical eNodeB. The typical eNodeB will randomly select one potential relay to forward the packet if there are multiple potential relays. After the relay is selected, the typical MTD will remain silent as if the packet has been transmitted successfully. Accordingly, the density of the active MTDs in the network remains as $p\lambda$. Denote the locations of inactive MTDs during the first transmission, the locations of active MTDs during the first transmission and retransmission as Φ_{in}^1, Φ_a^1 and Φ_a^2, respectively. Note Φ_{in}^1, Φ_a^1 and Φ_a^2 are not PPPs since points are not independently displaced after the selection of relays [85]. However, we approximate Φ_{in}^1, Φ_a^1 and Φ_a^2 as PPPs and this approximation is verified by simulation results.

If there is no potential relay, the typical MTD will retransmit the packet. To simplify the analysis, we only consider the case where the selected relay only retransmits once. Extensions on multiple retransmissions remains as our future work. Therefore, under the designed cooperative strategy, the typical eNodeB is in outage if: 1) there is a potential relay selected, however, the typical eNodeB fails to decode the packet after the retransmission from the potential relay; 2) there is no potential relay and the typical eNodeB fails to decode the packet after the retransmission from the typical MTD. In the following section, we analyze the outage probability of retransmission from MTD as well as this cooperative retransmission strategy.

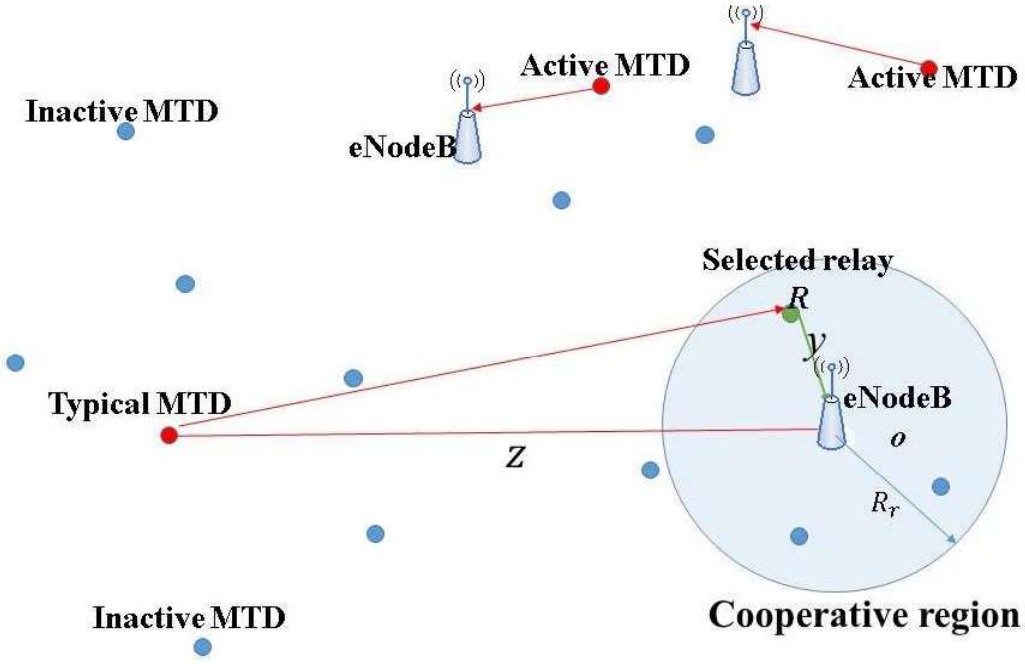

Figure 4.1: System model for massive MTC networks

4.2 Performance Analysis

This section presents a theoretical analysis on the outage probability of the designed cooperative strategy for massive MTC networks. In the considered massive MTC network, the SIR at the

typical eNodeB d during the first transmission can be expressed as,

$$SIR_{d,1} = \frac{S_{d,1}}{I_{d,1}} = \frac{G_{s,d,1} z^{-\alpha}}{\sum_{\mathbf{x}_i \in \Phi_a^1} G_{\mathbf{x},d,1} \|\mathbf{x}_i\|^{-\alpha}}, \tag{4.1}$$

where $S_{d,1}$ and $I_{d,1}$ denote the power of received signal and interference at the destination d during the first transmission, respectively. As a benchmark, the outage probability of the conventional MTD's retransmission, P^{re}, can be expressed as the outage probability in the first slot minus the probability that the retransmission in the following available slot success. Mathematically,

$$P^{re} = \mathbb{P}(SIR_{d,1} < T) - \mathbb{P}(SIR_{d,1} < T, SIR_{d,2} > T) \tag{4.2}$$

According to equation (2.15), $\mathbb{P}(SIR_{d,1} < T) = 1 - e^{-k_1}$ where $k_1 = \delta \pi \lambda p z^2 T^{\delta} \Gamma(1-\delta)\Gamma(\delta)$ and $\delta = \frac{2}{\alpha}$. By averaging over the small scale fading of the source-destination link in two time slots $G_{s,d,1}, G_{s,d,2}$, the probability that the retransmission in the following available slot succeed can be further expressed as

$$\mathbb{P}(SIR_{d,1} < T, SIR_{d,2} > T) = \mathbb{E}_{\{G\},\Phi}\left[(1 - e^{-TI_{d,1}z^{-\alpha}}) e^{-TI_{d,2}z^{-\alpha}}\right], \tag{4.3}$$

By averaging over random access strategy, the above equation can be simplified as

$$\begin{aligned} &\mathbb{P}(SIR_{d,1} < T, SIR_{d,2} > T) = \mathbb{E}_{\{G\},\Phi}\left[\Pi_{\mathbf{x}\in\Phi}(1 - p + pe^{-TG_{\mathbf{x},d,1}\|\mathbf{x}-D\|^{-\alpha}z^{\alpha}})\right] \\ &- \mathbb{E}_{\{G\},\Phi}\left[\Pi_{\mathbf{x}\in\Phi}(1 - p + pe^{-T\|\mathbf{x}-D\|^{-\alpha}G_{\mathbf{x},d,1}z^{\alpha}})\Pi_{\mathbf{x}\in\Phi}(1 - p + pe^{-T\|\mathbf{x}-D\|^{-\alpha}G_{\mathbf{x},d,2}z^{\alpha}})\right], \end{aligned} \tag{4.4}$$

By averaging over the small scale fading, the above equation can be simplified as

$$\begin{aligned} &\mathbb{P}(SIR_{d,1} < T, SIR_{d,2} > T) = \mathbb{E}_{\Phi}\left[\Pi_{\mathbf{x}\in\Phi}\left(1 - p + p\frac{1}{1 + T\|\mathbf{x}-D\|^{-\alpha}z^{\alpha}}\right)\right] \\ &- \mathbb{E}_{\Phi}\left[\Pi_{\mathbf{x}\in\Phi}\left(1 - p + p\frac{1}{1 + T\|\mathbf{x}-D\|^{-\alpha}z^{\alpha}}\right)^2\right], \end{aligned} \tag{4.5}$$

By using PGFL and further simplification on integrations, we can get

$$\mathbb{P}(SIR_{d,1} < T, SIR_{d,2} > T) = e^{-k_1} - e^{-2k_1 + p(1-\delta)k_1}. \tag{4.6}$$

Therefore, the outage probability under retransmission from the MTD is summarized in the following Lemma.

Lemma 8 *In a massive MTC network, the outage probability under pure retransmission from the MTD can be expressed as*

$$P^{re} = 1 - 2e^{-k_1} + e^{-2k_1 + p(1-\delta)k_1}, \tag{4.7}$$

where $k_1 = \delta\pi\lambda p z^2 T^{\delta}\Gamma(1-\delta)\Gamma(\delta)$ *and* $\delta = \frac{2}{\alpha}$.

Note that equation (4.7) takes temporal correlation of interference into account, i.e., interference at the first time-slot $I_{d,1}$ and second time-slot $I_{d,2}$ are temporally correlated. If we assume that $I_{d,1}$ and $I_{d,2}$ are independent, the retransmission outage probability can be expressed as $P^{re}_{ind} = 1 - 2e^{-k_1} + e^{-2k_1}$. As $P^{re}_{ind} < P^{re}$, we can find that the independent interference assumption underestimates the outage probability as in [86].

In the eNodeB side, instead of decoding the packet purely rely on the signals received in the second transmission slot, the eNodeB can combine the signals received in two time slots by energy accumulation or MRC so that the outage probability can be further reduced. In this case, the outage probability after the retransmission, $P^{re,EA}$, can be expressed as

$$P^{re,EA} = \mathbb{P}(SIR_{d,1} < T) - \mathbb{P}(SIR_{d,1} < T, SIR_{d,1} + SIR_{d,2} > T). \tag{4.8}$$

Using the same methodology developed in the first part of this dissertation, the probability that the SIR under energy accumulation is larger than the threshold while the SIR of the first transmission is smaller than the threshold under a fixed topology Φ and $SIR_{d,2}$ can be calculated in the following

steps.

$$
\begin{aligned}
&\mathbb{P}(SIR_{d,1} < T, SIR_{d,1} + SIR_{d,2} > T \,|\Phi, SIR_{d,2}) \\
&\overset{a}{=} \mathbb{E}_{\{G\},Aloha}\left[\exp\left(-z^{\alpha} T I_{d,1}(T - SIR_{s,d,2})^{+}\right) - \exp\left(-z^{\alpha} T I_{d,1} T\right)\right] \\
&\overset{b}{=} \Pi_{\mathbf{x}\in\Phi}\left(1 - p + p\frac{1}{1 + z^{\alpha}(T - SIR_{s,d,2})^{+}\|\mathbf{x} - D\|^{-\alpha}}\right) - \Pi_{\mathbf{x}\in\Phi}\left(1 - p + p\frac{1}{1 + z^{\alpha} T\|\mathbf{x} - D\|^{-\alpha}}\right)
\end{aligned} \tag{4.9}
$$

where $\overset{a}{=}$ comes from averaging over the small scale fading of the source-destination link; $\overset{b}{=}$ comes from averaging over the small scale fading and the random access. Denote $SIR_{d,2}$ as Ω and according to equation (A.6), the PDF of Ω given a fixed topology Φ can be expressed as

$$
f_{\Omega|\Phi}(\omega) = \sum_{\mathbf{x}\in\Phi} \frac{p\|\mathbf{x\text{-}D}\|^{-\alpha} z^{\alpha}}{(1 + \|\mathbf{x\text{-}D}\|^{-\alpha} z^{\alpha})^2 \omega} \prod_{\mathbf{y}\in\Phi, \mathbf{y}\neq\mathbf{x}} \left(1 - p + \frac{p}{1 + \|\mathbf{y\text{-}D}\|^{-\alpha} z^{\alpha}\omega}\right). \tag{4.10}
$$

Therefore, the probability that the eNodeB can decode the retransmission under energy accumulation can be expressed as

$$
\begin{aligned}
&\mathbb{P}(SIR_{d,1} < T, SIR_{d,1} + SIR_{d,2} > T) \\
&= \mathbb{E}\left[\int_0^{\infty} \Pi_{\mathbf{x}\in\Phi}\left(1 - p + p\frac{1}{1 + z^{\alpha}(T - \omega)^{+}\|\mathbf{x} - D\|^{-\alpha}}\right) f_{\Omega|\Phi}(\omega) d\omega\right] \\
&\quad - \mathbb{E}\left[\Pi_{\mathbf{x}\in\Phi}\left(1 - p + p\frac{1}{1 + z^{\alpha} T\|\mathbf{x} - D\|^{-\alpha}}\right)\right] \\
&\overset{a}{=} \int_0^{\infty}\int_{\mathbb{R}^2} \frac{\lambda p\|\mathbf{x\text{-}D}\|^{-\alpha} z^{\alpha}}{(1 + \|\mathbf{x\text{-}D}\|^{-\alpha} z^{\alpha}\omega)^2}\left(1 - p + p\frac{1}{1 + (T - \omega)^{+} z^{\alpha}\|\mathbf{x\text{-}D}\|^{-\alpha}}\right) d\mathbf{x} \\
&\quad \cdot e^{-\lambda\int_{\mathbb{R}^2} 1 - \left(1 - p + \frac{p}{1 + \|\mathbf{y\text{-}D}\|^{-\alpha} z^{\alpha}\omega}\right)\left(1 - p + p\frac{1}{1 + (T-\omega)^{+} z^{\alpha}\|\mathbf{y\text{-}D}\|^{-\alpha}}\right) d\mathbf{y}} d\omega - e^{-c_1} \\
&\overset{b}{=} \int_0^{\infty}\left(p\lambda c_3 z^2 \omega^{\frac{2}{\alpha} - 1} - c_2\lambda p^2 z^2 f_1(\omega)\right) e^{-\lambda p(1-p) c_1 z^2 f_2(\omega) - \lambda p^2 c_1 z^2 f_3(\omega)} d\omega - e^{-k_1},
\end{aligned} \tag{4.11}
$$

where $k_1 = \delta\pi\lambda p z^2 T^{\delta}\Gamma(1-\delta)\Gamma(\delta)$, $f_1(\omega) = (T-\omega)^{+}\omega^{\frac{2}{\alpha} - 2}{}_2F_1\left(1, 2 - \frac{2}{\alpha}; 3; 1 - \frac{(T-\omega)^{+}}{\omega}\right)$; $f_2(\omega) = \omega^{\frac{2}{\alpha}} + [(T-\omega)^{+}]^{\frac{2}{\alpha}}$; $f_3(\omega) = \frac{[(T-\omega)^{+}]^{1+\frac{2}{\alpha}} - \omega^{1+\frac{2}{\alpha}}}{(T-\omega)^{+} - \omega}$; $c_1 = 2\pi/\alpha B(1 - \frac{2}{\alpha}, \frac{2}{\alpha})$; $c_2 = \frac{2\pi B(2 - \frac{2}{\alpha}, 1 + \frac{2}{\alpha})}{\alpha}$; $c_3 = \frac{2\pi B(1 - \frac{2}{\alpha}, 1 + \frac{2}{\alpha})}{\alpha}$; $\overset{a}{=}$ comes from averaging over Φ and $\overset{b}{=}$ comes from Appendix A.2. The results on

the outage probability of combining retransmission with energy accumulation is summarized in the following Lemma.

Lemma 9 *In a massive MTC network, the outage probability under retransmission with energy accumulation from the MTD can be expressed as*

$$P^{re,EA} = 1 - \int_0^{\infty} \left(p\lambda c_3 z^2 \omega^{\frac{2}{\alpha}-1} - c_2 \lambda p^2 z^2 f_1(\omega) \right) e^{-\lambda p(1-p) c_1 z^2 f_2(\omega) - \lambda p^2 c_1 z^2 f_3(\omega)} d\omega, \quad (4.12)$$

where $f_1(\omega) = (T-\omega)^+ \omega^{\frac{2}{\alpha}-2} {}_2F_1\left(1, 2-\frac{2}{\alpha}; 3; 1-\frac{(T-\omega)^+}{\omega}\right)$; $f_2(\omega) = \omega^{\frac{2}{\alpha}} + [(T-\omega)^+]^{\frac{2}{\alpha}}$; $f_3(\omega) = \frac{[(T-\omega)^+]^{1+\frac{2}{\alpha}} - \omega^{1+\frac{2}{\alpha}}}{(T-\omega)^+ - \omega}$; $c_1 = \frac{2\pi}{\alpha} B(1-\frac{2}{\alpha}, \frac{2}{\alpha})$; $c_2 = \frac{2\pi B(2-\frac{2}{\alpha}, 1+\frac{2}{\alpha})}{\alpha}$; $c_3 = \frac{2\pi B(1-\frac{2}{\alpha}, 1+\frac{2}{\alpha})}{\alpha}$.

Similarly as the analysis in Appendix A.3, by replacing $(T-\omega)^+$ with $\frac{(T-\omega)^+}{1+\omega}$ in Lemma 9, we can get the outage probability in the case under mutual information accumulation, which is summarized in the following Lemma.

Lemma 10 *In a massive MTC network, the outage probability under retransmission with mutual information accumulation from the MTD can be expressed as*

$$P^{re,MIA} = 1 - \int_0^{\infty} \left(p\lambda c_3 z^2 \omega^{\frac{2}{\alpha}-1} - c_2 \lambda p^2 z^2 f_4(\omega) \right) e^{-\lambda p(1-p) c_1 z^2 f_5(\omega) - \lambda p^2 c_1 z^2 f_6(\omega)} d\omega, \quad (4.13)$$

where $f_4(\omega) = \frac{(T-\omega)^+ \omega^{\frac{2}{\alpha}-2}}{1+\omega} {}_2F_1\left(1, 2-\frac{2}{\alpha}; 3; 1-\frac{(T-\omega)^+}{\omega(1+\omega)}\right)$; $f_5(\omega) = \omega^{\frac{2}{\alpha}} + [\frac{(T-\omega)^+}{1+\omega}]^{\frac{2}{\alpha}}$; $c_1 = \frac{2\pi}{\alpha} B(1-\frac{2}{\alpha}, \frac{2}{\alpha})$; $c_2 = \frac{2\pi B(2-\frac{2}{\alpha}, 1+\frac{2}{\alpha})}{\alpha}$; $c_3 = \frac{2\pi B(1-\frac{2}{\alpha}, 1+\frac{2}{\alpha})}{\alpha}$; $f_6(\omega) = \frac{[\frac{(T-\omega)^+}{1+\omega}]^{1+\frac{2}{\alpha}} - \omega^{1+\frac{2}{\alpha}}}{\frac{(T-\omega)^+}{1+\omega} - \omega}$.

Another method to improve the performance of massive machine type communication network is to use cooperative transmission. Basically, if a MTD can decode the packet and the MTD is much close to the eNodeB, then this MTD can serve as a relay for the outage MTD. Under the designed cooperative strategy, the event that the typical eNodeB is in outage after retransmission can be divided into two exclusive events: 1) if there exists at least one potential relay and the typical eNodeB fails to decode the retransmission from the selected relay; 2) if there is no potential relay and the typical eNodeB fails to decode the retransmission packet from the typical MTD. Denote

the first transmission from the typical MTD fails as event B. Denote there is at least one potential relay as event A. Denote the retransmission from the selected relay succeeds as event E and denote retransmission from the typical MTD succeed as event F. The outage probability of the designed cooperative strategy can be expressed as

$$P^{co} = \mathbb{P}(B) - \mathbb{P}(A \cap B \cap E) - \mathbb{P}(A^c \cap B \cap F), \tag{4.14}$$

where A^c denotes the complement of A and $\mathbb{P}(B) = 1 - e^{-k_1}$ is the outage probability of the first transmission [80]. $\mathbb{P}(A \cap B \cap E)$ is the probability that the outage eNodeB successfully decode the retransmission from a selected relay. $\mathbb{P}(A^c \cap B \cap F)$ is the probability that there is no potential relay for the outage eNodeB and the outage eNodeB successfully decode the retransmission from the typical MTD. Note that event A, B and E are correlated together due to spatiotemporally correlated interference. Basically, the interference at the typical eNodeB during the first transmission $I_{d,1}$ and the interference at the typical eNodeB during the retransmission $I_{d,2}$ are temporally correlated; the interference at the typical eNodeB during the first transmission $I_{d,1}$ and the interference at the selected relay during the first transmission $I_{r,1}$ are spatially correlated. These spatiotemporally correlated interference will significantly affect the performance analysis of cooperative strategies. Before we go deep into the calculation of $\mathbb{P}(A \cap B \cap E)$, let's first look at the probability of finding potential relays while the eNB fails to decode the first transmission, i.e., $\mathbb{P}(A \cap B)$.

4.2.1 Probability of Finding Potential Relays

Recall that in a massive MTC network, the potential relays for an outage MTD are those inactive MTDs which meet two conditions: 1) the potential relays have successfully decoded the packet; 2) the potential relays are within the cooperative region $\mathscr{A}_r$. To simplify our analysis, we assume that for any inactive MTD $\mathbf{y}$ inside the cooperative region, its distance to the typical MTD and other active MTDs can be approximated to the corresponding distance to the typical eNodeB, i.e, $\|\mathbf{x} - \mathbf{y}\| \approx \|\mathbf{x}\|$, where $\mathbf{x} \in \Phi_a^k$. This assumption is accurate as most of the outage events happen

at the boundary of the cell, which means the radius of cooperative region is far smaller than the transceiver distance of the typical link, i.e., $R_r \ll z$. The accuracy of this approximation is further justified by simulation results in the following section. Note that within the cooperative region $\mathscr{A}_r$, the locations of inactive MTDs are HPPP with intensity of $(1-p)\lambda$. The number of inactive MTDs in $\mathscr{A}_r$, denoted as $\mathscr{N}$, is a Poisson random number with average $a = \pi R_r^2(1-p)\lambda$. The number of potential relays, denoted as $\mathscr{M}$, is also a random variable. It is quite difficult to directly calculate the expression of $\mathbb{P}(A \cap B)$ because event A includes various sub-events, i.e., different combinations of relays who can decode the packet. Instead, we can calculate the complement of event $A \cap B$. By De Morgan's law, the probability that there is at least one potential relay can be expressed as

$$\mathbb{P}(A \cap B) = 1 - \mathbb{P}(A^c) - \mathbb{P}(B^c) + \mathbb{P}(A^c \cap B^c), \tag{4.15}$$

where $\mathbb{P}(A^c)$ is the probability that no potential relay can be found after the first transmission; $\mathbb{P}(A^c \cap B^c)$ is the probability that the first transmission succeed while there is no potential relay. In the following, we show some detailed derivation of the probability that no potential relay can be found after the first transmission. Note that there are two cases that no potential relay can be found: 1) there is no inactive user in the cooperative region; 2) there are $k, k = 1, 2, ...,$ inactive users in the cooperative region, however, all these inactive users fail to decode the packet in the first slot. Therefore,

$$\mathbb{P}(A^c) = \mathbb{P}(\mathscr{N} = 0) + \sum_{k=1}^{\infty} \mathbb{P}(\mathscr{N} = k)\mathbb{P}(SIR_{k,1} < T, \cdots, SIR_{1,1} < T) \tag{4.16}$$

where $\mathscr{N}$ denotes the number of inactive users in the cooperative region. Recall that $\mathscr{N}$ is Poisson distributed with average of $a = \pi R_r^2(1-p)\lambda$, therefore, $\mathbb{P}(\mathscr{N} = 0) = e^{-a}$. By substituting the

expression of $SIR_{k,1}$ and averaging over the small scaling fading, we can get

$$\mathbb{P}(A^c) = e^{-a} + \sum_{k=1}^{\infty} \frac{e^{-a}a^k}{k!} \mathbb{E}\left[\prod_{j=1}^{k}(1-e^{-Tz^{\alpha}I_{j,1}})\right]. \tag{4.17}$$

It is not convenient to average over multiplication of multiple items, $\mathbb{E}\left[\prod_{j=1}^{k}(1-e^{-Tz^{\alpha}I_{j,1}})\right]$. Instead, we can express the multiplication out and get the following,

$$\mathbb{P}(A^c) = e^{-a} + \sum_{k=1}^{\infty} \frac{e^{-a}a^k}{k!} \mathbb{E}\left[1 + \sum_{j=1}^{k}(-1)^j C_k^j e^{-Tz^{\alpha}\sum_{i=1}^{j} I_{i,1}}\right], \tag{4.18}$$

where $C_k^j = \frac{k!}{j!(k-j)!}$. Then, we can do average on each items in the summation. By changing the summation in the exponent to the multiplication of exponential functions and note that $\sum_{k=0}^{\infty}\frac{a^k}{k!} = e^a$, we can get

$$\mathbb{P}(A^c) = 1 + \sum_{k=1}^{\infty} \frac{e^{-a}a^k}{k!} \sum_{j=1}^{k}(-1)^j C_k^j \mathbb{E}\left(\prod_{i=1}^{j}\prod_{\mathbf{x}_m\in\Phi_a^1} e^{-\frac{Tz^{\alpha}G_{m,i,1}}{\|\mathbf{x}_m\|^{\alpha}}}\right) \tag{4.19}$$

Averaging over the small scale fading $G_{m,i,1}$ and using the PGFL, we can get

$$\begin{aligned}\mathbb{P}(A^c) &= 1 + \sum_{k=1}^{\infty} \frac{e^{-a}a^k}{k!} \sum_{j=1}^{k}(-1)^j C_k^j e^{-2\pi p\lambda \int_0^{\infty}\left(1-\frac{1}{(1+Tz^{\alpha}v^{-\alpha})^j}\right)vdv} \\ &\triangleq 1 + \sum_{k=1}^{\infty} \frac{e^{-a}a^k}{k!} \sum_{j=1}^{k}(-1)^j C_k^j e^{-p\lambda g(j)},\end{aligned} \tag{4.20}$$

where $C_k^j = \frac{k!}{j!(k-j)!}$, $g(j) \triangleq \pi T^{\delta} z^2 \frac{\pi\delta}{\sin(\pi\delta)} \sum_{i=1}^{j} C_j^i \frac{\Gamma(\delta)}{\Gamma(i)\Gamma(\delta-i+1)}$ which is similar to the definition of F_n in [80]. The following Lema summaries the above derivation,

Lemma 11 *In a massive MTC network, the probability that no potential relay can be found after the first transmission is*

$$\mathbb{P}(A^c) = 1 + \sum_{k=1}^{\infty} \frac{e^{-a}a^k}{k!} \sum_{j=1}^{k}(-1)^j C_k^j e^{-p\lambda g(j)} \tag{4.21}$$

where $g(j) \triangleq \pi T^{\delta} z^2 \frac{\pi\delta}{\sin(\pi\delta)} \sum_{k=1}^{j} C_j^k \frac{\Gamma(\delta)}{\Gamma(k)\Gamma(\delta-k+1)}$.

In the following, we are going to derive the probability that there is no potential relay in the cooperative region while the first transmission is successful, i.e., $\mathbb{P}(A^c \cap B^c)$. Note that the event A and B are not independent, so the probability $\mathbb{P}(A^c \cap B^c)$ cannot be split into the product of two probabilities of $\mathbb{P}(A^c)$ and $\mathbb{P}(B^c)$. The result of $\mathbb{P}(A^c \cap B^c)$ is summarized in the following Lema and the proof is in the appendix.

Lemma 12 *In a massive MTC network, the probability that no potential relay can be found while MTD's first transmission is successful can be expressed as*

$$\mathbb{P}(A^c \cap B^c) = \sum_{k=1}^{\infty} \sum_{j=1}^{k} \frac{e^{-a} a^k}{k!} (-1)^j C_k^j e^{-p\lambda g(j+1)} + e^{-k_1}. \tag{4.22}$$

where $k_1 = \delta\pi\lambda p z^2 T^{\delta} \Gamma(1-\delta)\Gamma(\delta)$.

Proof 11 *See Appendix A.5.*

Substitute (4.21) (4.22) into (4.15), the probability of finding potential relays for the outage MTD can be summarized into the following theorem:

Theorem 5 *In a massive MTD network, the probability that the outage typical MTD can find at least one potential relay is*

$$\mathbb{P}(A \cap B) = \sum_{k=1}^{\infty} \sum_{j=1}^{k} \frac{e^{-a} a^k}{k!} (-1)^j C_k^j \left(e^{-p\lambda g(j+1)} - e^{-p\lambda g(j)} \right), \tag{4.23}$$

where $C_k^j \triangleq \frac{k!}{j!(k-j)!}$, $g(j) \triangleq \pi T^{\delta} z^2 \frac{\pi\delta}{\sin(\pi\delta)} \sum_{i=1}^{j} C_j^i \frac{\Gamma(\delta)}{\Gamma(i)\Gamma(\delta-i+1)}$.

Note that $\mathbb{P}(A \cap B)$ can also be interpreted as the portion of MTDs which are forwarding the data for other outage MTDs. In a massive MTC network, it is quite common that MTDs are inactive/idle for most of time. Therefore, by allowing inactive MTDs to forward the data of outage MTDs, we save the investment of deploying specific relays. Furthermore, for a specific deployed relay, it is

not guaranteed that the relay can decode the packet when the source MTD is in outage. However, in our designed cooperative strategy, only the inactive node which has already decoded the packet in the first time-slot is selected. Therefore, we can expect that our designed cooperative strategy can further reduce the outage probability. In the derivation of Theorem 5, the spatiotemporal correlation of interference is considered. As a benchmark, if the correlation of interference is neglected, i.e., interference at different locations and time slots are independent, the probability of finding potential relays for the outage MTD will be the multiplication of two events: the first event is the MTD is in outage, of which the probability can be expressed as $1-e^{-k_1}$; the second event is there is no potential relay in the cooperative region. Note that the number of inactive MTDs in the cooperative region is a Poisson distribution with an average of $a=\pi R_r^2(1-p)\lambda$. Since every node in the cooperative region can decode independently with a probability of e^{-k_1} (under the independent assumption), the number of potential relay in the cooperative region is also a Poisson distribution with an average of ae^{-k_1}. Therefore, under the independent assumption, the probability that there is at least one potential relay in the cooperative region, the second event, can be expressed as $1-e^{-ae^{-k_1}}$. Therefore, under independent interference assumption, the probability that the outage typical MTD can find at least one potential relay is summarized in the following Lemma.

Lemma 13 *In a massive MTC network, the probability that the outage typical MTD can find at least one potential relay under independent interference assumption is*

$$\mathbb{P}^*(A\cap B)=(1-e^{-k_1})(1-e^{-ae^{-k_1}}). \tag{4.24}$$

where $k_1=\delta\pi\lambda pz^2T^{\delta}\Gamma(1-\delta)\Gamma(\delta)$ *and* $a=\pi R_r^2(1-p)\lambda$.

4.2.2 Outage Probability Analysis

If the typical eNodeB can find a potential relay for the outage typical MTD, the selected relay will retransmit the packet to the typical eNodeB. Whether the typical eNodeB can decode the packet

after retransmission depends on the received signal and interference. Assume the potential relay $\mathbf{y}$ is selected to do the retransmission. The distance from $\mathbf{y}$ to the typical eNodeB, denoted as y, is a random variable. It is untractable to find the real distribution of y, however, under our previous assumption of $\|\mathbf{x}-\mathbf{y}\| \approx \|\mathbf{x}\|, \forall \mathbf{x} \in \Phi_a^k$, the distribution of y can be calculated out because all the inactive mobile user within the assist region will have an identical probability of becoming potential relays. The distribution of y is summarized into the following lemma:

Lemma 14 *In a massive MTC network, if the relay is uniformly randomly selected from potential relays, the distribution of the distance from the selected relay to the typical outage eNodeB, y, can be expressed as*

$$f_y(y) = \frac{2y}{R_r^2}. \tag{4.25}$$

Note that the locations of selected relays cannot be modeled as a PPP because the process of selecting relays is not an independent thinning of the original PPP. However, the location of active MTDs which includes selected relays and active MTDs can still be approximated as a PPP. This is because the active relays can be regarded as random displacement of outage MTDs and random displacement of a PPP will generate another PPP as indicated in [85].

It is quite challenging to directly calculate $P(A \cap B \cap E)$ as A denotes that there is at least one potential relay. Instead the probability of A^c is much easier to calculate. By De Morgan's law, we can interchange intersection and union. Therefore,

$$\begin{aligned}
&\mathbb{P}(A \cap B \cap E) \\
&= 1 - \mathbb{P}(A^c) - \mathbb{P}(B^c) - \mathbb{P}(E^c) + \mathbb{P}(A^c \cap B^c) + \mathbb{P}(A^c \cap E^c) + \mathbb{P}(B^c \cap E^c) - \mathbb{P}(A^c \cap B^c \cap E^c) \\
&= \mathbb{P}(A \cap B) - \mathbb{P}(E^c) + \mathbb{P}(A^c \cap E^c) + \mathbb{P}(B^c \cap E^c) - \mathbb{P}(A^c \cap B^c \cap E^c).
\end{aligned} \tag{4.26}$$

The probability that retransmission from the selected relay can be successfully decoded by the typical eNodeB can be expressed in the following lemma.

Lemma 15 *In a massive MTC network, the probability that the typical eNodeB can successfully*

decode the retransmission from the selected relay can be expressed as

$$\mathbb{P}(A \cap B \cap E) = \int_0^{R_r} P_{re}^s(y) 2y / R_r^2 dy, \tag{4.27}$$

where

$$P_{re}^s(y) = \sum_{k=1}^{\infty} \sum_{j=1}^{k} \frac{e^{-a} a^k}{k!} C_k^j \left(g_2(j+1, y) - g_2(j, y) \right), \tag{4.28}$$

which represents the probability that the typical eNodeB successfully decodes the retransmission from the selected relay given y, and

$$g_2(j, y) \triangleq \exp\left(-2\pi\lambda \int_0^{\infty} \rho - \left(1 - p + \frac{p}{1 + \rho^{-\alpha} y^{\alpha} T} \right) \left(1 - p + \frac{p}{(1 + \rho^{-\alpha} z^{\alpha} T)^j} \right) \rho d\rho \right). \tag{4.29}$$

Proof 12 *See Appendix A.6.*

If there is no potential relay in the cooperative region, the typical MTD will retransmit the packet. The probability that the typical eNodeB can successfully decode the retransmission packet from the typical MTD can be expressed in the following lemma.

Lemma 16 *In a massive MTC network, when there is no potential relay, the probability that MTD' retransmission succeeds is*

$$\mathbb{P}(A^c \cap B \cap F) = e^{-k_1} - e^{-a - 2k_1 + p(1-\delta)k_1} + \sum_{k=1}^{\infty} \sum_{j=1}^{k+1} \frac{(-1)^j e^{-a} a^k (k+1)}{j!(k+1-j)!} e^{-pg(j+1)\lambda}, \tag{4.30}$$

where $k_1 = \delta \pi \lambda p z^2 T^{\delta} \Gamma(1-\delta) \Gamma(\delta)$.

Proof 13 *Proof can be found in Appendix A.7.*

Note that here the retransmission probability $\mathbb{P}(A^c \cap B \cap F)$ is quite different from the retransmission probability defined in equation (4.7). This is because in our designed strategy retransmission

from the typical MTD only happens when there is no potential relay. Finally, the outage probability for a massive MTC network under our designed cooperative strategy can be obtained by substitute (4.27) and (4.30) to (4.14), which is summarized as:

Theorem 6 *In a massive MTC network, the outage probability for a typical MTD link under our designed cooperative strategy can be expressed as*

$$P^{co} = 1 - 2e^{-k_1} + e^{-a-2k_1+p(1-\delta)k_1} - \sum_{k=1}^{\infty}\sum_{j=1}^{k+1} \frac{(-1)^j e^{-a} a^k (k+1)}{j!(k+1-j)!} e^{-p\lambda(g(j)-(1-p)g(1)-p(g(j+1)-g(j)))}$$
$$- \sum_{k=1}^{\infty}\sum_{j=1}^{k} \frac{(-1)^j e^{-a} a^k}{j!(k-j)!} \int_0^{R_r} \frac{2y}{R_r^2}(g_2(j+1,y) - g_2(j,y))dy, \tag{4.31}$$

where $k_1 = \delta\pi\lambda p z^2 T^{\delta}\Gamma(1-\delta)\Gamma(\delta)$, $a = \pi R_r^2(1-p)\lambda$ *and* $g_2(j,y)$ *is defined in equation* (4.29).

4.3 Evaluation Results

In this section, numerical and Monte Carlo simulation results are presented to verify our theoretical analysis and to demonstrate the performance gain of mutual information accumulation as well as our designed cooperative strategy in massive MTC networks. Fig. 4.2 shows both simulation and numerical results on the outage probability of retransmission under three different strategies: pure retransmission, retransmission with energy accumulation and retransmission with mutual information accumulation. In this figure, $\lambda = 10^{-3}m^{-2}$, $p = 0.001$, $z = 400m$ and $\alpha = 4$. From this figure, we can observe that mutual information accumulation can reduce the network outage in both low SINR regime and high SINR regime compared to energy accumulation. Furthermore, we find that the outage probability achieved by mutual information accumulation will approximate to the outage probability of energy accumulation when the decoding threshold is low. However, when the decoding threshold is high, the outage probability of mutual information accumulation will be much lower that the outage probability of energy accumulation and the outage probability of energy accumulation approximates to the outage probability of retransmission. Basically, this

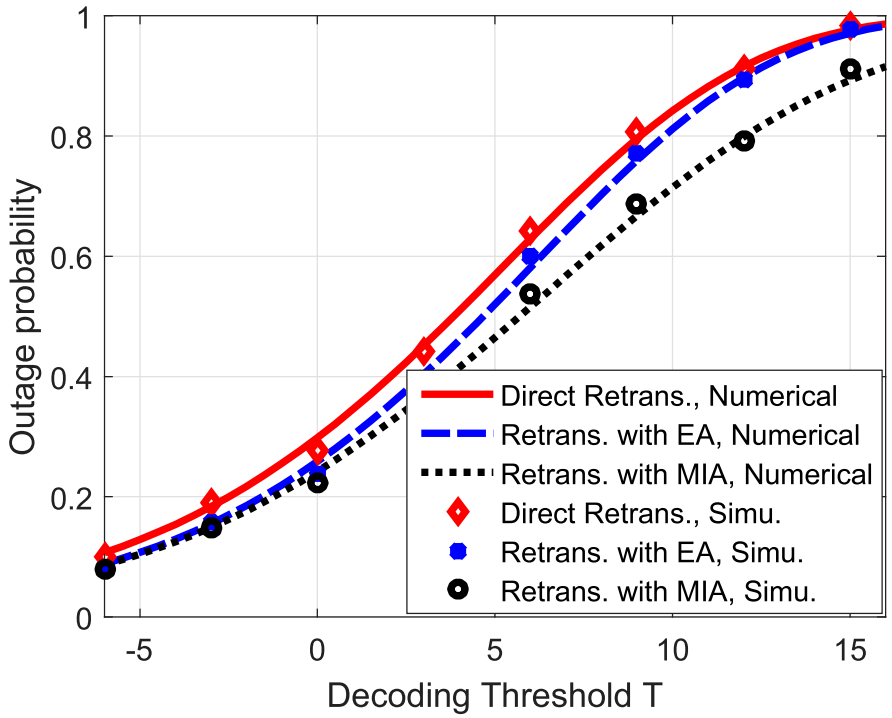

Figure 4.2: Compare of outage probability under three retransmission strategies

result indicates that in high SINR regime energy accumulation or MRC cannot reduce too much outage in MTC networks as the combined energy is not high enough for decoding. However, by directly combining mutual information, the destination can decode the packet. Fig. 4.3 shows the probability of finding potential relays as a function of the cooperative radius R_r. In this figure, $T = 2dB, \alpha = 4, p = 0.001, z = 400$. This figure justifies the correctness of our theoretical analysis. Furthermore, we can find that independent interference assumption overestimates the probability of finding potential relays and the corresponding results are far away from simulation results. Therefore, we can conclude that in massive MTC networks, the analysis has to consider spatiotemporal correlation of interference.

Fig. 4.4 presents simulation results as well as numerical results on the probability of outage for both conventional retransmission P^{re} and our cooperative strategy P^{co}. In this figure, each point is an average over 5,000 realizations and $\lambda = 10^{-3}m^{-2}, p = 0.001, \alpha = 4, z = 400m$. From this figure, we can see that our designed cooperative strategy can significantly reduce the outage

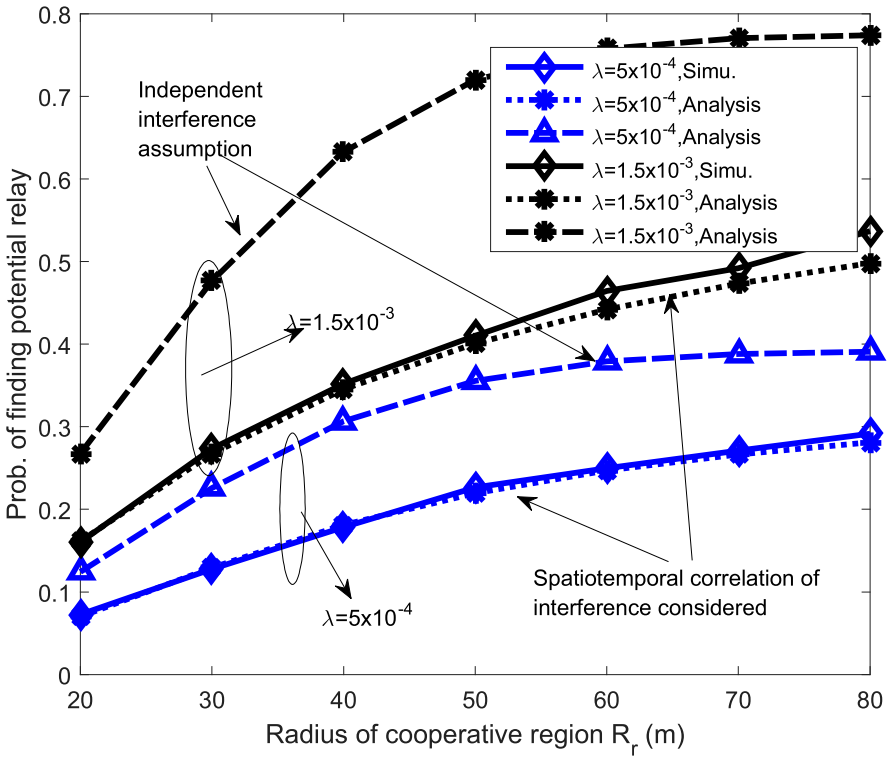

Figure 4.3: Probability of finding potential relays

probability compared to conventional retransmission. Specifically, with a decoding threshold of 2dB, the outage probability of massive MTC network with cooperative region of 65 m is 14.5% while corresponding conventional retransmission has an outage probability of 39.7%. Note that the outage probability of conventional retransmission is higher than the outage probability of the first time-slot transmission (which is 37.0%) due to the temporally correlated interference. The reason why our designed cooperative strategy can reduce the outage probability is because :1) the relay is selected only when it can decode the packet; 2) the selected relay within the cooperative region is much closer to the eNodeB. Furthermore, we can find that as the radius of cooperative region becomes small, the outage probability of cooperative communication will approach to the outage probability of conventional retransmission. This is because as the cooperative region reduces, it is difficult to find potential relays. Finally, the numerical results match simulation results quite well, which verifies our theoretical analysis and assumptions once more.

Fig. 4.5 shows simulation results of coverage probability as a function of cooperative radius.

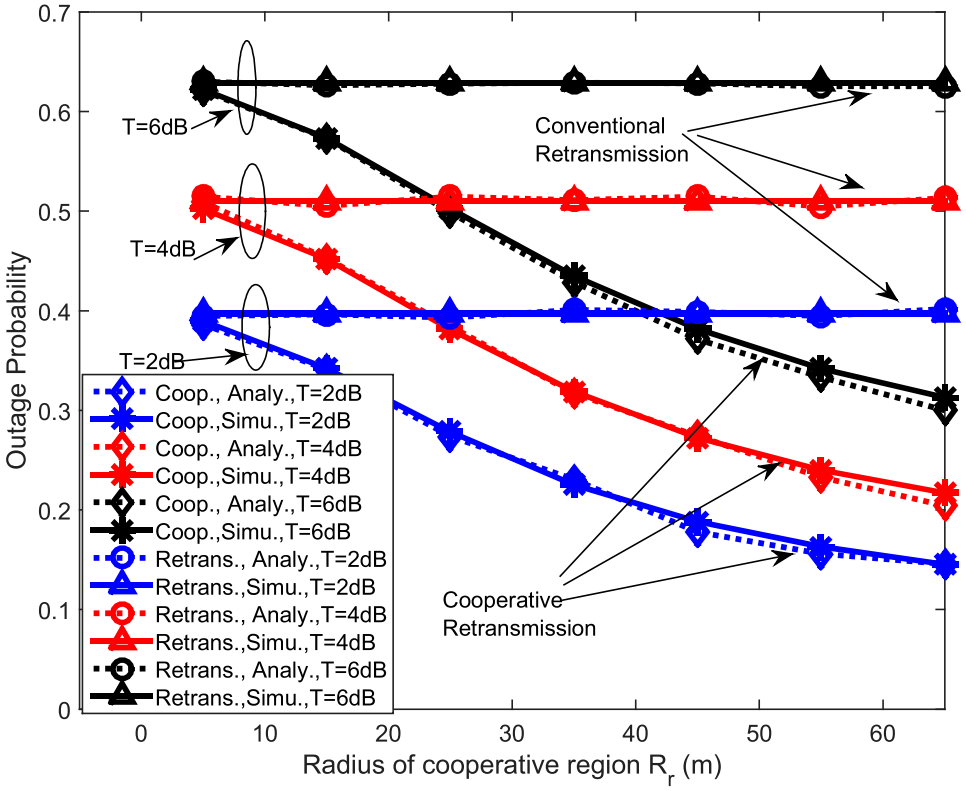

Figure 4.4: Outage probability as a function of cooperative radius

Four different strategies are compared: 1) retransmission from the typical MTD; 2) cooperative retransmission; 3) cooperative retransmission with energy accumulation; 4) cooperative retransmission with mutual information accumulation. In this figure, the source-destination distance is $z = 400m$, $\alpha = 4$, decoding threshold $T = 10$dB, access probability $p = 0.001$. From this figure, we can find that compared to retransmission, cooperative retransmission can improve the coverage probability from 0.15 to more than 0.45. Furthermore, compared to pure cooperation with no accumulation, energy accumulation can further improve the coverage probability by $10\% \sim 76\%$ under different cooperative radius.

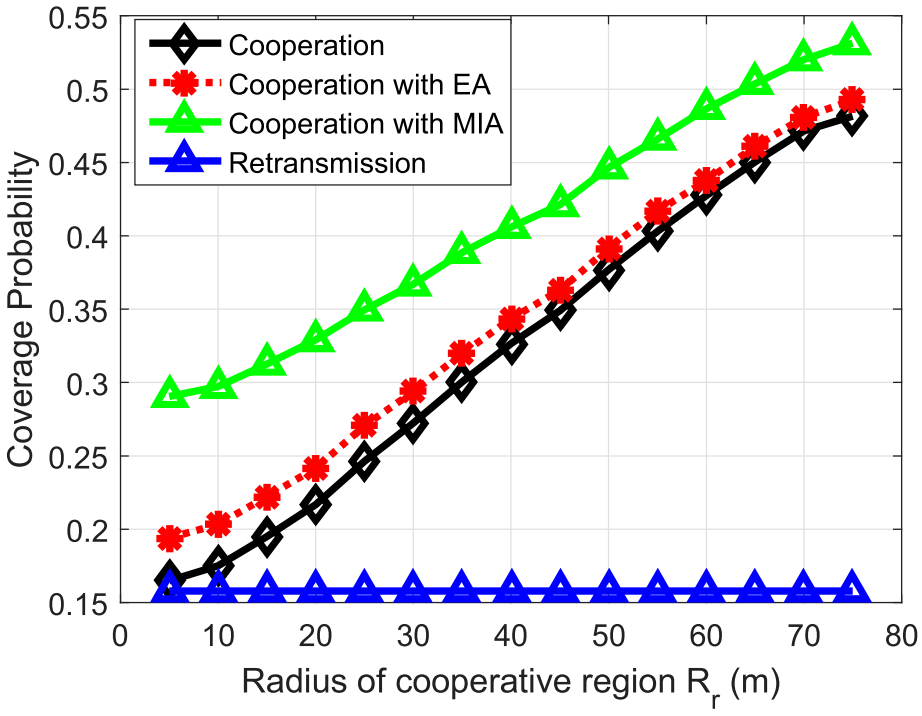

Figure 4.5: Coverage probability as a function of cooperative radius

4.4 Conclusions

In this chapter, we analyze the retransmission performance of massive MTC networks with mutual information accumulation. Furthermore, we design and analyze a novel cooperative strategy for massive MTC networks where inactive MTDs are allowed to act as relays for outage MTDs. Using point process theory, analytical expressions of outage probability for this kind of massive MTC network are obtained. Both numerical and simulation results show the potential of cooperative communication in massive MTC networks.

Chapter 5

Summary and Future Work

This dissertation is to make fundamental analysis on the performance of wireless networks with advanced physical layer technique, mutual information accumulation, and design new network scheduling/transmission protocols or strategies to explore the full potentials of mutual information in various wireless networks. To achieve this goal, we first make fundamental analysis on the asymptotic performance of mutual information accumulation in an infinite 2-dimensional(2-D) grid network. Then, we investigate the optimal routing in cognitive radio networks with mutual information accumulation and derive the corresponding closed-form cooperative gain obtained by applying mutual information accumulation in cognitive radio networks. Finally, we characterize the performance of mutual information accumulation in random networks using tools from stochastic geometry. The analysis presented in this dissertation guide us to develop both centralized and distributed routing and resource allocation algorithms for cognitive radio networks with mutual information accumulation. Furthermore, the analysis methodology provides us a solid tool to analyze the performance of massive machine type network with mutual information accumulation. The insights obtained from this work include the following system design guidelines.

- By exploring the broadcast nature of wireless channels, mutual information accumulation can provide much more gain in two dimensional or three dimensional networks compared to one dimensional network.

- Mutual information accumulation can provide better performance in the scenario where the signal-to-interference-plus-noise (SINR) ratio is high or when the decoding SINR threshold is high compared to energy accumulation. The performance of mutual information accumulation will approximate to the performance of energy accumulation in low SINR regime or when the decoding SINR threshold is low.

- Cooperative transmission using mutual information accumulation can achieve higher cooperative gain in cognitive radio network with tight interference threshold constraint. Cooperative transmission using mutual information accumulation can achieve higher cooperative gain in the scenario with high interference.

- In underlay cognitive radio networks, the optimal routing and resource allocation under mutual information accumulation is quite different from the that under traditional decode-and-forward strategy. Instead of allocating all the spectrum to the nodes in the route one-by-one, it may be beneficial to split spectrum resource between two neighbor nodes and let two nodes transmit concurrently.

- In random networks, spatiotemporal correlation of interference will strongly affect the performance analysis of wireless networks. Independent assumption on interference at different locations and in different time slots will lead to inaccurate analytical results.

- The optimal location of the relay node in a cooperative network with mutual information accumulation is much closer to the source node compared to the optimal location under energy accumulation or decode-and-forward strategy.

The results in this dissertation lead to new research questions on the topics of mutual information accumulation over wireless networks. Further extensions of mutual information accumulation over wireless networks include the following topics.

- Analysis of Queueing Delay in Wireless Networks with Mutual Information Accumulation: In this dissertation, the analysis on mutual information accumulation is focused on the trans-

mission of one packet. For a given packet, we know that mutual information accumulation can reduce the transmission time of this packet. We can expect that mutual information accumulation will also reduce the queueing delay in wireless networks. However, it is still unclear how much queue delay we can reduce by using mutual information accumulation, especially the coding delay may need to be taken into account when mutual information accumulation is used as new redundancy version of the packet needs to be generated. Based on the analytical results, revision on the back-pressure routing algorithm, which is one of the optimal scheduling and routing algorithms to achieve maximum stable throughput in wireless networks, may be needed to explore the full potential of mutual information accumulation in the scheduling of wireless networks.

- Analysis of Mutual Information Accumulation in Random Multi-hop Wireless Networks: In this dissertation, the analysis on mutual information accumulation in random networks is focused on a one-hop and two-hop cases. It is still unclear on the performance of mutual information accumulation in multi-hop random networks. Results on multi-hop networks will help us understand the achievable network throughput or the network capacity, which remains as an open question in information theory field. As we have already witnessed the complex expression of the coverage probability in a two-hop special case, multi-hop analysis will be much more challenging. Spatiotemporal correlated interference is one of the main obstacles. New approximation and simplification techniques are needed to get an elegant and accurate analytical results.

References

[1] "IMT Vision-Framework and overall objectives of the future development of IMT for 2020 and beyond," International Telecommunications Union (ITU), July 2015.

[2] "ITU ICT Facts and Figures - The world in 2015," International Telecommunications Union (ITU), May 2015.

[3] "Cisco visual networking index: Global mobile data traffic forecast update, 2014-2019," Cisco Systems, May 2015.

[4] "Cisco visual networking index: Forecast and methodology, 2014-2019," Cisco Systems, May 2015.

[5] IMT-2020 (5G) Promotion Group, "5G Vision and Requirements," Dec 2015.

[6] L. Liu, "On delay-sensitive communication over wireless networks," Ph.D. dissertation, Texas A&M University, 2008.

[7] P. Gupta and P. R. Kumar, "The capacity of wireless networks," vol. 46, no. 2, pp. 388–404, March 2000.

[8] M. Haenggi, *Stochastic Geometry for Wireless Networks*. Cambridge University Press, November 2012.

[9] K. Letaief and W. Zhang, "Cooperative communications for cognitive radio networks," *Proc. IEEE*, vol. 97, no. 5, pp. 878–893, May 2009.

[10] G. Caire and D. Tuninetti, "The throughput of hybrid-ARQ protocols for the Gaussian collision channel," *IEEE Trans. Inf. Theory*, vol. 47, no. 5, pp. 1971–1988, Jul 2001.

[11] R. Urgaonkar and M. J. Neely, "Optimal routing with mutual information accumulation in wireless networks," *IEEE J. Sel. Areas Commun.*, vol. 30, no. 9, pp. 1730–1737, October 2012.

[12] M. Luby, "Lt codes," in *Proc. IEEE FOCS 2002*, 2002, pp. 271–280.

[13] A. Shokrollahi, "Raptor codes," *IEEE Trans. Inf. Theory*, vol. 52, no. 6, pp. 2551–2567, June 2006.

[14] A. Molisch, N. Mehta, J. S. Yedidia, and J. Zhang, "Performance of fountain codes in collaborative relay networks," *IEEE Trans. Wireless Commun.*, vol. 6, no. 11, pp. 4108–4119, November 2007.

[15] B. Zhao and M. Valenti, "Practical relay networks: a generalization of hybrid-arq," *IEEE J. Sel. Areas Commun.*, vol. 23, no. 1, pp. 7–18, Jan 2005.

[16] S. Draper, L. Liu, A. Molisch, and J. S. Yedidia, "Cooperative transmission for wireless networks using mutual-information accumulation," *IEEE Trans. Inf. Theory*, vol. 57, no. 8, pp. 5151–5162, Aug 2011.

[17] J. Yang, Y. Liu, and S. Draper, "Optimal scheduling policies with mutual information accumulation in wireless networks," in *2012 IEEE INFOCOM*, March 2012, pp. 1062–1070.

[18] Y. Liu, J. Yang, and S. Draper, "Exploiting route diversity in multi-packet transmission using mutual information accumulation," in *2011 IEEE 49th Annu. Allerton Conf. on Commu., Contr., and Comput.*, September 2011, pp. 1793–1800.

[19] T. Girici and A. C. Kazez, "Energy efficient routing with mutual information accumulation," in *Proc. IEEE WiOpt 2012*, Paderborn, Germany, May 2012, pp. 425–430.

[20] T. J. Ali, S. Schedler, and V. Kuehn, "Energy minimisation in wireless multi-hop networks with mutual-information accumulation," in *Proc. VDE ISWCS 2013*, Ilmenau, Germany, Aug 2013, pp. 1–5.

[21] Y.-C. Liang, Y. Zeng, E. Peh, and A. T. Hoang, "Sensing-Throughput Tradeoff for Cognitive Radio Networks," *IEEE Trans. Wireless Commun.*, vol. 7, no. 4, pp. 1326–1337, April 2008.

[22] A. K. Sadek, K. J. R. Liu, and A. Ephremides, "Cognitive multiple access via cooperation: Protocol design and performance analysis," *IEEE Trans. Inf. Theory*, vol. 53, no. 10, pp. 3677–3696, Oct 2007.

[23] Q. Zhao and B. Sadler, "A survey of dynamic spectrum access," *IEEE Signal Process. Mag.*, vol. 24, no. 3, pp. 79–89, May 2007.

[24] L. B. Le and E. Hossain, "Resource allocation for spectrum underlay in cognitive radio networks," *IEEE Trans. Wireless Commun.*, vol. 7, no. 12, pp. 5306–5315, December 2008.

[25] H. Chen, L. Liu, J. Matyjas, and M. Medley, "Optimal resource allocation for sensing based spectrum sharing cognitive radio networks," in *Proc. IEEE GLOBECOM 2014*, Austin,TX, Dec 2014, pp. 899–904.

[26] M. Cesana, F. Cuomo, and E. Ekici, "Routing in cognitive radio networks: Challenges and solutions," *Ad Hoc Networks*, vol. 9, no. 3, pp. 228 – 248, 2011.

[27] Y. Hou, Y. Shi, and H. Sherali, "Optimal spectrum sharing for multi-hop software defined radio networks," in *Proc. IEEE INFOCOM 2007*, Anchorage, AK, May 2007, pp. 1–9.

[28] H. Chen, Q. Du, and P. Ren, "A joint routing and time-slot assignment algorithm for multi-hop cognitive radio networks with primary-user protection," *Internat. J. on Compu.,Commun. &Control*, vol. 7, no. 3, pp. 203–216, September 2012.

[29] K. Chowdhury and I. Akyildiz, "Crp: A routing protocol for cognitive radio ad hoc networks," *IEEE J. Sel. Areas Commun.*, vol. 29, no. 4, pp. 794–804, April 2011.

[30] M. Caleffi, I. Akyildiz, and L. Paura, "Opera: Optimal routing metric for cognitive radio ad hoc networks," *IEEE Trans. Wireless Commun.*, vol. 11, no. 8, pp. 2884–2894, August 2012.

[31] P. Gupta and P. Kumar, "The capacity of wireless networks," *IEEE Trans. Inf. Theory*, vol. 46, no. 2, pp. 388–404, Mar 2000.

[32] R. Yim, N. Mehta, A. Molisch, and J. Zhang, "Progressive accumulative routing: Fundamental concepts and protocol," *IEEE Trans. Wireless Commun.*, vol. 7, no. 11, pp. 4142–4154, November 2008.

[33] A. E. Khandani, J. Abounadi, E. Modiano, and L. Zheng, "Cooperative routing in static wireless networks," *IEEE Trans. Commun.*, vol. 55, no. 11, pp. 2185–2192, 2007.

[34] J. Chen, L. Jia, X. Liu, G. Noubir, and R. Sundaram, "Minimum energy accumulative routing in wireless networks," in *Proc IEEE INFOCOM 2005*, vol. 3, Miami, March 2005, pp. 1875–1886.

[35] W. Su, J. Matyjas, and S. Batalama, "Active cooperation between primary users and cognitive radio users in heterogeneous ad-hoc networks," *IEEE Trans. Signal Process.*, vol. 60, no. 4, pp. 1796–1805, April 2012.

[36] I. Maric and R. Yates, "Cooperative multihop broadcast for wireless networks," *IEEE J. Sel. Areas Commun.*, vol. 22, no. 6, pp. 1080–1088, Aug 2004.

[37] I. Maric and R. D. Yates, "Cooperative multicast for maximum network lifetime," *IEEE J. Sel. Areas Commun.*, vol. 23, no. 1, pp. 127–135, Jan 2005.

[38] Y. Hou, Y. Shi, and H. Sherali, "Spectrum sharing for multi-hop networking with cognitive radios," *IEEE J. Sel. Areas Commun.*, vol. 26, no. 1, pp. 146–155, Jan 2008.

[39] Cisco, "Cisco visual networking index: Global mobile data traffic forecast update 2015-2020 white paper," February 2016.

[40] J. Andrews, S. Buzzi, W. Choi, S. Hanly, A. Lozano, A. Soong, and J. Zhang, "What will 5G be?" *IEEE J. Sel. Areas Commun.*, vol. 32, no. 6, pp. 1065–1082, June 2014.

[41] H. S. Dhillon, H. C. Huang, and H. Viswanathan, "Wide-area wireless communication challenges for the internet of things," *CoRR*, vol. abs/1504.03242, 2015.

[42] T. C. y. Ng and W. Yu, "Joint optimization of relay strategies and resource allocations in cooperative cellular networks," *IEEE J. Sel. Areas Commun.*, vol. 25, no. 2, pp. 328–339, February 2007.

[43] G. Neonakis Aggelou and R. Tafazolli, "On the relaying capability of next-generation gsm cellular networks," *IEEE Pers. Commun.*, vol. 8, no. 1, pp. 40–47, Feb 2001.

[44] Z. Jingmei, S. Chunju, W. Ying, and Z. Ping, "Performance of a two-hop cellular system with different power allocation schemes," in *Proc. IEEE VTC2004-Fall*, vol. 6, Sept 2004, pp. 4538–4542.

[45] V. Sreng, H. Yanikomeroglu, and D. Falconer, "Coverage enhancement through two-hop relaying in cellular radio systems," in *Proc. IEEE WCNC 2002*, vol. 2, Mar 2002, pp. 881–885.

[46] G. Cocco, C. Ibars, and N. Alagha, "Cooperative coverage extension in heterogeneous machine-to-machine networks," in *Globecom Workshops (GC Wkshps), 2012 IEEE*, Dec 2012, pp. 1693–1699.

[47] C. Y. Ho and C. Y. Huang, "Energy-saving massive access control and resource allocation schemes for M2M communications in OFDMA cellular networks," *IEEE Wireless Commun. Lett.*, vol. 1, no. 3, pp. 209–212, June 2012.

[48] T. Abdelkader, K. Naik, A. Nayak, N. Goel, and V. Srivastava, "SGBR: A routing protocol for delay tolerant networks using social grouping," *IEEE Trans. Parallel Distrib. Syst.*, vol. 24, no. 12, pp. 2472–2481, Dec 2013.

[49] P. K. Verma, R. Verma, A. Prakash, A. Agrawal, K. Naik, R. Tripathi, T. Khalifa, M. Alsabaan, T. Abdelkader, and A. Abogharaf, "Machine-to-machine (M2M) communications: A survey," *Journal of Network and Computer Applications*, pp. –, 2016.

[50] C. Xie, K. C. Chen, and X. Wang, "To hop or not to hop in massive machine-to-machine communications," in *Wireless Communications and Networking Conference (WCNC), 2013 IEEE*, April 2013, pp. 1021–1026.

[51] S. Musa and W. Wasylkiwskyj, "Co-channel interference of spread spectrum systems in a multiple user environment," *IEEE Trans. Commun.*, vol. 26, no. 10, pp. 1405–1413, Oct 1978.

[52] E. Sousa and J. Silvester, "Optimum transmission ranges in a direct-sequence spread-spectrum multihop packet radio network," *IEEE J. Sel. Areas Commun.*, vol. 8, no. 5, pp. 762–771, Jun 1990.

[53] J. G. Andrews, F. Baccelli, and R. Ganti, "A tractable approach to coverage and rate in cellular networks," *IEEE Trans. Commun.*, vol. 59, no. 11, pp. 3122–3134, November 2011.

[54] F. Baccelli and B. Błaszczyszyn, "Stochastic geometry and wireless networks: Volume ii applications," *Found. Trends Netw.*, vol. 4, no. 1-2, pp. 1–312, January 2010.

[55] T. Novlan, H. Dhillon, and J. Andrews, "Analytical modeling of uplink cellular networks," *IEEE Trans. Wireless Commun.*, vol. 12, no. 6, pp. 2669–2679, June 2013.

[56] T. Novlan, R. Ganti, A. Ghosh, and J. Andrews, "Analytical evaluation of fractional frequency reuse for ofdma cellular networks," *IEEE Trans. Wireless Commun.*, vol. 10, no. 12, pp. 4294–4305, December 2011.

[57] X. Lin, J. G. Andrews, and A. Ghosh, "Spectrum sharing for device-to-device communication in cellular networks," *IEEE Trans. Wireless Commun.*, vol. 13, no. 12, pp. 6727–6740, Dec 2014.

[58] Q. Ye, M. Al-Shalash, C. Caramanis, and J. Andrews, "Device-to-device modeling and analysis with a modified matern hardcore bs location model," in *Global Communications Conference (GLOBECOM), 2013 IEEE*, Dec 2013, pp. 1825–1830.

[59] C. han Lee and M. Haenggi, "Interference and outage in poisson cognitive networks," *IEEE Trans. Wireless Commun.*, vol. 11, no. 4, pp. 1392–1401, April 2012.

[60] H. Dhillon, R. Ganti, F. Baccelli, and J. Andrews, "Modeling and analysis of k-tier downlink heterogeneous cellular networks," *IEEE J. Sel. Areas Commun.*, vol. 30, no. 3, pp. 550–560, April 2012.

[61] R. Ganti and M. Haenggi, "Interference and outage in clustered wireless ad hoc networks," *IEEE Trans. Inf. Theory*, vol. 55, no. 9, pp. 4067–4086, Sept 2009.

[62] M. Haenggi, "Diversity loss due to interference correlation," *Communications Letters, IEEE*, vol. 16, no. 10, pp. 1600–1603, October 2012.

[63] M. Haenggi and R. Smarandache, "Diversity polynomials for the analysis of temporal correlations in wireless networks," *IEEE Trans. Wireless Commun.*, vol. 12, no. 11, pp. 5940–5951, November 2013.

[64] J. Andrews, S. Weber, M. Kountouris, and M. Haenggi, "Random access transport capacity," *Wireless Communications, IEEE Transactions on*, vol. 9, no. 6, pp. 2101–2111, June 2010.

[65] R. Vaze, "Throughput-delay-reliability tradeoff with arq in wireless ad hoc networks," *IEEE Trans. Wireless Commun.*, vol. 10, no. 7, pp. 2142–2149, July 2011.

[66] R. Tanbourgi, H. Dhillon, J. Andrews, and F. Jondral, "Effect of spatial interference correlation on the performance of maximum ratio combining," *IEEE Trans. Wireless Commun.*, vol. 13, no. 6, pp. 3307–3316, June 2014.

[67] G. Nigam, P. Minero, and M. Haenggi, "Coordinated multipoint joint transmission in heterogeneous networks," *IEEE Trans. Commun.*, vol. 62, no. 11, pp. 4134–4146, Nov 2014.

[68] T. H. Cormen, C. E. Leiserson, R. L. Rivest, and C. Stein, *Introduction to Algorithms*, 3rd ed. The MIT Press, 2009.

[69] J. M. Ciofli, *A multicarrier primer.* ANSI T1E1, 1991, vol. 4.

[70] H. Balakrishnan, P. Iannucci, J. Perry, and D. Shah, "De-randomizing shannon: The design and analysis of a capacity-achieving rateless code," *CoRR*, vol. abs/1206.0418, 2012. [Online]. Available: http://arxiv.org/abs/1206.0418

[71] D. G. Luenberger and Y. Ye, *Linear and Nonlinear Programming*, 3rd ed., ser. International Series in Operations Research & Management Science. Springer, 2008.

[72] S. Draper, L. Liu, A. Molisch, and J. Yedidia, "Cooperative routing for wireless networks using mutual-information accumulation," *IEEE Trans. Inf. Theory*, vol. 57, no. 8, pp. 5151–5162, August 2011.

[73] Y. Shi, Y. Hou, H. Zhou, and S. Midkiff, "Distributed cross-layer optimization for cognitive radio networks," *IEEE Trans. Veh. Technol.*, vol. 59, no. 8, pp. 4058–4069, Oct 2010.

[74] R. Madan, S. Cui, S. Lall, and A. Goldsmith, "Cross-layer design for lifetime maximization in interference-limited wireless sensor networks," *IEEE Trans. Wireless Commun.*, vol. 5, no. 11, pp. 3142–3152, November 2006.

[75] N. Pantazis, S. Nikolidakis, and D. Vergados, "Energy-efficient routing protocols in wireless sensor networks: A survey," *IEEE Commun. Surveys Tuts.*, vol. 15, no. 2, pp. 551–591, Second 2013.

[76] L. Ding, T. Melodia, S. Batalama, J. Matyjas, and M. Medley, "Cross-layer routing and dynamic spectrum allocation in cognitive radio ad hoc networks," *IEEE Trans. Veh. Technol.*, vol. 59, no. 4, pp. 1969–1979, May 2010.

[77] M. Neely, E. Modiano, and C. Rohrs, "Dynamic power allocation and routing for time-varying wireless networks," *IEEE J. Sel. Areas Commun.*, vol. 23, no. 1, pp. 89–103, Jan 2005.

[78] H. Chen, P. Ren, L. Sun, and Q. Du, "A distributed routing and time-slot assignment algorithm for cognitive radio ad hoc networks with primary-user protection," in *Proc. ICST CHINACOM 2012*, Kunming, PRC, August 2012, pp. 470–474.

[79] A. Goldsmith, S. Jafar, I. Maric, and S. Srinivasa, "Breaking spectrum gridlock with cognitive radios: An information theoretic perspective," *Proceedings of the IEEE*, vol. 97, no. 5, pp. 894–914, May 2009.

[80] M. Haenggi and R. Smarandache, "Diversity polynomials for the analysis of temporal correlations in wireless networks," *IEEE Trans. Wireless Commun.*, vol. 12, no. 11, pp. 5940–5951, November 2013.

[81] Y. Zhou and W. Zhuang, "Opportunistic cooperation in wireless ad hoc networks with interference correlation," *Peer-to-Peer Networking and Applications*, pp. 1–15, 2015.

[82] G. Nigam, P. Minero, and M. Haenggi, "Spatiotemporal cooperation in heterogeneous cellular networks," *IEEE J. Sel. Areas Commun.*, vol. 33, no. 6, pp. 1253–1265, June 2015.

[83] H. S. Dhillon, H. Huang, H. Viswanathan, and R. A. Valenzuela, "Fundamentals of throughput maximization with random arrivals for M2M communications," *IEEE Trans. Commun.*, vol. 62, no. 11, pp. 4094–4109, Nov 2014.

[84] S. P. Weber, X. Yang, J. G. Andrews, and G. de Veciana, "Transmission capacity of wireless ad hoc networks with outage constraints," *IEEE Trans. Inf. Theory*, vol. 51, no. 12, pp. 4091–4102, Dec 2005.

[85] M. Haenggi, *Stochastic geometry for wireless networks*, 1st ed. Cambridge University Press, 2013.

[86] R. Tanbourgi, H. Dhillon, J. Andrews, and F. Jondral, "Effect of spatial interference correlation on the performance of maximum ratio combining," *IEEE Trans. Wireless Commun.*, vol. 13, no. 6, pp. 3307–3316, June 2014.

[87] I. Gradshteyn and I. Ryzhik, *Table of Integrals, Series, and Products*. Academic Press, 2007.

Appendix A

Proofs

A.1 Proof of Lemma 3

Proof 14 *The locations of active transmitters in the first and second time slot can be modeled as Poisson point processes $\Phi_{a,1}$ and $\Phi_{a,2}$, respectively. As the coverage probability is captured in* (2.15)*, in the following, we focus on deriving the coverage probability of forwarding packets from relay to the destination. The probability that the destination can successfully decode the packet from the relay can be expressed as*

$$\begin{aligned}
P_{r,d,2} &= \mathbb{P}(SIR_{s,d,1} < T, SIR_{s,r,1} > T, SIR_{r,d,2} > T) \\
&= \mathbb{P}\left(G_{d,1} < I_{d,1} T z^{\alpha}, G_{r,1} > I_{r,1} T y^{\alpha}, G_{k,2} > I_{d,2} T x^{\alpha}\right) \\
&= \mathbb{E}_{\Phi_{a,1},\Phi_{a,2},\{G\}}\left[\left(1 - e^{-I_{d,1} T z^{\alpha}}\right) e^{-I_{r,1} T y^{\alpha}} e^{-I_{d,2} T x^{\alpha}}\right] \\
&= \mathbb{E}_{\Phi_{a,1},\Phi_{a,2},\{G\}}\left[\exp(-I_{r,1} T y^{\alpha} - I_{d,2} T x^{\alpha})\right] - \mathbb{E}_{\Phi_{a,1},\Phi_{a,2},\{G\}}\left[\exp(-I_{r,1} T y^{\alpha} - I_{d,2} T x^{\alpha} - I_{d,1} T z^{\alpha})\right]
\end{aligned} \tag{A.1}$$

Now let's look at the two items in (A.1) *separately. For the first item,*

$$\begin{aligned}
&\mathbb{E}_{\Phi_{a,1},\Phi_{a,2},\{G\}}\left[\exp(-I_{r,1}Ty^{\alpha}-I_{d,2}Tx^{\alpha})\right]\\
&=\mathbb{E}_{\Phi,\{G\}}\left[\prod_{\boldsymbol{x},\boldsymbol{y}\in\Phi}\exp(G_{\boldsymbol{x}}\|\boldsymbol{x}-\boldsymbol{R}\|^{-\alpha}Ty^{\alpha}1_{\boldsymbol{x}\in\Phi_{a,1}})\exp(h_{\boldsymbol{y}}\|\boldsymbol{y}-\boldsymbol{D}\|^{-\alpha}Tx^{\alpha}1_{\boldsymbol{y}\in\phi_{a,2}})\right]
\end{aligned}\tag{A.2}$$

where the indicator function $1_{\boldsymbol{x}\in\Phi_{a,1}}$ *is decided by the slotted-aloha algorithm. Averaging over the slotted-aloha algorithm where we assume in each slot the nodes will independently access the spectrum with a probability p, we get,*

$$\begin{aligned}
&\mathbb{E}_{\Phi_{a,1},\Phi_{a,2},\{G\}}\left[\exp(-I_{r,1}Ty^{\alpha}-I_{d,2}Tx^{\alpha})\right]\\
&\overset{aloha}{=}\mathbb{E}_{\Phi,\{G\}}\left[\prod_{\boldsymbol{x}\in\Phi}\left(1-p+p\exp(-h_{\boldsymbol{x},1}\|\boldsymbol{x}-\boldsymbol{R}\|^{-\alpha}Ty^{\alpha})\right)\left(1-p+p\exp(-h_{\boldsymbol{x},2}\|\boldsymbol{x}-\boldsymbol{D}\|^{-\alpha}Tx^{\alpha})\right)\right]\\
&=\mathbb{E}_{\Phi}\left[\prod_{\boldsymbol{x}\in\phi}\left(1-p+\frac{p}{1+\|\boldsymbol{x}-\boldsymbol{R}\|^{-\alpha}Ty^{\alpha}}\right)\left(1-p+\frac{p}{1+\|\boldsymbol{x}-\boldsymbol{D}\|^{-\alpha}Tx^{\alpha}}\right)\right]\\
&=\exp\left(-\lambda\int_{\mathbb{R}^2}1-\left(1-p+\frac{p}{1+|\boldsymbol{x}-\boldsymbol{R}\|^{-\alpha}Ty^{\alpha}}\right)\left(1-p+\frac{p}{1+\|\boldsymbol{x}-\boldsymbol{D}\|^{-\alpha}Tx^{\alpha}}\right)d\boldsymbol{x}\right)
\end{aligned}\tag{A.3}$$

The main technique used here is PGFL. Coming to the second item,

$$\begin{aligned}
&\mathbb{E}_{\Phi_{a,1},\Phi_{a,2}}\left[\exp(-I_{r,1}Ty^{\alpha}-I_{d,2}Tx^{\alpha}-I_{d,1}Tz^{\alpha})\right]\\
&=\mathbb{E}_{\Phi}\left[\prod_{\boldsymbol{x}\in\Phi}e^{-G_{\boldsymbol{x},\boldsymbol{D},1}\|\boldsymbol{x}-\boldsymbol{R}\|^{-\alpha}Ty^{\alpha}1_{\boldsymbol{x}\in\Phi_{a,1}}}e^{-G_{\boldsymbol{x},\boldsymbol{R},1}\|\boldsymbol{x}-\boldsymbol{D}\|^{-\alpha}Tz^{\alpha}1_{\boldsymbol{x}\in\Phi_{a,1}}}e^{-G_{\boldsymbol{x},\boldsymbol{D},2}\|\boldsymbol{x}-\boldsymbol{D}\|^{-\alpha}Tx^{\alpha}1_{\boldsymbol{x}\in\Phi_{a,2}}}\right]\\
&=\mathbb{E}_{\Phi}\left[\prod_{\boldsymbol{x}\in\Phi}\left(1-p+pe^{-G_{\boldsymbol{x},\boldsymbol{D},1}\|\boldsymbol{x}-\boldsymbol{R}\|^{-\alpha}Ty^{\alpha}}e^{-G_{\boldsymbol{x},\boldsymbol{R},1}\|\boldsymbol{x}-\boldsymbol{D}\|^{-\alpha}Tz^{\alpha}}\right)\left(1-p+pe^{-G_{\boldsymbol{x},\boldsymbol{D},2}\|\boldsymbol{x}-\boldsymbol{D}\|^{-\alpha}Tx^{\alpha}}\right)\right]\\
&=e^{-\lambda\int_{\mathbb{R}^2}1-\left(1-p+\frac{p}{(1+\|\boldsymbol{x}-\boldsymbol{R}\|^{-\alpha}Ty^{\alpha})(1+\|\boldsymbol{x}-\boldsymbol{D}\|^{-\alpha}Tz^{\alpha})}\right)\left(1-p+\frac{p}{1+\|\boldsymbol{x}-\boldsymbol{D}\|^{-\alpha}Tx^{\alpha}}\right)d\boldsymbol{x}}
\end{aligned}\tag{A.4}$$

A.2 Proof of Lemma 4

Proof 15 *Given the topology Φ and $SIR_{r,d,2}$, the coverage probability at the second slot can be expressed as*

$$\begin{aligned}
&\mathbb{P}(SIR_{s,d,1} < T, SIR_{s,r,1} > T, SIR_{r,d,2} + SIR_{s,d,1} > T | \Phi, SIR_{r,d,2}) \\
&= \mathbb{P}\left((T - SIR_{r,d,2})^{+} I_{d,1} z^{\alpha} < G_{d,1} < I_{d,1} T z^{\alpha}, h_{r,1} > I_{r,1} T y^{\alpha} | \Phi, SIR_{r,d,2}\right) \\
&= \mathbb{E}_{\{G\}}\left[\exp\left(-(T - SIR_{k,d,2})^{+} I_{d,1} z^{\alpha} - I_{r,1} T y^{\alpha}\right) - \exp\left(-I_{d,1} T z^{\alpha} - I_{r,1} T y^{\alpha}\right) | \Phi, SIR_{r,d,2}\right] \\
&= \prod_{\boldsymbol{x} \in \Phi} \left(1 - p + p \frac{1}{(1 + (T - SIR_{r,d,2})^{+} z^{\alpha} \|\boldsymbol{x}\text{-}\boldsymbol{D}\|^{-\alpha})(1 + \|\boldsymbol{x}\text{-}\boldsymbol{R}\|^{-\alpha} T y^{\alpha})}\right) \\
&- \prod_{\boldsymbol{x} \in \Phi} \left(1 - p + p \frac{1}{1 + \|\boldsymbol{x}\text{-}\boldsymbol{D}\|^{-\alpha} T z^{\alpha}} \frac{1}{1 + \|\boldsymbol{x}\text{-}\boldsymbol{R}\|^{-\alpha} T y^{\alpha}}\right)
\end{aligned} \tag{A.5}$$

After getting the coverage probability for a fixed topology and a fixed $SIR_{r,d,2}$, we need to derive the distribution of $SIR_{r,d,2}$ under a given topology Φ. Denote $SIR_{r,d,2}$ as Ω, now we need to calculate the cumulative distribution function (CDF)for Ω given the topology Φ.

$$\begin{aligned}
&\mathbb{P}(\Omega \leq \omega | \Phi) \\
&= \mathbb{P}\left(G_{r,d,2} \leq I_{d,2} x^{\alpha} \omega | \Phi\right) \\
&= 1 - \mathbb{E}(\exp(-I_{d,2} x^{\alpha} \omega) | \Phi) \\
&= 1 - \mathbb{E}(\prod_{\boldsymbol{x} \in \Phi} \left(1 - p + p \exp(-G_{\boldsymbol{x},2} \|\boldsymbol{x}\text{-}\boldsymbol{D}\|^{-\alpha} x^{\alpha} \omega)\right) | \Phi) \\
&= 1 - \prod_{\boldsymbol{x} \in \Phi} \left(1 - p + \frac{p}{1 + \|\boldsymbol{x}\text{-}\boldsymbol{D}\|^{-\alpha} x^{\alpha} \omega}\right)
\end{aligned} \tag{A.6}$$

After getting the CDF of Ω, we can get the PDF of Ω by derivation as follows,

$$\begin{aligned}
f_{\Omega|\Phi}(\omega) &= \frac{\partial \mathbb{P}(\Omega \leq \omega | \Phi)}{\partial \omega} \\
&= \sum_{\boldsymbol{x} \in \Phi} \frac{p \|\boldsymbol{x}\text{-}\boldsymbol{D}\|^{-\alpha} x^{\alpha}}{(1 + \|\boldsymbol{x}\text{-}\boldsymbol{D}\|^{-\alpha} x^{\alpha})^2 \omega} \prod_{\boldsymbol{y} \in \Phi, \boldsymbol{y} \neq \boldsymbol{x}} \left(1 - p + \frac{p}{1 + \|\boldsymbol{y}\text{-}\boldsymbol{D}\|^{-\alpha} x^{\alpha} \omega}\right)
\end{aligned} \tag{A.7}$$

Therefore,the probability that the destination can decode the packet with energy accumulation in the second time slot can be obtained by averaging the result in equation (A.5) *over both* Ω *and* Φ*, which can be expressed as,*

$$
\begin{aligned}
P^{EA} &= \int_0^{\infty} \mathbb{E}_{\Phi}\left[\prod_{\boldsymbol{x}\in\phi}\left(1-p+p\frac{1}{1+(T-\omega)^{+}z^{\alpha}\|\boldsymbol{x}\text{-}\boldsymbol{D}\|^{-\alpha}}\frac{1}{1+\|\boldsymbol{x}\text{-}\boldsymbol{R}\|^{-\alpha}Ty^{\alpha}}\right) f_{\Omega|\Phi}(\omega)\right] d\omega \\
&\quad - \mathbb{E}_{\Phi}\left[\prod_{\boldsymbol{x}\in\Phi}\left(1-p+p\frac{1}{1+\|\boldsymbol{x}\text{-}\boldsymbol{D}\|^{-\alpha}Tz^{\alpha}}\frac{1}{1+\|\boldsymbol{x}\text{-}\boldsymbol{R}\|^{-\alpha}Ty^{\alpha}}\right)\right] \\
&= \int_0^{\infty} \mathbb{E}_{\Phi}\left[\sum_{\boldsymbol{x}\in\Phi}\frac{p\|\boldsymbol{x}\text{-}\boldsymbol{D}\|^{-\alpha}x^{\alpha}}{(1+\|\boldsymbol{x}\text{-}\boldsymbol{D}\|^{-\alpha}x^{\alpha}\omega)^2}\left(1-p+p\frac{1}{1+(T-\omega)^{+}z^{\alpha}\|\boldsymbol{x}\text{-}\boldsymbol{D}\|^{-\alpha}}\frac{1}{1+\|\boldsymbol{x}\text{-}\boldsymbol{R}\|^{-\alpha}Ty^{\alpha}}\right)\cdot\right. \\
&\left.\prod_{\boldsymbol{y}\in\Phi,\boldsymbol{y}\neq\boldsymbol{x}}\left(1-p+\frac{p}{1+\|\boldsymbol{y}\text{-}\boldsymbol{D}\|^{-\alpha}x^{\alpha}\omega}\right)\left(1-p+p\frac{1}{1+(T-\omega)^{+}z^{\alpha}\|\boldsymbol{y}\text{-}\boldsymbol{D}\|^{-\alpha}}\frac{1}{1+\|\boldsymbol{y}\text{-}\boldsymbol{R}\|^{-\alpha}Ty^{\alpha}}\right)\right] d\omega \\
&\quad - \exp\left(-\lambda_a\int_{\mathbb{R}^2} 1-\frac{1}{1+\|\boldsymbol{x}\text{-}\boldsymbol{D}\|^{-\alpha}Tz^{\alpha}}\frac{1}{1+\|\boldsymbol{x}\text{-}\boldsymbol{R}\|^{-\alpha}Ty^{\alpha}}d\boldsymbol{x}\right)
\end{aligned}
\tag{A.8}
$$

By[Theorem 8.9 in [8]], we have, for any measurable function $h(x)$*,*

$$
\mathbb{E}_{\Phi}\left[\sum_{\boldsymbol{x}\in\Phi} h(\boldsymbol{x},\Phi\setminus\{\boldsymbol{x}\})\right] = \int_{\mathbb{R}^2}\mathbb{E}^{!}_{\boldsymbol{x}}\left[h(\boldsymbol{x},\Phi)\right]\lambda d\boldsymbol{x} = \int_{\mathbb{R}^2}\mathbb{E}\left[h(\boldsymbol{x},\Phi)\right]\lambda d\boldsymbol{x} \tag{A.9}
$$

Therefore,

$$
\begin{aligned}
P^{EA} &= \int_0^{\infty}\int_{\mathbb{R}^2}\frac{p\|\boldsymbol{x}\text{-}\boldsymbol{D}\|^{-\alpha}x^{\alpha}}{(1+\|\boldsymbol{x}\text{-}\boldsymbol{D}\|^{-\alpha}x^{\alpha}\omega)^2}\left(1-p+p\frac{1}{1+(T-\omega)^{+}z^{\alpha}\|\boldsymbol{x}\text{-}\boldsymbol{D}\|^{-\alpha}}\frac{1}{1+\|\boldsymbol{x}\text{-}\boldsymbol{R}\|^{-\alpha}Ty^{\alpha}}\right)\cdot \\
&\mathbb{E}_{\Phi}\left[\prod_{\boldsymbol{y}\in\Phi,\boldsymbol{y}\neq\boldsymbol{x}}\left(1-p+\frac{p}{1+\|\boldsymbol{y}\text{-}\boldsymbol{D}\|^{-\alpha}x^{\alpha}\omega}\right)\left(1-p+p\frac{1}{1+(T-\omega)^{+}z^{\alpha}\|\boldsymbol{y}\text{-}\boldsymbol{D}\|^{-\alpha}}\frac{1}{1+\|\boldsymbol{y}\text{-}\boldsymbol{R}\|^{-\alpha}Ty^{\alpha}}\right)\right] d\omega \\
&\quad - \exp\left(-\lambda_a\int_{\mathbb{R}^2} 1-\frac{1}{1+\|\boldsymbol{x}\text{-}\boldsymbol{D}\|^{-\alpha}Tz^{\alpha}}\frac{1}{1+\|\boldsymbol{x}\text{-}\boldsymbol{R}\|^{-\alpha}Ty^{\alpha}}d\boldsymbol{x}\right) \\
&= \int_0^{\infty}\int_{\mathbb{R}^2}\frac{\lambda p\|\boldsymbol{x}\text{-}\boldsymbol{D}\|^{-\alpha}x^{\alpha}}{(1+\|\boldsymbol{x}\text{-}\boldsymbol{D}\|^{-\alpha}x^{\alpha}\omega)^2}\left(1-p+p\frac{1}{1+(T-\omega)^{+}z^{\alpha}\|\boldsymbol{x}\text{-}\boldsymbol{D}\|^{-\alpha}}\frac{1}{1+\|\boldsymbol{x}\text{-}\boldsymbol{R}\|^{-\alpha}Ty^{\alpha}}\right)d\boldsymbol{x}\cdot \\
&\quad e^{-\lambda\int_{\mathbb{R}^2}1-\left(1-p+\frac{p}{1+\|\boldsymbol{y}\text{-}\boldsymbol{D}\|^{-\alpha}x^{\alpha}\omega}\right)\left(1-p+p\frac{1}{1+(T-\omega)^{+}z^{\alpha}\|\boldsymbol{y}\text{-}\boldsymbol{D}\|^{-\alpha}}\frac{1}{1+\|\boldsymbol{y}\text{-}\boldsymbol{R}\|^{-\alpha}Ty^{\alpha}}\right)d\boldsymbol{y}}d\omega \\
&\quad - e^{-\lambda p\int_{\mathbb{R}^2}1-\frac{1}{1+\|\boldsymbol{x}\text{-}\boldsymbol{D}\|^{-\alpha}Tz^{\alpha}}\frac{1}{1+\|\boldsymbol{x}\text{-}\boldsymbol{R}\|^{-\alpha}Ty^{\alpha}}d\boldsymbol{x}}.
\end{aligned}
\tag{A.10}
$$

A.3 Proof of Lemma 5

Proof 16 *Similar to the steps in the proof of coverage probability under energy accumulation strategy, the coverage probability of mutual information accumulation can be calculated by first calculate the coverage probability under fixed topology and fixed $SIR_{r,d,2}$ and then average over the topology and the distribution of $SIR_{r,d,2}$. The coverage probability of mutual information accumulation under fixed topology and fixed $SIR_{r,d,2}$ can be expressed as*

$$
\begin{aligned}
&\mathbb{P}(SIR_{s,d,1} < T, SIR_{s,r,1} > T, \log(1+SIR_{r,d,2}) + \log(1+SIR_{s,d,1}) > \log(1+T) | \Phi, SIR_{r,d,2}) \\
&= \mathbb{P}(SIR_{s,d,1} < T, SIR_{s,r,1} > T, SIR_{s,d,1} > \frac{(T-SIR_{r,d,2})^+}{1+SIR_{r,d,2}} | \Phi, SIR_{r,d,2}) \\
&= \mathbb{P}\left(\frac{(T-SIR_{r,d,2})^+ I_{d,1} z^\alpha}{1+SIR_{r,d,2}} < G_{d,1} < I_{d,1} T z^\alpha, G_{r,1} > I_{r,1} T y^\alpha | \Phi, SIR_{r,d,2} \right) \\
&= \mathbb{E}\left[\exp\left(-\frac{(T-SIR_{r,d,2})^+ I_{d,1} z^\alpha}{1+SIR_{r,d,2}} - I_{r,1} T y^\alpha \right) - \exp\left(-I_{d,1} T z^\alpha - I_{r,1} T y^\alpha \right) | \Phi, SIR_{r,d,2} \right] \\
&= \prod_{\boldsymbol{x} \in \Phi} \left(1 - p + p \frac{1}{1 + \frac{(T-SIR_{r,d,2})^+ z^\alpha \|\boldsymbol{x}\text{-}\boldsymbol{D}\|^{-\alpha}}{1+SIR_{r,d,2}}} \frac{1}{1+\|\boldsymbol{x}\text{-}\boldsymbol{R}\|^{-\alpha} T y^\alpha} \right) \\
&\quad - \prod_{\boldsymbol{x} \in \Phi} \left(1 - p + p \frac{1}{1+\|\boldsymbol{x}\text{-}\boldsymbol{D}\|^{-\alpha} T z^\alpha} \frac{1}{1+\|\boldsymbol{x}\text{-}\boldsymbol{R}\|^{-\alpha} T y^\alpha} \right)
\end{aligned}
\tag{A.11}
$$

By averaging the conditional coverage probability over random topologies and the distribution of $SIR_{r,d,2}$, the coverage probability of mutual information accumulation can be expressed as

$$
\begin{aligned}
P^{MIA} &= \int_0^{\infty} \mathbb{E}_{\Phi}\left[\prod_{\boldsymbol{x}\in\Phi}\left(1-p+p\frac{1}{1+\frac{(T-\omega)^{+}z^{\alpha}\|\boldsymbol{x}\text{-}\boldsymbol{D}\|^{-\alpha}}{1+\omega}}\frac{1}{1+\|\boldsymbol{x}\text{-}\boldsymbol{R}\|^{-\alpha}Ty^{\alpha}}\right) f_{\Omega|\Phi}(\omega)\right] d\omega \\
&\quad - \mathbb{E}_{\Phi}\left[\prod_{\boldsymbol{x}\in\Phi}\left(1-p+p\frac{1}{1+\|\boldsymbol{x}\text{-}\boldsymbol{D}\|^{-\alpha}Tz^{\alpha}}\frac{1}{1+\|\boldsymbol{x}\text{-}\boldsymbol{R}\|^{-\alpha}Ty^{\alpha}}\right)\right] \\
&= \int_0^{\infty} \mathbb{E}_{\Phi}\left[\sum_{\boldsymbol{x}\in\phi}\frac{p\|\boldsymbol{x}\text{-}\boldsymbol{D}\|^{-\alpha}x^{\alpha}}{(1+\|\boldsymbol{x}\text{-}\boldsymbol{D}\|^{-\alpha}x^{\alpha}\omega)^2}\left(1-p+p\frac{1}{1+\frac{(T-\omega)^{+}z^{\alpha}\|\boldsymbol{x}\text{-}\boldsymbol{D}\|^{-\alpha}}{1+\omega}}\frac{1}{1+\|\boldsymbol{x}\text{-}\boldsymbol{R}\|^{-\alpha}Ty^{\alpha}}\right)\cdot\right. \\
&\quad \left.\prod_{\boldsymbol{y}\in\Phi,\boldsymbol{y}\neq\boldsymbol{x}}\left(1-p+\frac{p}{1+\|\boldsymbol{y}\text{-}\boldsymbol{D}\|^{-\alpha}x^{\alpha}\omega}\right)\left(1-p+p\frac{1}{1+\frac{(T-\omega)^{+}z^{\alpha}\|\boldsymbol{y}\text{-}\boldsymbol{D}\|^{-\alpha}}{1+\omega}}\frac{1}{1+\|\boldsymbol{y}\text{-}\boldsymbol{R}\|^{-\alpha}Ty^{\alpha}}\right)\right] d\omega \\
&\quad - \exp\left(-\lambda p\int_{\mathbb{R}^2}1-\frac{1}{1+\|\boldsymbol{x}\text{-}\boldsymbol{D}\|^{-\alpha}Tz^{\alpha}}\frac{1}{1+\|\boldsymbol{x}\text{-}\boldsymbol{R}\|^{-\alpha}Ty^{\alpha}}d\boldsymbol{x}\right) \\
&= \int_0^{\infty}\int_{\mathbb{R}^2}\frac{\lambda p\|\boldsymbol{x}\text{-}\boldsymbol{D}\|^{-\alpha}x^{\alpha}}{(1+\|\boldsymbol{x}\text{-}\boldsymbol{D}\|^{-\alpha}x^{\alpha}\omega)^2}\left(1-p+p\frac{1}{1+\frac{(T-\omega)^{+}z^{\alpha}\|\boldsymbol{x}\text{-}\boldsymbol{D}\|^{-\alpha}}{1+\omega}}\frac{1}{1+\|\boldsymbol{x}\text{-}\boldsymbol{R}\|^{-\alpha}Ty^{\alpha}}\right)d\boldsymbol{x}\cdot \\
&\quad e^{-\lambda\int_{\mathbb{R}^2}1-\left(1-p+\frac{p}{1+\|\boldsymbol{y}\text{-}\boldsymbol{D}\|^{-\alpha}x^{\alpha}\omega}\right)\left(1-p+p\frac{1}{1+\frac{(T-\omega)^{+}z^{\alpha}\|\boldsymbol{y}\text{-}\boldsymbol{D}\|^{-\alpha}}{1+\omega}}\frac{1}{1+\|\boldsymbol{y}\text{-}\boldsymbol{R}\|^{-\alpha}Ty^{\alpha}}\right)d\boldsymbol{y}}d\omega \\
&\quad - e^{-\lambda p\int_{\mathbb{R}^2}1-\frac{1}{1+\|\boldsymbol{x}\text{-}\boldsymbol{D}\|^{-\alpha}Tz^{\alpha}}\frac{1}{1+\|\boldsymbol{x}\text{-}\boldsymbol{R}\|^{-\alpha}Ty^{\alpha}}d\boldsymbol{x}}.
\end{aligned}
\tag{A.12}
$$

A.4 Proof of Lemma 6

Proof 17 *The first two-dimensional integration can be expressed as*

$$
\begin{aligned}
&\int_{\mathbb{R}^2}\frac{\lambda p\|\boldsymbol{x}\text{-}\boldsymbol{D}\|^{-\alpha}x^{\alpha}}{(1+\|\boldsymbol{x}\text{-}\boldsymbol{D}\|^{-\alpha}x^{\alpha}\omega)^2}\left(1-p+p\frac{1}{1+(T-\omega)^{+}z^{\alpha}\|\boldsymbol{x}\text{-}\boldsymbol{D}\|^{-\alpha}}\frac{1}{1+\|\boldsymbol{x}\text{-}\boldsymbol{R}\|^{-\alpha}Ty^{\alpha}}\right)d\boldsymbol{x} \\
&\approx \int_{\mathbb{R}^2}\frac{\lambda p\|\boldsymbol{x}\|^{-\alpha}x^{\alpha}}{(1+\|\boldsymbol{x}\|^{-\alpha}x^{\alpha}\omega)^2}\left(1-p+p\frac{1}{1+(T-\omega)^{+}z^{\alpha}\|\boldsymbol{x}\|^{-\alpha}}\frac{1}{1+\|\boldsymbol{x}\|^{-\alpha}Ty^{\alpha}}\right)d\boldsymbol{x} \\
&= \int_0^{\infty}\frac{2\pi p\lambda x^{\alpha}\rho^{-\alpha+1}}{(1+x^{\alpha}\omega\rho^{-\alpha})^2}d\rho - \int_0^{\infty}\frac{2\pi p^2\lambda x^{\alpha}\rho^{-\alpha+1}}{(1+x^{\alpha}\omega\rho^{-\alpha})^2}\left[1-\frac{1}{(1+(T-\omega)^{+}z^{\alpha}\rho^{-\alpha})(1+Ty^{\alpha}\rho^{-\alpha})}\right]d\rho
\end{aligned}
\tag{A.13}
$$

Let's first address the second integration in equation (A.13) *and denote* $a_0 = (T-\omega)^+ z^\alpha, b_0 = Ty^\alpha, c_0 = x^\alpha\omega$. *Using the equation that*

$$1 - \frac{1}{(1+ax)(1+bx)} = \frac{a}{a-b}\left(1 - \frac{1}{1+ax}\right) - \frac{b}{a-b}\left(1 - \frac{1}{1+bx}\right), \tag{A.14}$$

The second integration in equation (A.13) *can be simplified as*

$$\begin{aligned}
&\int_0^\infty \frac{2\pi p^2\lambda x^\alpha \rho^{-\alpha+1}}{(1+x^\alpha\omega\rho^{-\alpha})^2}\left[1 - \frac{1}{(1+(T-\omega)^+ z^\alpha\rho^{-\alpha})(1+Ty^\alpha\rho^{-\alpha})}\right]d\rho \\
&= \frac{a_0^2}{a_0-b_0}\int_0^\infty \frac{2\pi p^2\lambda x^\alpha\rho^{-2\alpha+1}}{(1+c_0\rho^{-\alpha})^2(1+a_0\rho^{-\alpha})}d\rho - \frac{b_0^2}{a_0-b_0}\int_0^\infty \frac{2\pi p^2\lambda x^\alpha\rho^{-2\alpha+1}}{(1+c_0\rho^{-\alpha})^2(1+b_0\rho^{-\alpha})}d\rho \\
&\overset{t=\rho^{-\alpha}}{=\!=\!=} \frac{2\pi p^2\lambda x^\alpha}{(a_0-b_0)\alpha}\int_0^\infty \frac{a_0^2 c_0^{2/\alpha-2}t^{1-2/\alpha}}{(1+t)^2(1+a_0t/c_0)}dt - \frac{2\pi p^2\lambda x^\alpha}{(a_0-b_0)\alpha}\int_0^\infty \frac{b_0^2 c_0^{2/\alpha-2}t^{1-2/\alpha}}{(1+t)^2(1+b_0t/c_0)}dt \\
&\overset{a}{=} \frac{2\pi p^2\lambda x^\alpha B(2-\frac{2}{\alpha}, 1+\frac{2}{\alpha})}{(a_0-b_0)\alpha c_0^{2-\frac{2}{\alpha}}}(a_0^2 {}_2F_1(1,2-\frac{2}{\alpha};3;1-a_0/c_0) - b_0^2 {}_2F_1(1,2-\frac{2}{\alpha};3;1-b_0/c_0)) \\
&\triangleq p^2\lambda x^\alpha c_2 h_0(a_0,b_0,c_0),
\end{aligned} \tag{A.15}$$

where $\overset{a}{=}$ *comes from the equation (3.197.5) in [87] and* ${}_2F_1(a,b;c;z) = \frac{\Gamma(c)}{\Gamma(b)\Gamma(c-b)}\int_0^1 t^{b-1}(1-t)^{c-b-1}(1-tz)^{-a}dt$ *is the hypergeometric function;* $h_0(a_0,b_0,c_0) \triangleq \frac{(a_0^2 {}_2F_1(1,2-\frac{2}{\alpha};3;1-a_0/c_0) - b_0^2 {}_2F_1(1,2-\frac{2}{\alpha};3;1-b_0/c_0))}{(a_0-b_0)c_0^{2-\frac{2}{\alpha}}}$; $c_2 \triangleq \frac{2\pi B(2-\frac{2}{\alpha},1+\frac{2}{\alpha})}{\alpha}$. *The first integration in equation* (A.13) *can be simplified as*

$$\int_0^\infty \frac{2\pi p\lambda x^\alpha\rho^{-\alpha+1}}{(1+x^\alpha\omega\rho^{-\alpha})^2}d\rho = \frac{2\pi p\lambda x^2\omega^{\frac{2}{\alpha}-1}}{\alpha}B(1-\frac{2}{\alpha},1+\frac{2}{\alpha}) \triangleq p\lambda c_3 x^2\omega^{\frac{2}{\alpha}-1}, \tag{A.16}$$

where $c_3 \triangleq \frac{2\pi B(1-\frac{2}{\alpha},1+\frac{2}{\alpha})}{\alpha}$. *Similar to the results in equation* (2.23)*, the second two-dimensional integration can be simplified in the following:*

$$
\begin{aligned}
&\int_{\mathbb{R}^2} 1-\left(1-p+\frac{p}{1+\|\boldsymbol{y}\text{-}\boldsymbol{D}\|^{-\alpha}x^{\alpha}\boldsymbol{\omega}}\right)\left(1-p+p\frac{1}{1+(T-\boldsymbol{\omega})^{+}z^{\alpha}\|\boldsymbol{y}\text{-}\boldsymbol{D}\|^{-\alpha}}\frac{1}{1+\|\boldsymbol{y}\text{-}\boldsymbol{R}\|^{-\alpha}Ty^{\alpha}}\right)d\boldsymbol{y}\\
&\approx p(1-p)\int_{\mathbb{R}^2} 1-\frac{1}{1+\|\boldsymbol{x}\|^{-\alpha}c_0}d\boldsymbol{x}+p(1-p)\int_{\mathbb{R}^2} 1-\frac{1}{(1+\|\boldsymbol{x}\|^{-\alpha}a_0)(1+\|\boldsymbol{x}\|^{-\alpha}b_0)}d\boldsymbol{x}\\
&\qquad+p^2\int_{\mathbb{R}^2} 1-\frac{1}{(1+\|\boldsymbol{x}\|^{-\alpha}a_0)(1+\|\boldsymbol{x}\|^{-\alpha}b_0)(1+\|\boldsymbol{x}\|^{-\alpha}c_0)}d\boldsymbol{x}\\
&=p(1-p)c_1\left(c_0^{2/\alpha}+\frac{b_0^{1+\frac{2}{\alpha}}}{b_0-a_0}+\frac{a_0^{1+\frac{2}{\alpha}}}{a_0-b_0}\right)\\
&\qquad+p^2c_1\left(\frac{(b_0)^{2+\frac{2}{\alpha}}}{(b_0-a_0)(b_0-c_0)}+\frac{(a_0)^{2+\frac{2}{\alpha}}}{(a_0-b_0)(a_0-c_0)}+\frac{(c_0)^{2+\frac{2}{\alpha}}}{(c_0-b_0)(c_0-a_0)}\right)\\
&\triangleq p(1-p)c_1h_1(a_0,b_0,c_0)+p^2c_1h_2(a_0,b_0,c_0),
\end{aligned}
\tag{A.17}
$$

where $h_1(a_0,b_0,c_0) \triangleq c_0^{2/\alpha}+\frac{b_0^{1+\frac{2}{\alpha}}}{b_0-a_0}+\frac{a_0^{1+\frac{2}{\alpha}}}{a_0-b_0}$, *and* $h_2(a_0,b_0,c_0) \triangleq \frac{(b_0)^{2+\frac{2}{\alpha}}}{(b_0-a_0)(b_0-c_0)}+\frac{(a_0)^{2+\frac{2}{\alpha}}}{(a_0-b_0)(a_0-c_0)}+\frac{(c_0)^{2+\frac{2}{\alpha}}}{(c_0-b_0)(c_0-a_0)}$.

A.5 Proof of Lemma 12

Proof 18

$$
\begin{aligned}
&\mathbb{P}(A^c \cap B^c) = \mathbb{P}(\mathscr{M} = 0, SIR_{d,1} > T) \\
&= \mathbb{P}(\mathscr{N} = 0)\mathbb{P}(SIR_{d,1} > T) + \sum_{k=1}^{\infty} \mathbb{P}(\mathscr{N} = k)\mathbb{P}(SIR_{k,1} < T, \cdots, SIR_{1,1} < T, SIR_{d,1} > T) \\
&= \sum_{k=1}^{\infty} \frac{e^{-a}a^k}{k!} \mathbb{E}\left(e^{-Tz^{\alpha}I_{d,1}} \prod_{j=1}^{k} (1 - \exp(-Tz^{\alpha}I_{j,1})) \right) + e^{-a-k_1} \\
&= \sum_{k=1}^{\infty} \frac{e^{-a}a^k}{k!} \mathbb{E}\left(\sum_{j=1}^{k} (-1)^j C_k^j \exp(-Tz^{\alpha} \sum_{i=0}^{j} I_{i,1}) \right) + \sum_{k=1}^{\infty} \frac{e^{-a}a^k}{k!} \mathbb{E}\left(\exp(-Tz^{\alpha}I_{d,1}) \right) + e^{-a-k_1} \\
&= \sum_{k=1}^{\infty} \sum_{j=1}^{k} \frac{e^{-a}a^k}{k!} (-1)^j C_k^j e^{-p\lambda g(j+1)} + e^{-k_1},
\end{aligned}
\tag{A.18}
$$

where $C_k^j = \frac{k!}{j!(k-j)!}$, $g(j) \triangleq \pi T^{\delta} z^2 \frac{\pi\delta}{\sin(\pi\delta)} \sum_{i=1}^{j} C_j^i \frac{\Gamma(\delta)}{\Gamma(i)\Gamma(\delta-i+1)}$ *which is similar to the definition of* F_n *in [80].*

A.6 Proof of Lemma 15

Proof 19 *The following proof is to calculate each item in the right hand of equation* (4.26)*. Here we only list the calculation of* $\mathbb{P}(A^c \cap B^c \cap E^c)$*, others are omitted and can be derived following the*

similar steps. Given a specific y, $\mathbb{P}(A^c \cap B^c \cap E^c)$ can be calculated as

$$
\begin{aligned}
&\mathbb{P}(A^c \cap B^c \cap E^c) \\
&= \mathbb{P}(\mathscr{M} = 0, SIR_{d,1} > T, SIR_{d,2} < T) \\
&= \mathbb{P}(\mathscr{N} = 0)\mathbb{P}(SIR_{d,1} > T) + \sum_{k=1}^{\infty} \mathbb{P}(\mathscr{N} = k)\mathbb{P}(SIR_{k,1} < T, \cdots, SIR_{d,2} < T, SIR_{d,1} > T) \\
&= \sum_{k=1}^{\infty} \mathbb{P}(\mathscr{N} = k)\mathbb{E}\left[e^{-I_{d,1}Tz^{\alpha}} \prod_{j=1}^{k}(1 - e^{-I_{j,1}Tz^{\alpha}})\right] + e^{-a-c_1} \\
&\quad - \sum_{k=1}^{\infty} \mathbb{P}(\mathscr{N} = k)\mathbb{E}\left[e^{-I_{d,1}Tz^{\alpha}} e^{-I_{d,2}Ty^{\alpha}} \prod_{j=1}^{k}(1 - e^{-I_{j,1}Tz^{\alpha}})\right] \\
&= \mathbb{P}(A^c \cap B^c) - \sum_{k=1}^{\infty} \mathbb{P}(\mathscr{N} = k)\mathbb{E}\left[\frac{(1 + \sum_{j=1}^{k}(-1)^j C_k^j e^{-Tz^{\alpha}\sum_{i=1}^{j} I_i})}{e^{I_{d,1}Tz^{\alpha} + I_{d,2}Ty^{\alpha}}}\right] \\
&= \mathbb{P}(A^c \cap B^c) - g_2(1,y) - \sum_{k=1}^{\infty}\sum_{j=1}^{k} \frac{e^{-a}a^k(-1)^j}{j!(k-j)!} g_2(j+1,y),
\end{aligned}
$$

where $g_2(j,y)$ is defined as

$$
\begin{aligned}
g_2(j,y) &= \mathbb{E}\left[e^{-Ty^{\alpha}I_{d,2}} e^{-Tz^{\alpha}\sum_{i=k-j+1}^{k} I_{i,1}}\right] \\
&= e^{-2\pi\lambda \int_0^{\infty} \rho - \left(1-p+\frac{p}{1+\rho^{-\alpha_y}\alpha_T}\right)\left(1-p+\frac{p}{(1+\rho^{-\alpha_z}\alpha_T)^j}\right)\rho d\rho}.
\end{aligned} \tag{A.19}
$$

Averaging over the distribution of y, the lemma is proved.

A.7 Proof of Lemma 16

Proof 20 *Note that the condition of MTD's retransmission is that there is no potential relay can be found. Therefore, the condition that $\mathscr{M} = 0$ should hold.*

$$\begin{aligned}
&\mathbb{P}(A^c \cap B \cap F) = \mathbb{P}(SIR_{d,2} > T, \mathscr{M} = 0, SIR_{d,1} < T) \\
&\overset{a}{=} \sum_{k=0}^{\infty} \mathbb{P}(\mathscr{N} = k)\mathbb{P}(SIR_{d,2} > T, SIR_{j,1} < T, 0 \le j \le k) \\
&\overset{b}{=} \sum_{k=0}^{\infty} \mathbb{P}(N = k)\mathbb{E}\left[\exp(-TI_{d,2}z^{\alpha})\prod_{j=1}^{k+1}(1-\exp(-Tz^{\alpha}I_{j,1}))\right] \\
&\overset{c}{=} \sum_{k=1}^{\infty} \mathbb{P}(N = k)\mathbb{E}\left[\exp(-Tz^{\alpha}I_{d,2})\prod_{j=1}^{k+1}(1-\exp(-Tz^{\alpha}I_{j,1}))\right] + e^{-a}\mathbb{P}(SIR_{d,2} > T, SIR_{d,1} < T) \\
&= \sum_{k=1}^{\infty}\sum_{j=1}^{k+1} \frac{(-1)^j e^{-a} a^k (k+1)}{j!(k+1-j)!} e^{-p\lambda(g(j)-(1-p)g(1)-p(g(j+1)-g(j)))} + e^{-k_1} - e^{-a-2k_1+p(1-\delta)k_1}
\end{aligned} \tag{A.20}$$

where $\overset{a}{=}$ comes from we number out every relay in the cooperative region and all relays in the region failed to decode the packet; denote $SIR_{0,1} = SIR_{d,1}$ to make the expression more simple; $\overset{b}{=}$ comes from averaging over small scale fading; $\overset{c}{=}$ comes from splitting the first summation item, i.e., $k = 0$, out.